

Study of Adaptive Radio Resource Allocation Using Cross Layer Design in OFDMA Systems

Arfianto Fahmi¹, Dadang Gunawan²

¹Electrical Engineering Department, University Of Indonesia
New Campus Of UI Depok 16424 Indonesia, arfianto.fahmi@gmail.com

²Electrical Engineering Department, University Of Indonesia
New Campus Of UI Depok 16424 Indonesia, guna@eng.ui.ac.id

Abstract — This paper reviews some recent research in the area of Adaptive radio resource allocation (ARRA) in OFDMA systems due to change of wireless channel. To accommodate high speed communications which have the various of service and quality of services, the resource allocation strategies need to be combined with some scheduling and priority scheme (part of MAC layer) to improve spectral efficiency, to maintain fairness among users and to maintain utility usage of radio resources. This combined scheme we call cross-layer design, where this scheme has become one of the most recent topics in the areas of wireless networks beyond 3G. Some on-going research in this area is also briefly reviewed and in this paper.

Keywords— OFDMA, cross layer design, adaptive radio resource allocation, scheduling.

1. Introduction

Future wireless and communication system are expected to offer high speed communication for support a large number of user and various of service with certain quality of service requirements. OFDMA (Orthogonal Frequency Division Multiple Access) system is one of the access technology used in some wireless access technology standards such as WiMAX and LTE. Challenges of the future of wireless technology is more limited frequency spectrum and the total transmit power and the nature of wireless channels, where there is a tendency exposed to the effects of intersymbol interference (ISI) in broadband wireless communications. To combat these challenges, the OFDMA technology suitable for use as it can against the nature of wireless channels that are selective fading.

In mobile applications, wireless channel changes must be anticipated by implementing an intelligent adaptive radio resource management algorithms by interacting in both the physical and the media access control (MAC) layers, where allocation of radio resources (subcarriers and power) to each user must be made adaptively depending on channel conditions.

In practice, the radio resource allocation procedures that involve the physical layer and MAC layer can be modelled as an optimization problem where the objective and constraints can be determined based on the quality of service from the user, the type of service (real time or non real time) and network limitations. Based on the objective function and constraints, there are three categories of radio resource allocation strategy that is based on throughput (efficiency), based on fairness and based on the utility. Radio resource allocation problem in OFDMA networks with K users and N subcarriers are divided into two parts, the first part is determining the number of subcarriers to be allocated to each user and the second part is how to allocate the power in each subcarrier. all these parts is based on Channel State Information (CSI) that is sent by each user.

By combining Resources allocation and scheduling scheme with certain priorities will be more efficient resource allocation because the allocation is based on objectivity function that will be reached which is determined from the quality of service and type of service from each user. This paper reviews the three categories of radio resource allocation strategy in OFDMA systems and their advantages and weaknesses. This study involves the scheduling and priority schemes to be combined with the three categories above and describe the research opportunities of the three categories above.

2. Adaptif Radio Resources Allocation Strategies

Radio resource allocation strategy is divided into three categories algorithm: Based on the throughput (spectral efficiency), based on fairness and based on the utility. The following description of the three algorithms as follows :

2.1 Throughput – Based Resource Allocation

In this scheme, the objectivity to be achieved is to maximize the aggregate system throughput with the total system power transmit constraints [1], [2], [3]. The Scheme with such objectivity can be achieved using the allocation of each subcarrier scheduling schemes to the users with best channel quality conditions and distributed power using water-filling algorithm. The algorithms this category is maximizing the total throughput of the system while supporting each users with its fixed rate [4]. The downside of this category is for users who experience the condition of propagation of poor quality, so that the fairness of each user is not awake. And when viewed from user's service point of view type that uses real-time service does not get priority. Scheduling scheme that can be used to maximize throughput is MAXSINR [5], where resources are allocated to the user with the best SINR. From the results of research [5] proved that, compared with Round-Robin scheme and the proportional fair scheduling scheme, By using MAXSINR scheduling will get a higher system throughput.

2.2 Fairness – Based Resource Allocation

In this scheme of objectivity to be achieved is to achieve a criterion of fairness between users. Fairness in resource allocation stating how the same resources are distributed to each user and always a trade off between fairness and throughput. Fairness can be stated in terms of different parameters - different. Fairness can be stated in terms of bandwidth allocation where each user get the same number of subcarriers [6], or it can be stated with power where each user get the same allocation of resources and can also be expressed with the same data rate [2]. In principle, fairness can express quality of service for each user. If objectivity is the proportionality of resource allocation among users, the optimization is called a constrained optimization with fairness [7]. In [7] also defined fairness index parameters in the term of proportional rate constraints with a maximum value of 1 which means that all users will achieve the same data rate (fairest case). Absolute Proportional fairness can be achieved using Max-Min Fairness (MMF) allocation which gives priority to the allocation of the user who has low-speed data or in other words MMF resource scheduling will give more priority to users who have the worst channel quality, so the throughput will be achieved will be equal to other users [2]. MMF scheduling scheme will maintain the fairness of each user but the throughput (spectral efficiency), the system will shrink. Allocation scheme that considers the fairness and throughput is Proportional Fair (PF) allocation. In this scheme combines MAXSINR and MMF, where the total system throughput will achieve the minimum requirements while maintaining fairness among users. In this scheme, resources are assigned to users Who Are Experiencing the best channel conditions [5].

2.3 Utility – Based Resource Allocation

In this scheme, the objectivity to be achieved is a utility function that will be used to quantify the benefits of usage of certain resources, which are used in utility theory to evaluate the level of communication networks ability to meet the needs of the user's service quality requirements. Utility also offers a tangible metric for network provisioning when application performance is the key concern. Utility in wireless resource allocation is used to build a bridge between physical layer and the MAC layer and to balance the efficiency and fairness to achieve cross-layer optimization [8].

To achieve the level of customer satisfaction and to managing resources and quality of services which are different, the utility function can be used as a key role. Application of traffic and different parameters may have different utility functions. Generally there are two approaches to obtain the utility function. The first approach for specific types of applications, the utility function can be obtained by sophisticated subjective surveys. Another approach is to design utility functions based

on the nature of traffic and in accordance with fairness. Optimization based on utility aims is to maximize utility on the system due to the limited ability of the physical layer. Note that in this optimization, constraints come only from physical layer. We put other constraints regarding Qos into the optimization objective utility functions through mathematical methods of the physical meanings of those constraints. This optimization has two advantages [8]:

- For new application, we need only change the corresponding utility function and still use the existing optimization structure is not changed
- Because the optimization constraints determine the system capacity region, this mechanism makes fairness, stability and quality of service tractable.

So, the most important decision to make in utility-based optimization problem is to choose the utility function properly according to the objective of the system. In [8], Song et al. has developed two radio resource allocation scheme based on utility. The scheme has been developed are Dynamic subcarrier allocation with fixed power allocation (DSA), Adaptive Power allocation with fixed subcarrier allocation (APA), and combining DSA and APA. In these studies include two scenarios on the rate of continuous (without changing modulation) and at the rate of discrete (discrete modulation).

3. General Model System

In general, modeling of the radio resource allocation in OFDMA systems can be modeled as follows:

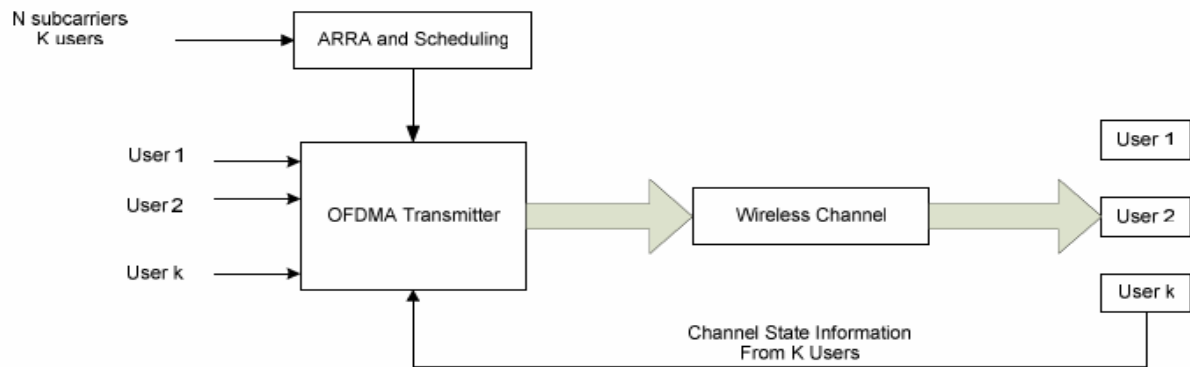


Fig 1. General model system in downlink resource allocation

The system consists of K users and N subcarriers, it is assumed the information CSI (Channel State Information) is already known and ARRA with the certain scheduling algorithm will work on the basis of channel state information submitted by a user. Throughput-based resource allocation can be modeled mathematically as follows [9]:

$$\max: R_T = \frac{B}{N} \sum_{k=1}^K \sum_{n=1}^N c_{k,n} \log_2 \left(1 + \frac{p_{k,n} h_{k,n}^2}{N_o \frac{B}{N}} \right)$$

Subject to :

$$C1: c_{k,n} \in \{0,1\}, \quad \forall k, n$$

$$C2: c_{k,n} = 1, \quad \forall n$$

$$C3: p_{k,n} \geq 0, \quad \forall k, n$$

$$C4: \sum_{k=1}^K \sum_{n=1}^N c_{k,n} p_{k,n} \leq P_{total}$$

$$C5: \text{User Rate Requirements}$$

(1)

The first two constraints (C1-C2) are on subcarrier allocation to ensure that each subcarrier is assigned to only one user. The next two constraints (C3 – C4) are on power allocation where P_{total} is the total transmit power of system. C5 is the user rate requirements.

While the Fairness-based resource allocation can be modeled mathematically as follows [7]:

$$\max: R_T = \frac{B}{N} \sum_{k=1}^K \sum_{n=1}^N c_{k,n} \log_2 \left(1 + \frac{p_{k,n} h_{k,n}^2}{N_o \frac{B}{N}} \right)$$

Subject to :

$$\text{C1: } c_{k,n} \in \{0,1\}, \quad \forall k, n$$

$$\text{C2: } c_{k,n} = 1, \quad \forall n$$

$$\text{C3: } p_{k,n} \geq 0, \quad \forall k, n$$

$$\text{C4: } \sum_{k=1}^K \sum_{n=1}^N c_{k,n} p_{k,n} \leq P_{\text{total}}$$

$$\text{C5: } R_1 : R_2 : \dots : R_K = \alpha_1 : \alpha_2 : \dots : \alpha_K \quad (2)$$

Objective of this allocation is to maximize the total rate within the total power constraint of the system while maintaining rate proportionality among the users indicated in C5. Here $\{\alpha_1, \alpha_2, \dots, \alpha_K\}$ is the set of predetermined proportional constraints where α_K is a positive real number with $\alpha_{\min} = 1$ for the user with the least required proportional rate.

Utility – based resource allocation used the concept of utility function $U(\cdot)$ to formulate the problem of resource allocation. Utility function maps the network resources a user into real number and is a function of the user's data rate. This problem is formulated as [8][9] :

$$\max: \sum_{k=1}^K U_k(R_k)$$

Subject to :

$$\text{C1: } S_i \cap S_j = \phi, \quad \forall i, j \in k, i \neq j$$

$$\text{C2: } \bigcup_k S_k \subseteq \{1, 2, \dots, N\}$$

$$\text{C3: } p_{k,n} \geq 0, \quad \forall k, n$$

$$\text{C4: } \sum_{k=1}^K \sum_{n=1}^N c_{k,n} p_{k,n} \leq P_{\text{total}} \quad (3)$$

Where $U_k(R_k)$ is the utility function for the k th user, R_k is user's data rate, S_k is the set of subcarriers assigned to user k for which $c_{k,n} = 1$ and $\bigcup_k S_k$ is the union of all subcarrier sets. The first two constraints ensure no sharing in subcarriers and the objective of this allocation is to maximize the sum utility within the power budget P_{total} .

4. Optimization Of Adaptif Radio Resource Allocation

Third radio resource allocation strategies above should be solved using optimization methods because there are constraints that must be met to achieve the objectivity of the allocation of resources. Optimization method which is used use three approaches: Relaxation method, problem splitting method and heuristics method

4.1 Relaxation – Optimization Method

This optimization method allows the allocation of the number of bits in each subchannel is not an integer, so the simpler the process of computing. By allowing non-integer numbers then the optimization problem turned into a problem Linear Programming (LP) and can be solved by more efficient. LP solution must be re-evaluated as the integer solutions are feasible only when viewed from the system's point of view. Usually this solution is done by giving back subchannel - subchannel to the user with the largest fraction of non-integer. The approach was first performed by Wong et al [10] [11].

4.2 Problem Splitting – Optimization Method

In this method, the optimization is divided into two processes, the first process is determining the amount required to meet the data rate requirements and the second process is the allocation of subchannels for certain users subchannel in which the determination was made per user by using the matching algorithm [11] [12]

4.3 Heuristics – Optimization Method

In this method, the optimization is based on the search procedure. One approach that has been done is by Kivanc et al [13]. In [13] determining the number of required user subchannel is done by greedy algorithm based on SINR (BABS Algorithm) and subchannel allocation algorithm is done by amplitude craving greedy (ACG Algorithm). The Simulations show that the power required using optimization BABS / ACG smaller than Wong relaxation, and more efficient computing 100 times than Wong Relaxation.

5. Research Opportunities

Cross layer design of an adaptive radio resource allocation and scheduling techniques in OFDMA systems offer many advantages. Among them achieve a balance between high throughput and fairness among users. Related to these advantages there are several related research opportunities that are still to be explored.

5.1 Utility Function Design for Specific Applications

Research which has be done by Song et al [8] introduce a utility function to link between the physical layer and MAC layer does not specify any particular type of real-time traffic (RT) or non real time (NRT). Opportunity to design a utility function, especially for real time traffic is still open for now due to the behavior of different traffic will impact the designs of different utility functions as well. In addition, there are also open to design a utility function for mixed applications (real-time and non real time).

5.2 Scheduler Design for Achieving Real-time Traffic QoS

Real time traffic scheduler schemes require modifications to achieve the QoS such as delay, packet drop and delay fairness between applications. Several studies have been conducted, scheduler design is only done to keep RT traffic but less NRT QoS traffic in a single system.

5.3 Joint Design of Adaptive Scheduler and Adaptive Radio Resource Allocation

Adaptive scheduler technique is done by adjusting the packet length and buffer length adaptively to achieve RT traffic delays are smaller. But the design of adaptive scheduler is still associated with limited power and subcarriers that existed at the Adaptive Radio Resource allocation.

5.4 Design Utility Function on Unperfect CSI Conditions

Research had been conducted, generally CSI information already available. This condition is difficult to be realized due to wireless channel conditions are susceptible to noise and multipath. It takes a certain utility function that can anticipate the CSI imperfection information by entering the channel mismatch factors to allocate the radio resources.

5.5 Utility Function Design in MIMO OFDMA System for Real Time Traffic

The future developments are to combine the scheme of OFDMA systems with MIMO (Multiple Input Multiple Output). Where the radio resources in MIMO_OFDMA systems are: Power, subcarriers and the number of transmit and receive antennas. Utility functions are needed to accommodate these limitations.

5.6 Design Of Adaptive Radio Resource Allocation Algorithm using Utility-Based in Multicell Conditions

Research on the ARRA-utility based on generally carried out at the single cell. By designing multicell conditions then the user who suffered a bad propagation condition (cell border) can perform cell selection procedure to the adjacent cell using cell selection strategies with utility approach - based. Users will camp on to a cell that has greater utility functions.

5.7 Design Low Complexity Algorithm using Utility-Based in Multicell Conditions

Design of resource allocation algorithm which is a function of the number of users and the number of subcarriers as well as limitations in physical layer will be more complex due to the increasing number of users and the number subcarrier. And so we need a algorithm scheme that low complexity while still achieving objectivity.

6. Conclusion

ARRA algorithm in OFDMA systems offer many advantages which can accommodate the problem of throughput and fairness as well as providing real-time and non real time. The limited radio resources in OFDMA systems is anticipated by implementation of utility-based allocation scheme and combining with a certain scheduling technique.

Utility functions needed to bridge the existing parameters in the physical layer (subcarriers, power) with the scheduling parameters to achieve optimality between the two layers so that objectivity can be achieved.

The research opportunities are open to design the utility functions in accordance with environmental conditions (single cells or multicell) and behavioral traffic (RT or NRT) and keep the user's QoS Among fairness and required also trade off between complexity and objectivity to be achieved

Acknowledgment

The first author is a lecturer in Telkom Institute of Technology Bandung and now pursuing his doctorate degree in University of Indonesia.

References

- [1] J. Jang and K.B.Lee, "Transmit Power power adaptation For multiuser OFDM systems," IEEE Journal on Selected Areas in Communications, vol. 21, no.2, pp 171 – 178, 2003
- [2] W.Rhee and J.M Cioffi, " Increase in capacity of multiuser OFDM system using dynamic subchannel allocation," in Proc. IEEE VTC, vol. 2, pp. 1085 – 1089, May 2000
- [3] E.B. Rodrigues and F Casadevall, " Adaptive Radio Resource Allocation Framework for Multi-User OFDM," IEEE VTC 2009

- [4] H. Yin and H. Liu, "An efficient multiuser loading algorithm for OFDM based broadband wireless System," in *proc.IEEE Globecom*, vol 1, pp 103 – 107, November 2000.
- [5] G. Miao and N Himayat, "Low complexity utility based resource allocation for 802.16 OFDMA Systems," in *Proc. WCNC 2008 pp 1465 - 1470*.
- [6] Y. Otani, S. Ohno, K. Ann Donny Teo, and T Hinamoto, "Subcarrier allocation for multiuser OFDM system," in *proc. Asia-pacific conference on communication.*, pp 1073-1077.
- [7] Z.Shen, J.G Andrews, and B.L Evans, "Adaptive resource allocation in multiuser OFDM systems with proportional rate constrains," in *IEEE Trans Wireless Commun.*, vol 4, pp 2726 – 2723, November 2005.
- [8] G.Song and Y.(G) Li, "Cross Layer Optimization for OFDM Wireless Network – Part I and Part II," in *IEEE Trans Wireless Commun.*, vol 4,no 2, pp 614 – 634, mar 2005.
- [9] S.Sadr, A Anpalagan, and K Raahemifar, "Suboptimal Rate Adaptive Resource Allocation for Downlink OFDMA Systems," in *EURASIP International Journal of Vehicular Technology.*, vol 2009.
- [10] C.Y. Wong, R.S. Cheng, K.B. Letaief, and R. Murch, "Multiuser OFDM with adaptive subcarrier, bit and power allocation," *IEEE Journal on Selected Areas of Communications*, vol. 17, no. 10, pp. 1747–1758, October 1999.
- [11] M. Bohge, J. Gross, M. Meyer, A Wolisz, "Dynamic Resource Allocation in OFDM System : An overview of cross layer optimization principles and techniques," *Telecommunication Networks Group, TU Berlin*, 2006.
- [12] A. Schrijver, *Combinatorial Optimization*, Springer, 2003.
- [13] D. Kivanc, G. Li, and H. Liu, "Computationally efficient bandwidth allocation and power control for OFDMA," *IEEE Transactions on Wireless Communications*, vol. 2, no. 6, pp. 1150–1158, Nov 2003.

Multiresolution Analysis Using Quaternion Matrix-Valued Wavelets

Mawardi Bahri

Department of Mathematics, Hasanuddin University, Makassar, Indonesia

E-mail: mawardibahri@gmail.com

Abstract

In this paper, we introduce quaternion matrix-valued wavelets using a complex representation of a quaternion matrix. We then formulate scaling and wavelet functions using quaternion matrix multiresolution analysis (QMMRA). With these formulations, we obtain coefficients of highpass and lowpass filters of QMMRA.

Keywords: quaternion matrix-valued wavelets; quaternion matrix multiresolution analysis; highpass and lowpass filters

1 Introduction

Recently, the extension of the theory of scalar-valued wavelets to the matrix-valued wavelets has been introduced in [1, 7] using the theory of paraunitary matrix filterbanks. This extension is not straightforward, mainly due to the inherent property of non-commutativity of matrix multiplications. Matrix-valued signals are often encountered in applications, such as video images, multispectral images and color images.

It is well-known fact that a quaternion matrix can be identified with a complex representation matrix (see e.g. [5] and the references therein). In this paper, we study matrix-valued wavelets of quaternion matrix-valued signals. We investigate scaling and wavelet functions using QMMRA. The Fourier transform in a complex representation matrix introduced in this paper is not the same with that in matrix-valued function of [2, 3].

The quaternion algebra over \mathbb{R} denoted by \mathbb{H} is an associative non-commutative four-dimensional algebra,

$$\mathbb{H} = \{q = q_0 + \mathbf{i}q_1 + \mathbf{j}q_2 + \mathbf{k}q_3 \mid q_0, q_1, q_2, q_3 \in \mathbb{R}\}, \quad (1)$$

which obey Hamilton's multiplication rules

$$\mathbf{i}\mathbf{j} = -\mathbf{j}\mathbf{i} = \mathbf{k}, \quad \mathbf{j}\mathbf{k} = -\mathbf{k}\mathbf{j} = \mathbf{i}, \quad (2)$$

and

$$\mathbf{k}\mathbf{i} = -\mathbf{i}\mathbf{k} = \mathbf{j}, \quad \mathbf{j}^2 = \mathbf{j}^2 = \mathbf{k}^2 = \mathbf{i}\mathbf{j}\mathbf{k} = -1. \quad (3)$$

The quaternion conjugate of a quaternion q is given by

$$\bar{q} = q_0 - \mathbf{i}q_1 - \mathbf{j}q_2 - \mathbf{k}q_3, \quad q_0, q_1, q_2, q_3 \in \mathbb{R}. \quad (4)$$

For any quaternion valued matrix $X = (x_{ij}) \in \mathbb{H}^{m \times n}$, the transpose of X is $X^T = (x_{ji}) \in \mathbb{H}^{n \times m}$; the conjugate transpose of X is $X^\dagger = (\overline{x_{ji}}) \in \mathbb{H}^{n \times m}$. A matrix $X = (x_{ij}) \in \mathbb{H}^{m \times n}$ is then called Hermitian if $X = X^\dagger$ and unitary if $XX^\dagger = X^\dagger X = I_n$.

Lemma 1 Let $X \in \mathbb{H}^{m \times n}$ and $Y \in \mathbb{H}^{n \times p}$ be given. Then

$$(i). \quad \overline{\overline{X}} = X, \quad (X^\dagger)^\dagger = X.$$

$$(ii). \quad (XY)^\dagger = Y^\dagger X^\dagger.$$

$$(iii). \quad (XY)^{-1} = Y^{-1}X^{-1}, \quad \text{if } X \text{ and } Y \text{ are invertible.}$$

$$(iv). \quad (\overline{X})^{-1} = \overline{(X^{-1})}, \quad (X^\dagger)^{-1} = (X^{-1})^\dagger, \quad \text{if } X \text{ is invertible.}$$

An arbitrary a quaternion valued matrix $X \in \mathbb{H}^{m \times n}$ can be written as [5]

$$X = X_1 + \mathbf{j}X_2, \quad (5)$$

where $X_1, X_2 \in \mathbb{C}^{m \times n}$ are complex matrices. We note that equation (5) has the complex representation (the quaternionic adjoint matrix) noted γ_X of the form

$$\gamma_X = \begin{pmatrix} X_1 & -\bar{X}_2 \\ X_2 & \bar{X}_1 \end{pmatrix}. \quad (6)$$

2 Notations on Quaternion Matrix-Valued Spaces

Let

$$L^2(\mathbb{R}, \mathbb{C}^{2m \times 2m}) = \left\{ \Phi(x) = \begin{pmatrix} \phi_1(x) & -\bar{\phi}_2(x) \\ \phi_2(x) & \bar{\phi}_1(x) \end{pmatrix} \right\}, \quad (7)$$

denotes the space of quaternion matrix-valued functions defined on \mathbb{R} with values in $\mathbb{C}^{2m \times 2m}$.

The matrix Fourier transform Φ on \mathbb{R} is then defined by

$$\hat{\Phi}(\omega) = \int_{\mathbb{R}} \Phi(x) D(e^{-i\omega x}, e^{i\omega x}) dx, \quad (8)$$

where $D(e^{-i\omega x}, e^{i\omega x})$ is a $2m \times 2m$ diagonal matrix. The inverse of the above matrix Fourier transform is given by

$$\Phi(x) = \frac{1}{2\pi} \int_{\mathbb{R}} \hat{\Phi}(\omega) D(e^{i\omega x}, e^{-\omega x}) d\omega, \quad (9)$$

By inserting (8) to (7) we immediately obtain

$$\hat{\Phi}(\omega) = \begin{pmatrix} \int_{\mathbb{R}} \phi_1(x) e^{-i\omega x} dx & -\int_{\mathbb{R}} \bar{\phi}_2(x) e^{i\omega x} dx \\ \int_{\mathbb{R}} \phi_2(x) e^{-i\omega x} dx & \int_{\mathbb{R}} \bar{\phi}_1(x) e^{i\omega x} dx \end{pmatrix} \quad (10) \quad (ii).$$

or

$$\hat{\Phi}(\omega) = \begin{pmatrix} \hat{\phi}_1(\omega) & -\bar{\hat{\phi}}_2(\omega) \\ \hat{\phi}_2(\omega) & \bar{\hat{\phi}}_1(\omega) \end{pmatrix}. \quad (11) \quad (iii).$$

It is convenient to introduce the inner product of two quaternion matrix-valued functions $\Phi, \Psi \in L^2(\mathbb{R}, \mathbb{C}^{2m \times 2m})$ as follows

$$\langle \Phi, \Psi \rangle = \int_{\mathbb{R}} \Phi(x) \Psi^\dagger(x) dx. \quad (12)$$

Note that the inner product (12) is not inner product in the common sense that requires to be real-valued.

We say that the scaling function $\Phi(x) \in L^2(\mathbb{R}, \mathbb{C}^{2m \times 2m})$ is orthonormal if

$$\langle \Phi(\cdot - k_1), \Phi(\cdot - k_2) \rangle = \delta_{k_1, k_2} I_{2m}, \quad \forall k_1, k_2 \in \mathbb{Z}, \quad (13)$$

where δ_{k_1, k_2} is Kronecker symbol and I_{2m} is the $2m \times 2m$ identity matrix.

3 Quaternion Matrix-Valued Multiresolution Analysis

In this section, we introduce quaternion matrix-valued multiresolution analysis (QMMRA).

Definition 1 We say that the quaternion matrix of function $\Phi \in L^2(\mathbb{R}, \mathbb{C}^{2m \times 2m})$ generates a quaternion matrix-valued multiresolution analysis (QMMRA) if the subspaces

$$V_j = \text{span}\{2^{-j/2} \Phi(2^{-j}x - k) : k \in \mathbb{Z}\}$$

are nested,

$$\dots \subset V_{-2} \subset V_{-1} \subset V_0 \subset V_1 \subset V_2 \dots$$

such that the following four axioms are satisfied:

(i). The space $L^2(\mathbb{R}; \mathbb{C}^{2m \times 2m})$ is the closure of the union of all V_j and the intersection of all V_j is empty, i.e.

$$\overline{\bigcup_{j \in \mathbb{Z}} V_j} = \overline{\lim_{j \rightarrow \infty} V_j} = L^2(\mathbb{R}; \mathbb{C}^{2m \times 2m}), \quad (14)$$

and

$$\bigcap_{j \in \mathbb{Z}} V_j = \lim_{j \rightarrow -\infty} V_j = \{\mathbf{0}\}. \quad (15)$$

$$X(x) \in V_j \Leftrightarrow X(2x) \in V_{j+1}, j \in \mathbb{Z}. \quad (16)$$

(ii). There exists a function $\Phi(x) \in V_0$ such that

$$\{\Phi(x - k), k \in \mathbb{Z}\} \quad (17)$$

is an orthonormal basis in V_0 . The function $\Phi(x)$ is called a quaternion matrix-valued scaling function.

Since $V_0 \subset V_1$, any function in V_0 can be expanded in terms of the basis functions $\Phi_{1,k} = \sqrt{2} \Phi(2x - k)$ of V_1 . In particular, the scaling function $\Phi \in V_0$ can be expanded in terms of $\{\Phi_{1,k}\}$ as

$$\Phi(x) = \sqrt{2} \sum_k H_k \Phi(2x - k), \quad (18)$$

where H_k are constant matrices. Equation (18) is called a quaternion matrix-valued dilation equation.

Lemma 2 The scaling coefficients $\{H_k\}$ of equation (18) satisfies the normality condition, i.e.

$$\sum_k H_k H_{k-2l}^\dagger = I_{2m} \delta_{0l}, \quad \forall l \in \mathbb{Z}. \quad (19)$$

Proof. Notice first that by repeated applications of Equation (23) follows from (18) we have

$$\begin{aligned} \Phi(x)\Phi^\dagger(x-l) &= \sqrt{2} \sum_k H_k \Phi(2x-k)\Phi^\dagger(x-l) \\ &= 2 \sum_k H_k \Phi(2x-k) \\ &\quad \times \left(\sum_m H_m \Phi(2x-2l-m) \right)^\dagger. \quad (20) \end{aligned}$$

$$\begin{aligned} \hat{\Phi}(\omega) &= \int_{\mathbb{R}} \Phi(x) D(e^{-i\omega x}, e^{i\omega x}) dx \\ &\stackrel{(18)}{=} \sum_k \sqrt{2} H_k \int_{\mathbb{R}} \Phi(2x-k) D(e^{-i\omega x}, e^{i\omega x}) dx \\ &= \sum_k \frac{H_k}{\sqrt{2}} D(e^{-\frac{i\omega}{2}}, e^{\frac{i\omega}{2}}) \int_{\mathbb{R}} \Phi(2x-k) \\ &\quad \times D(e^{-i(2x-k)\frac{\omega}{2}}, e^{i(2x-k)\frac{\omega}{2}}) d(2x-k) \\ &\stackrel{(9)}{=} \sum_k \frac{H_k}{\sqrt{2}} D(e^{-\frac{i\omega}{2}}, e^{\frac{i\omega}{2}}) \hat{\Phi}\left(\frac{\omega}{2}\right) \\ &= m_0\left(\frac{\omega}{2}\right) \hat{\Phi}\left(\frac{\omega}{2}\right). \quad (24) \end{aligned}$$

By integrating both sides of (20) with respect to x we get

$$\begin{aligned} I_{2m} \delta_{0l} &= 2 \sum_k H_k \left(\sum_m \frac{1}{2} \int_{\mathbb{R}} \Phi(2x-k)\Phi^\dagger(2x-2l-m) d(2x) H_m^\dagger \right) \\ &= \sum_k \sum_m H_k I_{2m} \delta_{k,2l+m} H_m^\dagger \\ &= \sum_k H_k H_{k-2l}^\dagger. \quad (21) \end{aligned}$$

This completes the proof of (19).

Let us define

$$m_0(\omega) = \sum_k \frac{H_k}{\sqrt{2}} D(e^{-ik\omega}, e^{ik\omega}). \quad (22)$$

If m_0 is a 2π -periodic function in $L^2(\mathbb{R}, \mathbb{C}^{2m \times 2m})$, the function m_0 is called the *lowpass filter* associated with the quaternion matrix-valued scaling function Φ . The dilation equation (18) becomes

$$\hat{\Phi}(\omega) = m_0\left(\frac{\omega}{2}\right) \hat{\Phi}\left(\frac{\omega}{2}\right). \quad (23)$$

Without loss of generality we assume $\Phi(0) = I_{2m}$, iterating (23) leads to

$$\hat{\Phi}(\omega) = m_0\left(\frac{\omega}{2}\right) m_0\left(\frac{\omega}{4}\right) \cdots = \prod_{n=1}^{\infty} m_0\left(\frac{\omega}{2^n}\right). \quad (25)$$

The above equation implies

$$m_0(0) = I_{2m}, \quad \sum_k H_k = \sqrt{2} I_{2m}. \quad (26)$$

Similarly, according to (18) we have the *quaternion matrix-valued wavelet equation*

$$\Psi(x) = \sqrt{2} \sum_{k \in \mathbb{Z}} G_k \Phi(2x-k), \quad (27)$$

□ for some $2m \times 2m$ matrices $\{G_k\}_{k \in \mathbb{Z}}$.

Lemma 3 *If the integer translated quaternion matrix-valued wavelet functions $\Psi(x-l)$ form an orthonormal, we have*

$$\sum_k G_k G_{k-2l}^\dagger = I_{2m} \delta_{0l}. \quad (28)$$

We define the highpass filter

$$m_1(\omega) = \sum_k \frac{G_k}{\sqrt{2}} D(e^{-i\omega x}, e^{i\omega x}), \quad (29)$$

where m_1 is also a 2π -periodic function. The Fourier transform of the wavelet equation (27) becomes therefore

$$\hat{\Psi}(\omega) = m_1\left(\frac{\omega}{2}\right) \hat{\Phi}\left(\frac{\omega}{2}\right). \quad (30)$$

Lemma 4 The quaternion matrix-valued scaling function $\Phi(x)$ is orthonormal if and only if

$$\sum_{l=-\infty}^{\infty} \hat{\Phi}(\omega + 2\pi l) \hat{\Phi}^\dagger(\omega + 2\pi l) = I_{2m}. \quad (31)$$

In terms of m_0 (31) has the form

$$m_0(\omega) m_0^\dagger(\omega) + m_0(\omega + \pi) m_0^\dagger(\omega + \pi) = I_{2m}. \quad (32)$$

Proof. Using the inverse matrix Fourier transform (9) gives ($k \in \mathbb{Z}$)

$$\begin{aligned} & \delta_{k,0} I_{2m} \\ &= \int_{\mathbb{R}} \Phi(x) \Phi^\dagger(x-k) dx \\ &= \int_{\mathbb{R}} \left(\frac{1}{2\pi} \int_{\mathbb{R}} \hat{\Phi}(\omega) D(e^{i\omega x}, e^{-i\omega x}) d\omega \right) \Phi^\dagger(x-k) dx \\ &= \frac{1}{2\pi} \int_{\mathbb{R}} \hat{\Phi}(\omega) \int_{\mathbb{R}} \left(\Phi(x-k) D(e^{-i\omega(x-k)}, e^{i\omega(x-k)}) \right)^\dagger \\ & \quad \times d(x-k) D(e^{i\omega k}, e^{-i\omega k}) d\omega \\ &= \frac{1}{2\pi} \int_{\mathbb{R}} \hat{\Phi}(\omega) \hat{\Phi}^\dagger(\omega) D(e^{i\omega k}, e^{-i\omega k}) d\omega \\ &= \frac{1}{2\pi} \int_0^{2\pi} \sum_{l=-\infty}^{\infty} \hat{\Phi}(\omega + 2\pi l) \hat{\Phi}^\dagger(\omega + 2\pi l) \\ & \quad \times D(e^{i\omega k}, e^{-i\omega k}) d\omega. \end{aligned} \quad (33)$$

Since the $k = 0$ coefficient of $\sum_{l=-\infty}^{\infty} \hat{\Phi}(\omega + 2\pi l) \hat{\Phi}^\dagger(\omega + 2\pi l)$ equals I_{2m} and all the other coefficients are zero matrix, this implies that

$$\sum_{l=-\infty}^{\infty} \hat{\Phi}(\omega + 2\pi l) \hat{\Phi}^\dagger(\omega + 2\pi l) = I_{2m}.$$

Therefore (31) in Lemma 4 was proved.

Inserting (23) into the left-hand side of (31) and separating the even and odd integer terms give

$$\begin{aligned} & \sum_{l=-\infty}^{\infty} \hat{\Phi}(\omega + 2\pi l) \hat{\Phi}^\dagger(\omega + 2\pi l) \\ &= \sum_{l=-\infty}^{\infty} m_0\left(\frac{\omega + 2\pi l}{2}\right) \hat{\Phi}\left(\frac{\omega + 2\pi l}{2}\right) \\ & \quad \left(m_0\left(\frac{\omega + 2\pi l}{2}\right) \hat{\Phi}\left(\frac{\omega + 2\pi l}{2}\right) \right)^\dagger \\ &= \sum_{l=-\infty}^{\infty} m_0(\omega + \pi l) \hat{\Phi}(\omega + \pi l) \hat{\Phi}^\dagger(\omega + l) m_0^\dagger(\omega + \pi l) \\ &= \sum_{k=-\infty}^{\infty} m_0(\omega + 2\pi k) \hat{\Phi}(\omega + 2\pi k) \\ & \quad \times \hat{\Phi}^\dagger(\omega + 2\pi k) m_0^\dagger(\omega + 2\pi k) + \\ & \quad \sum_{k=-\infty}^{\infty} m_0(\omega + (2k+1)\pi) \hat{\Phi}(\omega + (2k+1)\pi) \\ & \quad \times \hat{\Phi}^\dagger(\omega + (2k+1)\pi) m_0^\dagger(\omega + (2k+1)\pi). \end{aligned} \quad (34)$$

According to (22), $m_0(\omega)$ is 2π -periodic. Therefore

$$\begin{aligned} & \sum_{l=-\infty}^{\infty} \hat{\Phi}(\omega + 2\pi l) \hat{\Phi}^\dagger(\omega + 2\pi l) \\ &= m_0(\omega) \sum_{k=-\infty}^{\infty} \hat{\Phi}(\omega + 2\pi k) \hat{\Phi}^\dagger(\omega + 2\pi k) m_0^\dagger(\omega) + \\ & \quad m_0(\omega + \pi) \sum_{k=-\infty}^{\infty} \hat{\Phi}(\omega + 2\pi k) \\ & \quad \times \hat{\Phi}^\dagger(\omega + 2\pi k) m_0^\dagger(\omega + \pi). \end{aligned} \quad (35)$$

Using (31) we finally obtain

$$m_0(\omega) m_0^\dagger(\omega) + m_0(\omega + \pi) m_0^\dagger(\omega + \pi) = I_{2m}.$$

This proves (32). \square

4 Conclusion

Using the basic concepts of a complex representation of a quaternion matrix and its Fourier transform we introduced quaternion-valued wavelets. We then constructed quaternion-valued multiresolution analysis. Using the spectral representation of the Fourier transform, we derived several important properties such as the highpass and lowpass filters. \square

References

- [1] A. T. Walden and A. Serroukh, Wavelet Analysis of Matrix-Valued Times-series, Proc. R. Soc. Lond. A 458 (2002), 157-179.
- [2] L. Cui, B. Zhai and T. Zhang, Existence and Design of Biorthogonal Matrix-Valued Wavelets, Nonlinear Analysis, 10 (5) (2009), 2679-2687.
- [3] J. Han, Z. Cheng and Q. Chen, A Study of Biorthogonal Multiple Vector-Valued Wavelets, Chaos, Soliton and Fractals, 40 (4) (2009), 1574-1587.
- [4] P. Zhao, G. Liu and C. Zhao, A Matrix-Valued Wavelet KL-Like Expansion for Wide-Sense Stationary Random Processes, IEEE Transaction on Signal Processing 52 (4) (2004), 914-920.
- [5] F. Zhang, Quaternion and Matrices of Quaternions, Linear Algebra and its applications, 251 (1997), 21-57.
- [6] J. X. He and B. Yu, Wavelet Analysis of Quaternion-Valued Times-series, International Journal of Wavelet, Multiresolution and Information Processing 3(2) (2005), 233-346.
- [7] X. G. Xia and B. W. Sutter, Vector-Valued Wavelets and Vector Filter Banks. IEEE Transaction on Signal Processing 44(3), 508-518 (1996)
- [8] E. B. Corrochano, The Theory and Use of the quaternion wavelet transform. Journal of Mathematical Imaging and Vision 24(1), 19-35 (2006)
- [9] J. B. Kuipers, Quaternions and Rotation Sequences, Princeton University Press, NJ (1999)
- [10] S. Mallat, A Wavelet Tour of Signal Processing, second ed., Academic Press, San Diego, CA (1999)
- [11] B. Mawardi, E. Hitzer, A. Hayashi and R. Ashino, *An Uncertainty Principle for Quaternion Fourier Transform*, Comput. Math. Appl. 56(9)(2008), 2411-2417.
- [12] B. Mawardi and E. Hitzer, *Clifford Algebra $Cl_{3,0}$ -Valued Wavelet Transformation, Clifford Wavelet Uncertainty Inequality and Clifford Gabor Wavelets*, Int. J. Wavelets Multiresolut. Inf. Process., 5(6)(2007), 997-1019.
- [13] B. Mawardi, E. Hitzer, R. Ashino and R. Vailancourt, Windowed Fourier transform of two-dimensional quaternionic signals, Applied Mathematics and Computation, 216(8), 2366-2379 (2010).

Digital Image Compression using Quantization Method

Armin Lawi¹ and Hendra²

Department of Mathematics, Hasanuddin University
Jl. Perintis Kemerdekaan Km. 10, Makassar 90245, INDONESIA

¹armin@unhas.ac.id, ²hendra@unhas.ac.id

Abstract. A digital image (or an image) has some important information contents that adversely make its file has a big size and thus causing a problem in storing and dispatching. Therefore, it is necessary to compress or reduce the file size of an image. A quantization approach is one method in compressing huge file size of an image and it is effectively decreasing the number of colors in an image. This paper uses the quantization method with two clustering methods, i.e., *k*-means and *k*-medoid. These two methods based on determining the closest properties of data which is classified the data into a same cluster. The methods have been tested and analyzed with some images that have color characteristics variably. Our result shows that the two methods can compress the file size of an image without unnecessary changes in the visual information of the original or host image.

Keywords: Clustering, *k*-means, *k*-medoid, color pallete, quantization, image compression.

1. Introduction

Digital image (or image) is a vital thing and has being an integral part of our life. In some occasions, image can be used as a tool in showing a reason, interpretation, illustration, representation, memory, education, communication, evaluation, navigation, survey, entertainment, and so on. An image has important information inside, therefore its file size is usually large and it causes problems in storing and sending, i.e., it needs big size of storage and takes some times in delivering. Therefore, it is necessary to compress the file size of an image in order to reduce its size without losing visual information inside the image.

Quantization is a simple and effective approach in compressing the number of colours in an image. It guarantees the colour in the resulted image can be controlled and will not different with the original image. Using the decreasing number of colours into some certain clusters, the size file of an image can be compressed.

In this paper, we study two data clustering methods, i.e., *k*-means and *k*-medoid, which are used to quantize the colour in an image so that the size can be compressed. The two methods utilize a group of data with the same characteristic is classified into a same group such that all members in each partition has their similarity according to an arbitrary matrix. The basic idea in these methods is to determine the measurement of property closest between data in order to classify them into the same cluster.

2. Fundamentals

2.1. Color Quantization

The type of quantization which is commonly used is the uniform quantization and minimum variance quantization. In uniform quantization, colours in RGB are uniformly divided into the same size, whereas in the minimum variance quantization, the colours are divided into small groups with different sizes depend on the colour distribution in the image. For some given colours, minimum variance quantization gives better result than the uniform one since its quantization are processed based on the actual data (Wijaya M. Ch dan Prijono A, 2007).

While processing the quantization, we can apply a tolerance function in order to determine the size of color pieces. For instance, we can specify the 0.1 tolerance of the end color area which is cut in ten pieces of the length of RGB color area. The number of color areas can be given as follows.

$$n = (\lfloor 1 / \text{tol} \rfloor + 1)^3 \quad (1)$$

Each color area represents a color in the output image. Therefore, the maximum colormap length in the ouput image is n . We can also hide the colors which are not appear in the original image so that the length can actually less than n (Wijaya M. Ch dan Prijono A, 2007).

2.2. Peak Signal to Noise Ratio (PSNR)

Fidelity measurement of an image can be evaluated using Mean Squared Error (MSE) and Peak Signal to Noise Ratio (PSNR). MSE and PSNR can be calculated using the equations (2) and (3), respectively. In the equation (2), $I(x, y)$ and $I'(x, y)$ are the grey level of original and output image, respectively, in the position (x, y) . X and Y are, respectively, length and width of the image. In the equation (3), m is the possible maximum value of the image. For instance, the maximum value of 8 bit image is 255 (Fahmi, 2008).

$$MSE = \frac{1}{XY} \sum_x \sum_y [I(x, y) - I'(x, y)]^2 \quad (2)$$

$$PSNR = 10 \log \frac{m^2}{MSE} \quad (3)$$

For 24 bit image, PSNR is the same with 8 bit image, however, its MSE is calculated with the average of summation of the three components using the equation (4).

$$PSNR = 10 \cdot \log_{10} \left(\frac{m^2}{\frac{MSE(R) + MSE(G) + MSE(B)}{3}} \right) \quad (4)$$

3. Clustering Methods

We use two cluster methods as the building blocks, i.e., the k -means and k -medoid. The two methods work as follows.

3.1. k -Means Algorithm

Basically, k -means works in two steps; i.e., detecting center and searching members of each cluster. Let k is an integer number, and then k -means algorithm works as follows.

1. Determine k clusters with randomly initial clusters are Z_1, Z_2, \dots, Z_k of n points X_1, X_2, \dots, X_n .
2. Initiate k to cluster centers (that can be randomly selected) and marks points $X_i, i = 1, 2, \dots, n$, into cluster $C_j, j \in \{1, 2, \dots, k\}$, if $\|X_i - Z_j\| < \|X_i - Z_p\|, p = 1, 2, \dots, k$ and $j \neq p$.
3. Evaluate the new cluster centers $Z_1^*, Z_2^*, \dots, Z_k^*$ with $Z_i^* = \frac{1}{n_i} \sum_{X_j \in C_i} X_j, i = 1, 2, \dots, k$

where, n_i is the number of elements belong to cluster C_i .

4. Check all data and put them into the nearest center (and the cluster center is not evaluated again). If $Z_i^* = Z_i, i = 1, 2, \dots, k$ the process is terminated, otherwise back to step 2.

Note that k -means may not be converged to non-optimal value (Nur H. W dan Badriyah T, 2005).

3.2. k -Medoid Algorithm

k -Medoid or Partition Around Medoids (PAM) works well for small number of data but it is not good for large data. k -medoid places points in a cluster as initial points. While searching some clusters, k -medoid try to determine a representative object called *medoid*. When a medoid is determined, all objects that are not medoid anymore are grouped into most similar medoid.

Let n objects are given with p variables that want to be classified into k ($< n$) clusters. Suppose we define variable j and object i as X_{ij} ($i = 1, \dots, n; j = 1, \dots, p$), k -medoid works as follows [5].

1. Using Euclidean distance as the difference measure, evaluate distance between parts of all object as

$$\text{the following equation, } d_{ij} = \sqrt{\sum_{\alpha=1}^p (X_{i\alpha} - X_{j\alpha})^2}, i = 1, 2, \dots, n; j = 1, 2, \dots, n.$$

2. Evaluate p_{ij} to determine initial cluster center using, $p_{ij} = \frac{d_{ij}}{\sum_{i=1}^n d_{il}}, i = 1, 2, \dots, n; j = 1, 2, \dots, n.$

3. Evaluate $\sum_{i=1}^n p_{ij}$ of all object and their increasing order with $j = 1, 2, \dots, n$. Select object k which has a minimum value as the initial medoid.
4. Search data of each object cluster to the nearest medoid.
5. Mark the cluster position of the k medoid. If most similar medoid has been found then terminate, otherwise repeat steps 2 and 3 until the nearest medoid is found.

4. Result and Comparison Analysis

The k -means and k -medoid cluster algorithms have been implemented to the images in Figure 2. This section presents our testing and analysis for all host images in Figure 1.

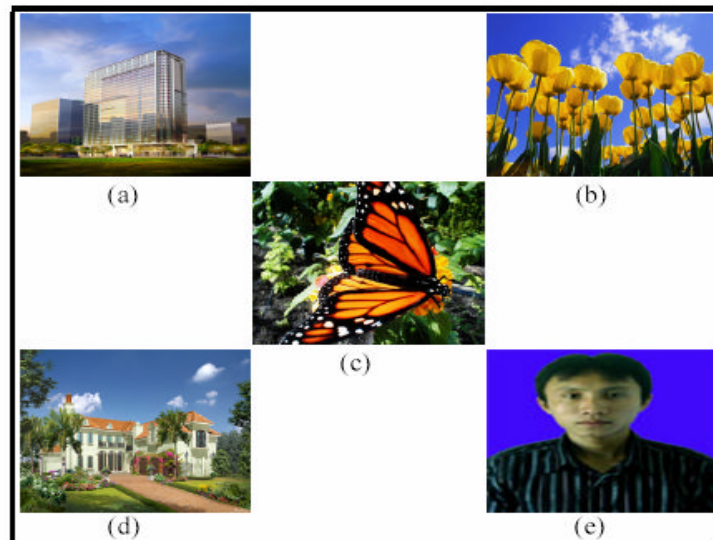


Figure 1. (a) Building.bmp, (b) Tulips.bmp, (c) Butterfly.bmp, (d) House.bmp, (e) Picture.bmp

Host images in Figure 7 are saved in BMP format with dimension 256×256 pixels. Clustering k -means and k -medoid are applied to the host images. The numbers of color neighbour for the testing are 5, 20 and 100. These color neighbors are used to analyze the comparison of resulted images using k -means and k -medoid

4.1. Number of Iterations

Comparisons of the number of iteration for both two algorithms are given in Figure 2.

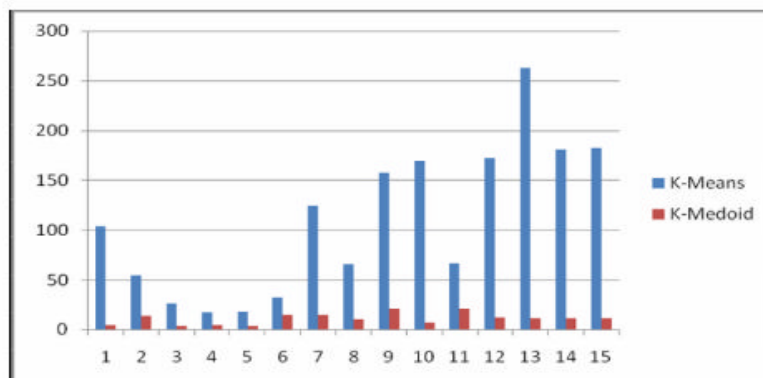


Figure 2. Bar Diagram of Iteration Comparison of K -Means and K -Medoid

4.2. File Size Comparisons

After implementing the two quantization methods to the host images, the size of files are compressed. Table 1 shows the decreasing size of files of the host images.

Table 1. Comparison changes of file size with initial size 192 KB

Neighbors Color	Host Images	k -Means	k -Medoid
5	Building.bmp	4.91 KB	4.57 KB
	Tulips.bmp	7.66 KB	7.82 KB
	Butterfly.bmp	9.57 KB	10.5 KB
	House.bmp	8.27 KB	8.38 KB
	Picture.bmp	4.26 KB	5.02 KB
20	Building.bmp	11.0 KB	11.1 KB
	Tulips.bmp	17.1 KB	17.9 KB
	Butterfly.bmp	19.9 KB	21.2 KB
	House.bmp	17.4 KB	17.8 KB
	Picture.bmp	10.2 KB	12.4 KB
100	Building.bmp	22.3 KB	22.4 KB
	Tulips.bmp	34.9 KB	36.3 KB
	Butterfly.bmp	40.3 KB	41.7 KB
	House.bmp	33.6 KB	34.1 KB
	Picture.bmp	24.7 KB	25.1 KB

4.3. Image Quality

PSNR is used to measure the quality of the reconstructed images compare to their host. The higher PSNR value means the reconstructed image did not cause necessary decreasing to the host image. Based on our result which is given in Figure 3, it can be seen that PSNR values of k -means and k -medoid are nearly the same.

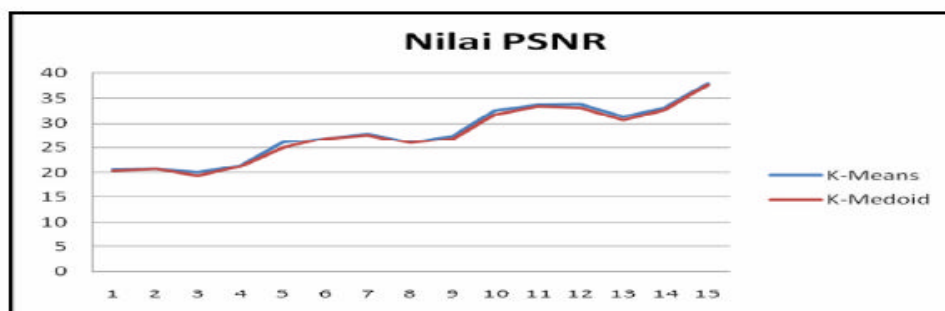


Figure 3. Comparison of PSNR values of k -means and k -medoid

References

- [1] Andi S. B., and Herman P. *Tips dan Konsep Konversi Warna*. Forum Grafika Digital. <http://www.xgdigital.com/index.php/2007112130/news/latest/tips>, 2009.
- [2] Andrianto, Heri, and Agus Prijono. *Menguasai Matriks dan Vektor*. Bandung: Rekayasa Sains, July 2006.
- [3] Castleman, K.R., *Digital Image Processing*. Prentice Hall, Englewood Clift, 2006.
- [4] Fahmi. *Studi dan Implementasi Watermarking Citra Digital dengan Menggunakan Fungsi Hash*. Sekolah Teknik Elektro dan Informatika, Institut Teknologi Bandung, 2008.
- [5] Hsiu-Hui Lee dan Shih-Chieh Lo, *A Method For Performing Color Reduction In Index Images*. Dept. Computer Science and Information Eng., National Taiwan University. Taipei, Taiwan, 2004.
- [6] Jiawei, H., Kamber, M. *Data Mining Concepts and Techniques*, Morgan Kaufmann, 2001
- [7] Marvin Ch. Wijaya dan Agus Prijono. November 2007. *Pengolahan Citra Digital Menggunakan Matlab*. Informatika Bandung, 2007.
- [8] Nur Hana Wijaya dan Tessy Badriyah. *Segmentasi Data Pemasaran Menggunakan Algoritma G-Kmeans*. Institut Teknologi Sepuluh Nopember. Surabaya, July 2005.

Time Reduction In Encrypting And Decrypting With Rsa Algorithm Using Distributed Computing

Jhonsong Hoya¹ and Armin Lawi²

¹Department of Informatics Engineering, STMIK Kharisma Makassar, Jl. Baji Ateka No. 20, Makassar

²Department of Mathematics, Hasanuddin University, Jl. Perintis Kemerdekaan Km. 10, Makassar

I. INTRODUCTION

One technique for securing data is to encrypting it. Data encryption is a way of encoding in which data's characters in file is encoded so that it doesn't have any mean to others [1]. While effort to restore data's characters that have been encoded in its original state based on its encryption rule is called decryption. There's a lot of encryption algorithm in use today such as Data Encryption Standard (DES), IDEA, and RSA. In encoding the data, encryption algorithm involves computing process both arithmetic operations and logic operations. For data in small size, encryption process will be done fast enough. Instead of data in huge size or even massive size, the encryption process will have more time to be done. From the earliest test we have done, we got a data as result from encrypting and decrypting in serial test. That referred to Table 1 (a table of testing result for encrypting and decrypting in serial).

TABLE I. TABLE TESTING RESULT FOR ENCRPTING AND DECRYPTING IN SERIAL

TESTING			
KEY (bit)	SIZE (KB)	TIME (minutes)	
		ENCRYPT	DECRYPT
1,024	207	0.01871	0.21371
1,024	512	0.03978	0.53195
1,024	1,040	0.07463	1.09070
1,024	2,089	0.14768	2.19821
1,024	5,132	0.33903	5.29725
1,024	10,180	0.67001	10.57082
2,048	207	0.02833	0.71708
2,048	512	0.05903	1.74901
2,048	1,040	0.11570	3.61115
2,048	2,089	0.22516	7.07922
2,048	5,132	0.54600	17.49470
2,048	10,180	1.06911	34.83820
4,096	1,040	0.20436	13.26713

Data in Table 1 was tested using Intel Core 2 Duo processor with clock speed 2.10 GHz. It marked red in a key with 1024 bit length and the file size is "1040 KB", the time for encrypting is approximately "0.075 minutes" and the time for decrypting is approximately "1.019 minutes".

From Table 1 as testing result, there is a fact that increment of key length or file size may cause more time to complete the process. To perform encryption and decryption for small file size is not take a long time. But it

is different if file with huge size will be encrypted or decrypted cause take a slightly long time. So we suggest reducing encryption and decryption time in RSA algorithm using distributed computing.

Distributed computing is a part of parallel computing which puts the parts of program separately into more than one computer and run the programs simultaneously to perform a particular job [2]. The goal is to accelerate processing time or computing time.

II. THEORY

A. RSA Algorithm

Key generation:

- Generate two large prime integers, p and q
- Calculate $m = (p-1)*(q-1)$
- Calculate $n = p*q$
- Choose e which relatively prime to m
- Find d , so that $e*d = 1 \text{ mod } (m)$, or $d = (1+nm)/e$
- Public key: (e,n)
- Private key: (d,n)

For example, BB encrypts message M to AA. Steps that BB must be done like this:

- Get AA's authentic public key (e,n)
- Represent message M in the interval $[0, n-1]$
- Calculate $C = (M^e) \text{ mod } n$
- Send C to AA

To decrypt, AA should be use private key d to produce $M = (C^d) \text{ mod } n$

Application example: here i select a small number for easier calculation. But in real application select large prime numbers to improve security.

$$p = 3$$

$$q = 11$$

$$n = 3 * 11 = 33$$

$$m = (3-1)*(11-1) = 20$$

$$e = 2 \Rightarrow \text{gcd}(e,20) = 2$$

$$e = 3 \Rightarrow \text{gcd}(e,20) = 1 \text{ (yes)}$$

$$n = 0 \Rightarrow e = 1/3$$

$$n = 1 \Rightarrow e = 21/3 = 7 \text{ (yes)}$$

$$\text{public key: } (3,33)$$

$$\text{private key: } (7,33)$$

checking the numbers, try to encrypt the plain text "2", $C = (2^3) \text{ mod } 33 = 8$. Try to decrypt the chiper text "8", $M = (8^7) \text{ mod } 33 = 2097152 \text{ mod } 33 = 2$.

B. Distributed Computing

Distributed computing is a method of computer processing in which the parts of different programs running simultaneously on two or more computers that communicate with each other in the network [3]. Distributed computing is a part of parallel computing , parallel computing is a method of processing on

computer where the parts of different programs running simultaneously on two or more computers and those computers communicate with each other via a network to accomplish a particular job. Huge computational process is divided into several sections and these parts are distributed to a number of computer node (often called a worker) in the network to be completed, the processing result in node is returned to propagator (often called a manager).

The reverse of distributed computing is centralized computing, where there are computer and software doing requested computation process from connected client, so that centralized computing burden server's performance as a result server require the great resources.

The main purpose of distributed computing is to improve computation performance. The more things can be done simultaneously, the more work that can be resolved. The easiest analogy is if you can boil water while chopping onions when you are cooking, you would need time less than if you do these things by sequence/serial.

Performance in distributed computing is measured by how much increase in speed (speed up) obtained in using parallel technique. Informally, if you cut the onions alone takes 1 hour and with the help of friend, both of you can done it in half hour then you gain a speed by 2 times.

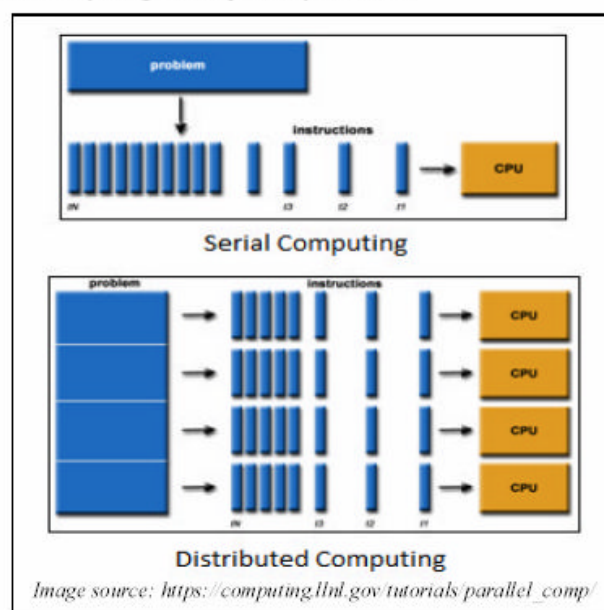


Figure 1. Comparison of serial and distributed

There are limits in an effort to create a computer program run more efficiently through increased speed, known as Amdahl law. The idea is that we only be able to improve the efficiency of computer programs limits to certain parts of program, which can be parallel. Then the part that have to be done by sequence will determine final performance.

C. Java Socket

Java programming language provides socket classes in java.net package. These socket classes are used to represent the connection between a client program and a server program [5]. Java.net package provides two main class, there are Socket class that is implemented by the client and Server Socket class that is implemented by the server program. The following important steps for the development of server programs (worker):

- Includes classes in java.net package
- Preparing the Server Socket object and port number that will be used
- Monitoring/listening on port and receive/accept any connection request from client.
- Preparing the line to write to Socket and to read from Socket.

- Close the connection.

Then for the client (manager) program shown in the following scenarios:

- Includes classes in java.net package.
- Preparing the Socket object, IP number, port number that will be used.
- Connection request to the server via IP and port number of the server.
- If connection request is accepted by server then client prepare the line to write to and to read from Socket.
- Close the connection.

In this paper, communication between client and server on distributed computer system is designed using java socket based stream communication using TCP protocol.

III. DESIGN OF SYSTEM

This system is built using Java programming language and both thread and cryptograph librarys that had been provided by Java. Techniques that is used in research are:

- Using Java programming language, with IDE of NetBeans 6.7.1
- Using JDK 1.6
- Using Java Threads.
- Client-Server asynchronous communication model with Socket.
- Connection oriented based.
- TCP/IP Protocol.
- Using cryptograph library that had been provided by Java.

Encryption algorithm in this research using RSA algorithm that is very well known reliability to secure the data.

The distributed system will be built consists of client (manager) and server (worker). Where client choosing the file that will be encrypted/decrypted and then divide it to workers to work together.

In a brief scene that occurs in client side that are starting from the selecte file, then connect to the available workers. After that create a number of Thread according to the number of worker to divide the file. Then each of Threads sends the piece of file to the worker and wait until worker send back the result of file (encrypted file or decrypted file). This client side is GUI based.

In a brief scene that occur in server side is starting from worker waiting for connection from client then waiting for file from client after that process the file like encrypring or decrypting. Then after the process was completed, the result of file is sent back to client. This server side is text based.

Encryption/decryption process starts from selecting the file in client/manager side, then connect to the available workers. After that create a number of Thread according to the numbers of workers to devide the file. Then each of Threads sends the piece of file to the worker and wait until worker send back the result of file (encrypted file or decrypted file). After all pieces of result file was obtained by client/manger, client/manager merge the pieces of result file into one file. While in the worker side, waiting for connection from manager then waiting for job which requested by manager (file that will be encrypted/decrypted). After obtain the job, worker start to work and the result is sent to manager. In detail software architecture shown in Figur 2.

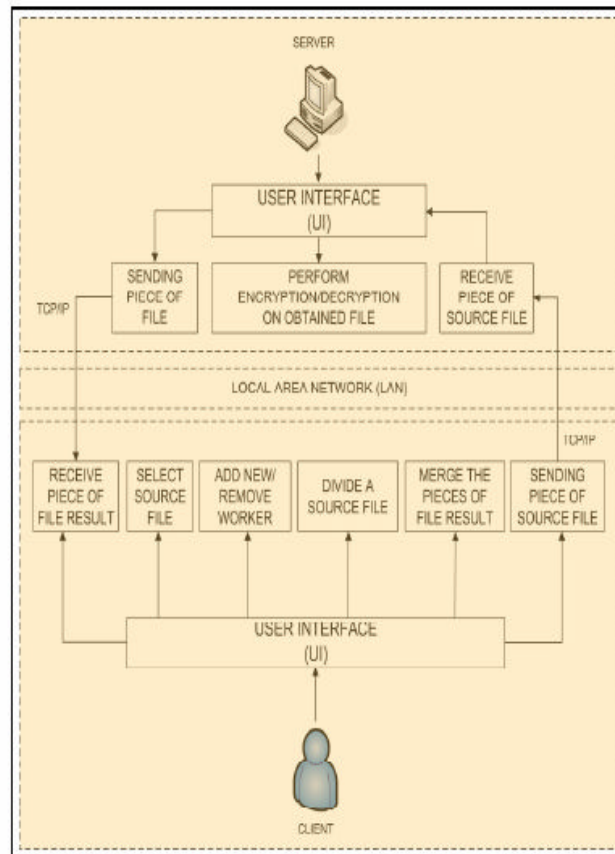


Figure 2. Software architecture

Encryption/decryption process is done by distributed. Because the source file is not encrypted/decrypted in client, but divided by client into several small piece and distributed to the workers to be processed, workers will do encryption/decryption on part file without regard each other. After that client waiting for all pieces of result file is sent back from worker and merge those files into unified whole file.

In general, the client algorithm shown as follows:

- 1: Read the file which will be encrypted/decrypted
- 2: Determine the status of operation, whether encrypting or decrypting
- 3: Prepare the public key for encrypting or private key for decrypting.
- 4: Perform connection using java socket to worker which will help in distributed computing process.
- 5: Divide file based on the number of worker which have been connected.
- 6: Send each file fragment to each worker and the status of operation also the selected key.
- 7: Waiting until all the worker job was collected in client.
- 8: Perform merge to all the file fragments from the workers process.
- 9: Disconnect the connection to the worker
- 10: Done

In general, the client algorithm shown as follows:

- 1: Open a connection for the client by using java socket.
- 2: Wait until there are clients which ask for connection (asking for helping in encrypting/decrypting)
- 3: Receive file fragment, operation code also the key from manager.
- 4: Process the file that was obtained using operation code and key.
- 5: Send back the process result to manager.
- 6: Disconnect the connection from client.
- 7: Repeat again from bagining.

IV. TESTING

Testing using executable (exe) file format with size is “3.94 MB” and “8.29MB”. Testing is using one client computer and five worker computer which doing encryption or decryption. Specification for workwe theses six computer are CPU Pentium 4 with “1.88 GHz” and “512MB” of RAM. Here are the result of testing encryption and decryption process:

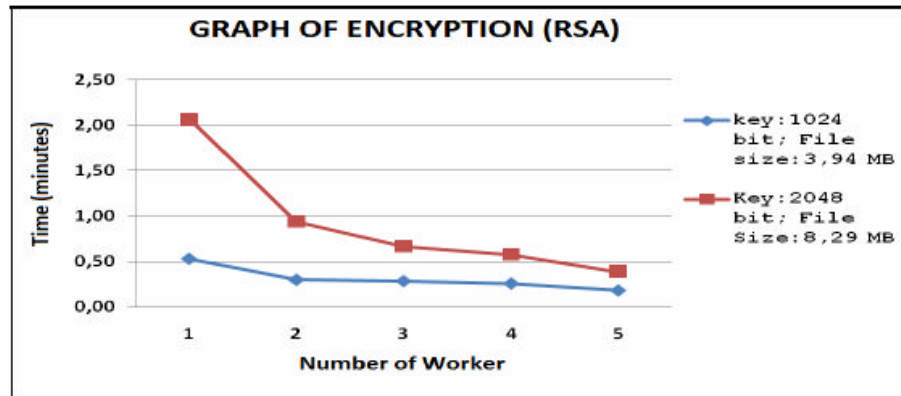


Figure 3. Graph of encryption with RSA algorithm

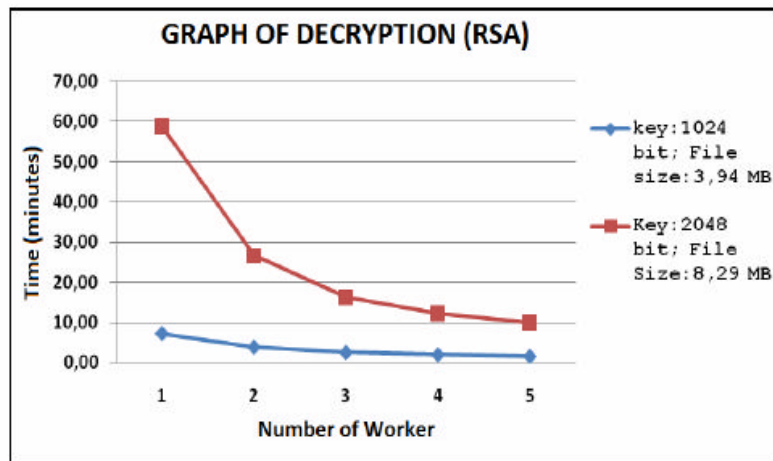


Figure 4. Graph of decryption with RSA algorithm

From figure 3 and 4 shows that process time for encryption and decryption in the distributed system can be reduced. Encryption using the RSA algorithm with 1024 bit key with “3.94 MB” of file size for one worker that takes time about “0.5 minutes” but with five workers is reduced to “0.2 minutes”. While RSA encryption with 2048 bit key length with “8.29 MB” of file size for one worker that takes time about “2.1 minutes” but with five workers is reduced to “0.4 minutes”. As for decryption using RSA algorithm with 1024 bit key length with “3.94 MB” of file size for one worker that takes time about “7.3 minutes” but with five workers is reduced to “1.5 minutes”. And for RSA with 2048 bit key length with “8.29 MB” of file size for one worker that takes time about “58.8 minutes” but with five workers is reduced to “10 minutes”.

V. CONCLUSION

From the result of tests can be concluded that there is a reduction in the time or the reduction of time to encryption and decryption process, so that the encryption and decryption much faster in distributed computing. It is distributed computing that we suggest could be an option to secure large or huge scale of data using RSA algorithm in encryption and decryption.

The system can be used in the financial sector such us banking, in military can be used to secure a very important and large data such us complex of weapons data, complex of defence system data, and many more.

REFERENCES

- [1] Fajar, M., Sudirman, "Design of Protection Using Encryption System", Journal of Computer Science Kharisma Tech, Vol. 2 No. 2. ISSN: 1907-2317
- [2] Fajar, M., Zainuddin, Z., Hasanuddin, Z., "Distributed Computer System for Rendering Application", International Proceedings, Makassar International Conference on Electrical Engineering and Informatics (MICEEI 2008). ISBN:978-979-18765-0-6
- [3] Akbar, Z., Supraedi, "Spacial Design and Implementation of Distributed Filtering Using Socket API for Digital Image Processing", Paper of Information System KNSI 2007
- [4] R. Rivest, A. Shamir, Adleman, "Method for Digital Signature and Public Key Cryptosystem", Communication ACM, Series 21, 1978, pages 120 to 126. MIT, April 1977
- [5] Liang, "Java Programming", Prentice-Hall, 2004

EDFA Simulation on Optical Fiber Communication System

#A.Achmad¹, N.N.R.A. Mokobombang,²

R.R.P. Muhlis³, J.J.N. Ferdiansyah⁴, and Z. Muslimin⁵

¹Electrical Engineering Department, Hasanuddin University, Makassar

E-mail: andani@unhas.ac.id , andani60@yahoo.com

²Electrical Engineering Department, Hasanuddin University, Makassar

E-mail: novv@unhas.ac.id

ABSTRACT

Fiber Optics is the high-speed technology of communication. However, it needs an amplifier because the velocity of a long distance communication will decrease. The commonly used amplifier is repeater, where the device changes the optical signals into electricity, and then back to optical signals. That matter, which becomes the weakness of the repeater. The weakness of the electronic repeater as encouraging the use of EDFA (Erbium Doped Fiber Amplifier).

Without signal alteration in the form of optical-electronic-optical makes EDFA to be efficient by economically and in terms of technology. The simulation shows the difference in gain that generated by using different wavelengths both on optical source and EDFA pump. The pump power are 10-100 mW with wavelengths are 980 nm and ,1480 nm, and optical source wavelength is 1,550 nm.

The result presents when the pump power is higher, it increases gain. The pump power of 20mW, 30mW, 40mW, 50mW, and 60mW, pump wavelength 980nm, signal power -22dBm with a length of EDFA 4m produces gain as 33.2 dB, 35dB, 36dB, 36.5 dB and 37.3 dB.

Keywords: *Optical Fiber Communication Systems, EDFA, Gain*

1. Introduction

Around the globe lately, the approach taken to anticipate an increase in the amount of communication connection demand is to build new networks not connected to each other. Although the addition of the submarine cable network does not cause the sea floor into the hustle and bustle with cables from the existing network, but several years later two technologies namely Erbium-doped fiber amplifier (EDFA) and Wavelength Division Multiplexing (WDM) to streamline use of existing networks.

If we look more further to fiber optic technology, a continued development of fiber optic communication system is necessary to boost the power of light transmitted through fiber optics. Strengthening the power on Optical Fiber Communication Systems are generally using fiber optics which is doped by Erbium atoms or often called by EDFA (Erbium doped fiber amplifier). We had the idea to design a simulation model of EDFA in optical fiber communication systems to describe the amplification system. The paper describes "Simulation of EDFA by using a wavelength at the Optical Fiber Communications Systems".

In light of what is mentioned on the above background, the problem can be formulated as follows: (1) How to create a model simulation analysis of EDFA in Optical Fiber Communication Systems that implement WDM as its multiplexing techniques; and (2) How to gain characteristic Wavelength Division Multiplexing-tech optical fiber communication systems with the application of EDFA as the amplification system.

2. System Overview

WDM (Wavelength Division Multiplexing) technology is basically a transport technology to distribute various types of traffic (data, voice, and video) in a transparent manner, using a wavelength (λ) varying within a single fiber simultaneously. Implementation of WDM can be applied both on the network long haul (long distance) and for short haul applications (short distance). WDM popular because it allows to expand network capacity without increasing the amount of fiber. By using WDM and amplifier, to create additional service capacity to improve the infrastructure of these optics, without having to add an existing

network line. Capacity of the relationship can be developed only by increasing the multiplexers and demultiplexers are used.

2.1. EDFA Definition and Architecture

EDFA (Erbium Doped Fiber Amplifier) is an Optical Amplifier that working at a wavelength of 1550 nm. It has an active medium in the form of silica fiber length of 10 meters - 30 meters doped with Erbium (Er). Optical amplifier uses Optical Pumping by using light (photons) with a shorter wavelength. [5]

EDFA works on the principle of optical amplification. The process is similar to the generation of the laser beam. EDFA system configuration consists of a few meters of fiber doped by Erbium ions (Er^{3+}), pump laser, coupler, and isolator. Doped fiber Er^{3+} ions acts as the gain medium to provide reinforcement to the signal applied to it. Pump laser provides the energy needed to produce a population inversion in the fiber. Next step, the signal enters EDF (Erbium Fiber Doped, - case of optical amplification). An Optical Amplifier consists of a doped fiber, one or more pump laser, a passive wavelength coupler, optical isolator and tap coupler as shown by the following figure [5]:

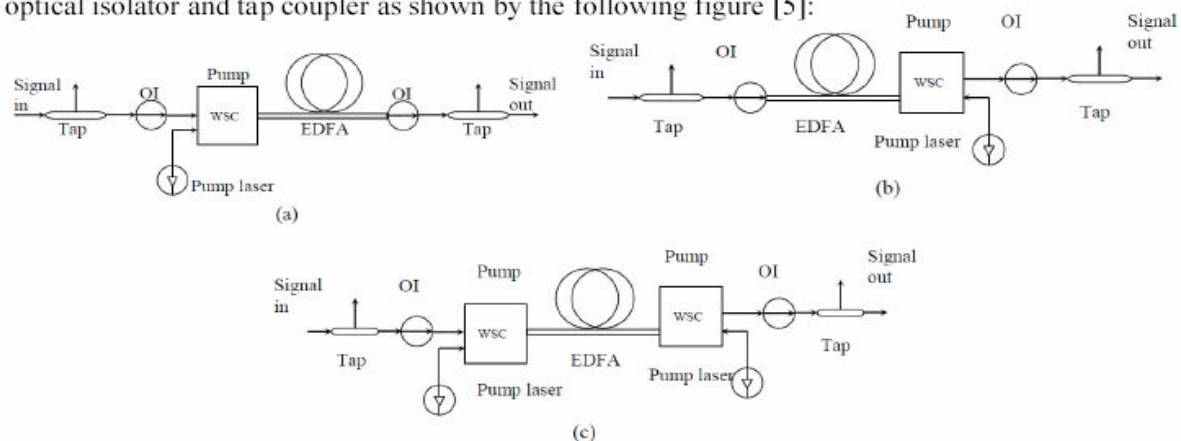


Figure 1: EDFA configuration

(a). Codirectional pumping. (b). Counterdirectional pumping. (c). Dual pumping

Thus far, WSC (Wavelength Selector Coupler) includes a combination of pump and signal power into the fiber to couple the wavelength 980/1550 nm or 1480/1550 nm. Pump light is usually injected into the fiber in the same direction as the direction signal, this method is known as co-directional pumping and shown by figure 1a. Another method when the direction opposite to pumping light signal direction as in the figure 1b is called counter-directional pumping. Next, when the combination of two above is applied together, it is called dual pumping shown by the figure 1c. Dual pumping has larger resultant gain among the three. Co-directional pumping has good noise performance but has the smallest gain

2.2. Energy System in three levels

Energy diagram of a three-level system is a solution approach to mathematically model for Erbium ions are reviewed by three levels of energy. The three-level system describes the structure of the Er^{3+} energy levels relevant to the process of strengthening EDFA. It can occur when there is a migration from level 2 to level 1, and at least half of the overall population of Erbium ions must be doped at level 2 [7].

2.3. EDFA Simulation

EDFA modeling is designed in a system of 3 levels. Equations in Mathematics model are related to the propagation of light flux, inversion Erbium ions, and the process of absorption and emission cross section, effect of the overlap parameters to calculate EDFA gain produced.

3. Designing EDFA Simulation

Modeling is done by treating the EDFA in the system of 3 levels. Thereby, the mathematical model for the EDFA-3 level system is described in the Three Levels of Energy System diagram. Other equations associated with the propagation of light flux, the population inversion Erbium ions, and the process of

absorption and emission cross section were included in this equation, the effect of the overlap parameters involved in calculating EDFA gain is produced.

3.1. EDFA modeling

EDFA modeling is designed in a system of 3 levels. Equations in Mathematics model are related to the propagation of light flux, inversion Erbium ions, and the process of absorption and emission cross section, effect of the overlap parameters to calculate EDFA gain produced.

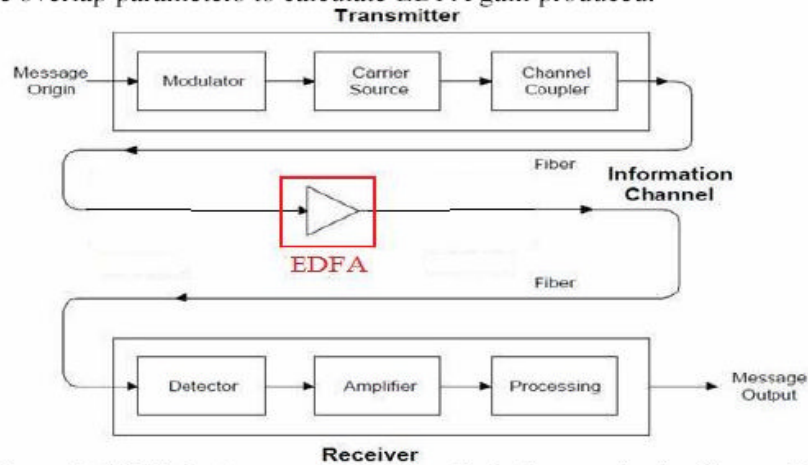


Figure 2: EDFA implementation on Fiber Optic Communication System [13]

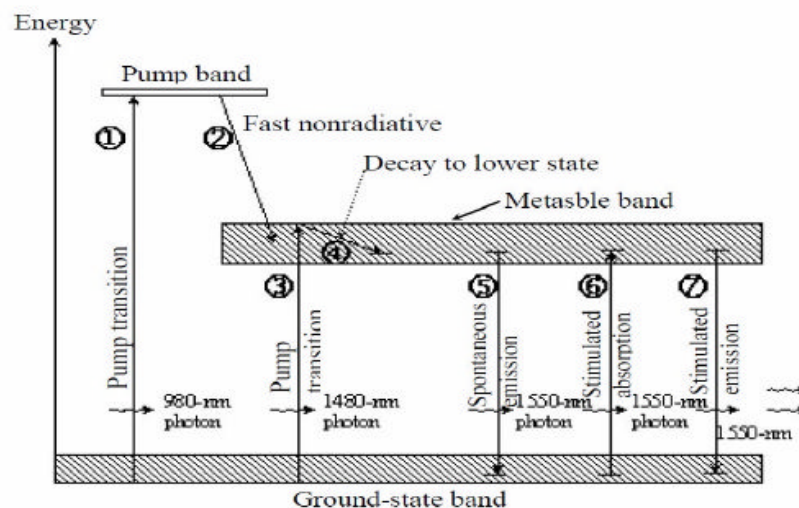


Figure 3: Simplified energy-level of the various transition processes for ion Er^{3+} in silica [5]

A pump laser with a wavelength of 980 nm is used to excite Er^{3+} ions from ground state to a level below the pump level describing in Figure 3. The excited ions will decay soon (less than $1 \mu\text{s}$) from the pump level to the meta-stable band indicated by the process (2). During this transition the energy released in the form of heat or vibration, the ions exciting the band tend to gather on the lower level of the metastable band.

The possibility of the pump laser wavelengths is 1480 nm, where the photon energy is similar to the photon signal. The 1480-nm photon energy is absorbed to excite electrons from the ground state and metastable bands straight into the top level as shown in process (3), these electrons tend to go down to lower levels of the metastable bands appear on the process (4) and then re- to ground state without any external stimulation signal photons as indicated by process (5). This transition is called Spontaneous Emission and noise in optical amplifiers. Process (6) shows the signal photon is absorbed by the ions rising to the level of metastable band. Then the photon signal will trigger excited ions in metastable band to return to the ground state together with new photon produce emissions equal to the photon signal.

It is a mathematical solution approach used in the modeling of EDFA amplifier. The diagram shows that Er³⁺ ions are relevant to the strengthening process. Obtained equation (3.1), (3.2), and (3.3) below:

$$\frac{dN_1}{dt} = \frac{N_2}{\tau_{21}} - (N_1 - N_3)W_p + (N_2 - N_1)W_s \quad (3.1) \quad \frac{dN_2}{dt} = -\frac{N_2}{\tau_{21}} + \frac{N_3}{\tau_{32}} - (N_2 - N_1)W_s \quad (3.2)$$

$$\frac{dN_3}{dt} = -\frac{N_3}{\tau_{32}} + (N_1 - N_3)W_p \quad (3.3)$$

Where the pump photon absorption rate is $W_p = \phi_p \sigma_s$, and the speed of the signal photon emission $W_s = \phi_s \sigma_s$. Strengthening the EDFA population inversion occurs between level 1 and level 2, and at least half of the overall Erbium ion populations must be excited at level 2. It calculates in advance the level of population at level 2 (N_2) to quantify the value of population inversion $N_2 - N_1$, showing in equation (3.4):

$$N_2 - N_1 = \frac{\phi_p \sigma_p - \Gamma_{21}}{\Gamma_{21} + 2\phi_s \sigma_s + \phi_p \sigma_p} N \quad (3.4)$$

In the case of indecent dimensional light field intensity derived from the light field through relationship can be stated as follows:

$$I(z) = \frac{P(z)\Gamma}{A_{eff}} \quad (3.5) \quad \Gamma = \left(1 - e^{-r^2/w^2}\right) \quad (3.6)$$

Where:

Overlap factor Γ = (confinement factor), which is the value that describes the overlap between the Erbium ions with light field mode. A_{eff} = effective cross-sectional area distribution of Erbium ions (m^2). w = radius of modes for the signal and pump (m^2).

3.2 Strengthening the Small Signal Range

A mathematical explanation clarifies the strengthening of the signal power which is illustrated through a medium after a pump power. Strengthening small-signal per unit length of fiber for strong pump power showed a very simple, namely the number of Erbium and emission cross section signal. To get the maximum amount of reinforcement for small signal range, use the equations in chapter 2. First input signal needs to be given for a particular pump power, input signal having strengthened as expected. Given pump power can be determined using equation (3.9):

$$P_p(z) = P_p(0) \exp^{-(\sigma_a N_s z / 2)} \quad (3.9)$$

In order to obtain the maximum gain as in equation (3.10), and in units (dB) is expressed in equation (3.11):

$$g_{mak} = \sigma_s (N_2 - N_1)_{mak} \quad (3.10) \quad G(db) = 10 \log e^{g_{mak} L} \quad (3.11)$$

3.3. Strengthening the Signal Saturation

Interesting phenomenon indicated that the saturation intensity (I_{sat}) is not constant, but increasing linearly with pump power. A high saturation occurs for signals at high power levels that changing the length of EDFA pump power as expressed:

$$P_p(z) = P_p(0) \exp^{-(\sigma_a N_s z / 2)} \quad (3.12)$$

Then the pumping intensity and magnitude of changes in the pumping power intensity expressed by the following equation:

$$I'_p(z) = \frac{I_p(z)}{I_{th}} = \frac{P_p(0)}{I_{th} A_{eff}} e^{-(\sigma_a N_s z / 2)} \quad I_p(z) = \frac{P_p(z)}{A_{eff}} = \frac{P_p(0)}{A_{eff}} e^{-(\sigma_a N_s z / 2)}$$

$$\text{Where } I_{th} = \frac{h\nu_p}{\sigma_p \tau_2} \quad (3.15)$$

Saturation intensity as expressed as $I_{sat}(z) = \frac{1+I'_p(z)}{2\eta}$, and signal intensity changes to the length of EDFA as stated $\frac{dI'_s(z)}{dz} = I_{sat}(z) \left(\frac{I'_p-1}{I'_p+1} \right) \sigma_s N$. Substitution (z) into the differential equation for the change in signal intensity against the distance will produce the following equation:

$$\begin{aligned} \frac{dI'_s(z)}{dz} &= I_{sat}(z) \left(\frac{I'_p-1}{I'_p+1} \right) \sigma_s N \\ &= \frac{1+I'_p}{2\eta} \left(\frac{I'_p-1}{I'_p+1} \right) \sigma_s N \\ &= \frac{\sigma_s N}{2\eta} (I'_p(z) - 1) \\ &= \frac{\sigma_s N}{2\eta} \left(\frac{P_p(0)}{I_{th} A_{eff}} e^{-(\sigma_p N \cdot z)/2} - 1 \right) \\ \frac{dI'_s(z)}{dz} &= \frac{\sigma_s N}{2\eta} \left(\frac{P_p(0)}{I_{th} A_{eff}} e^{-(\sigma_p N \cdot z)/2} - 1 \right) \end{aligned} \quad (3.16)$$

As a summary, equation (3.17) is used to calculate the maximum gain for the range of signal saturation.

$$G(\text{dB}) = 10 \log \left(\frac{\frac{\sigma_s P_p(0)}{\eta \sigma_p I_{th} A_{eff}} (1 - e^{-(\sigma_p N L)/2}) + \frac{P_s(0)}{A_{eff} I_{th}} - \frac{\sigma_s N}{2\eta} L}{\frac{P_s(0)}{A_{eff} I_{th}}} \right)$$

or

$$G(\text{dB}) = 10 \log \left(\frac{\frac{\sigma_s P_p(0)}{\eta \sigma_p I_{th} A_{eff}} + \frac{P_s(0)}{A_{eff} I_{th}} - \frac{\sigma_s P_p(0)}{\eta \sigma_p I_{th} A_{eff}} e^{-(\sigma_p N L)/2} - \frac{\sigma_s N}{2\eta} L}{\frac{P_s(0)}{A_{eff} I_{th}}} \right) \quad (3.17)$$

Data used in the simulation analysis is derived from IEEE journals and some reference books. However, parameters can be changed according to the needs of this research.

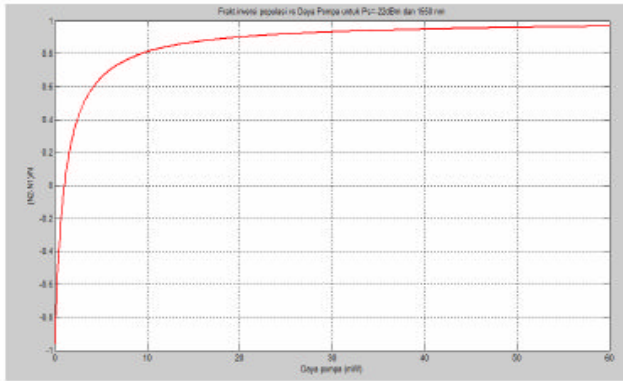
4. Analysis on EDFA Simulation

Observations were carried out by varying the input signal power parameters in order to obtain the minimum value that can still be amplified by EDFA, up to a maximum value of the resulting reinforcement. Signal wavelength used is 1,550 nm. There are two Pump wavelengths used, namely 980 nm, and 1,480 nm. Data obtained from the simulation results using MATLAB version 7, which are in accordance with the existing modeling system in the point (3).

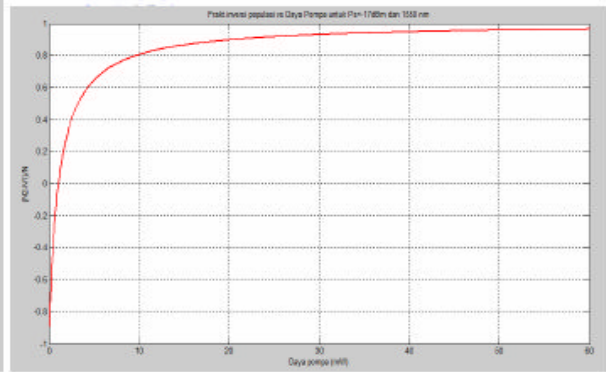
4.1 Population Inversion Fractional Calculation of Pump Power

The simulation on a three-level system aims to find out the threshold value. Threshold value is a value indicating that the initial strengthening will occur, and also showed that the number of Erbium ions in level 2 equals the number of Erbium ions in level 1.

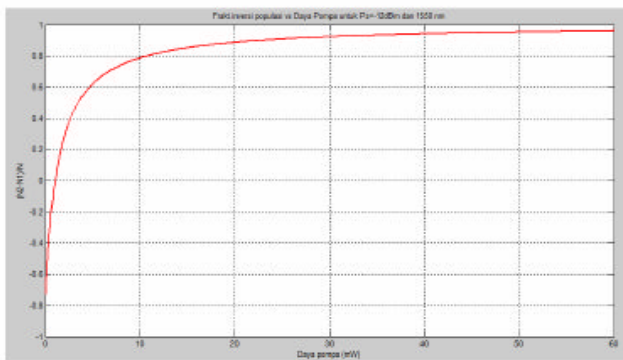
4.1.1. Simulation for Pump Wavelength 980 nm



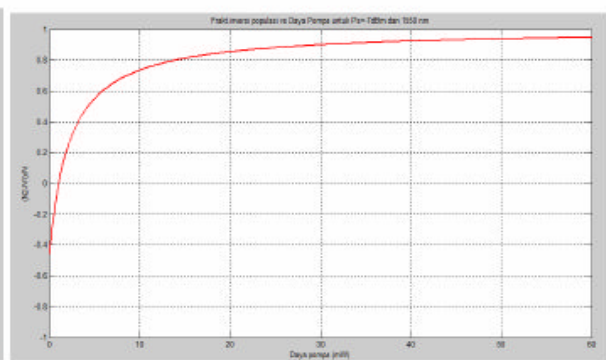
(a) Power signal -22 dBm



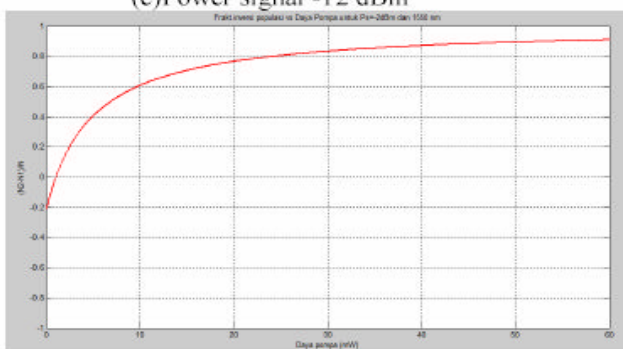
(b) Power signal -17 dBm



(c) Power signal -12 dBm



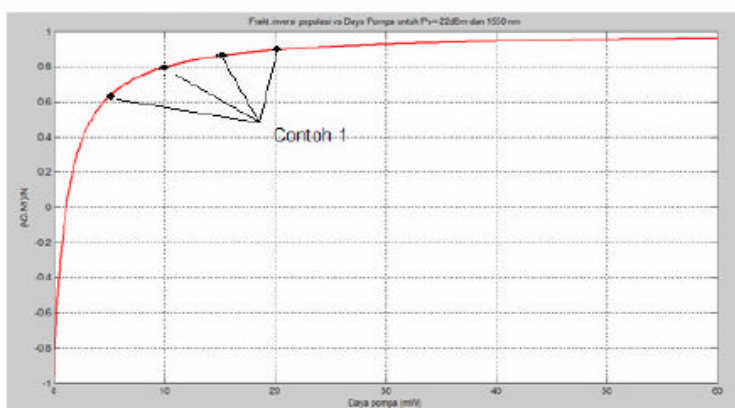
(d) Power signal -7 dBm



(e) Power signal -2 dBm

Figure 4: Fractional Inversion Population Characteristics On The Pump To Pump Wavelength 980 nm.

4.1.2 Simulation for pump wavelength 1480 nm



Simulation Calculation Example 1

If the optical fiber communication systems and signal wavelength EDFA pumping each 1,550nm and 980nm, the radius of the core fiber amplifier (EDFA), the signal power -22 dBm, EDFA pump power of 5mW, 10mW, 15mW and 20mW, cross section cross section pump and signal 1.9. and 6.6. lifetime at level 2 10ms, overlap factor signals and EDFA pump is 0.43 and 0.79. So the value of population inversion is as follows:

Where:

$$h=6,626 \cdot 10^{-34} \text{ Js}, c=3 \cdot 10^8 \text{ m/s}, \lambda_p=980 \text{ nm}, \lambda_s=1550 \text{ nm}, r=1.55 \text{ } \mu\text{m}, \sigma_p=1,9 \cdot 10^{-25} \\ , \sigma_s=6,6 \cdot 10^{-25}, P_p=10 \text{ mW daya pompa}, P_s=-22 \text{ dBm}=-52 \text{ dB}, \tau_{21}=0,01 \text{ s}, \Gamma_s=0,43 \text{ s}^{-1}, \Gamma_p=0,79 \text{ s}^{-1}$$

Then the calculation is:

$$\Gamma_{21} = \frac{1}{\tau_{21}} = \frac{1}{0,01} = 100$$

$$V_p = \frac{c}{\lambda_p} = \frac{3 \cdot 10^8}{980 \cdot 10^{-9}} = 3,06 \cdot 10^{14} \text{ Hz}$$

$$V_s = \frac{c}{\lambda_s} = \frac{3 \cdot 10^8}{1550 \cdot 10^{-9}} = 1,94 \cdot 10^{14} \text{ Hz}$$

$$P_s = 10^{-52} = 6,31 \cdot 10^{-6} \text{ watt}$$

$$A_{\text{eff}} = 2 \cdot \pi \cdot r$$

$$A_{\text{eff}} = 2 \cdot 3,14 \cdot 1,55 \cdot 10^{-6} = 7,55 \cdot 10^{-12} \text{ m}^2$$

$$I_{p5} = \frac{P_p \cdot \Gamma_p}{A_{\text{eff}}} = \frac{0,005 \cdot 0,79}{7,55 \cdot 10^{-12}} = 5,23 \cdot 10^8$$

$$I_{p10} = \frac{P_p \cdot \Gamma_p}{A_{\text{eff}}} = \frac{0,01 \cdot 0,79}{7,55 \cdot 10^{-12}} = 1,05 \cdot 10^9$$

$$I_{p15} = \frac{P_p \cdot \Gamma_p}{A_{\text{eff}}} = \frac{0,015 \cdot 0,79}{7,55 \cdot 10^{-12}} = 1,57 \cdot 10^9$$

$$I_{p20} = \frac{P_p \cdot \Gamma_p}{A_{\text{eff}}} = \frac{0,02 \cdot 0,79}{7,55 \cdot 10^{-12}} = 2,09 \cdot 10^9$$

$$I_s = \frac{P_s \cdot \Gamma_s}{A_{\text{eff}}} = \frac{5,37 \cdot 10^{-6} \cdot 0,43}{7,55 \cdot 10^{-12}} = 3,6 \cdot 10^5$$

$$\phi_{p5} = \frac{I_p}{h \cdot V_p} = \frac{5,7 \cdot 10^8}{6,626 \cdot 10^{-34} \cdot 3,06 \cdot 10^{14}} = 2,58 \cdot 10^{27}$$

$$\phi_{p10} = \frac{I_p}{h \cdot V_p} = \frac{5,7 \cdot 10^8}{6,626 \cdot 10^{-34} \cdot 3,06 \cdot 10^{14}} = 5,16 \cdot 10^{27}$$

$$\phi_{p15} = \frac{I_p}{h \cdot V_p} = \frac{5,7 \cdot 10^8}{6,626 \cdot 10^{-34} \cdot 3,06 \cdot 10^{14}} = 7,74 \cdot 10^{27}$$

$$\phi_{p20} = \frac{I_p}{h \cdot V_p} = \frac{5,7 \cdot 10^8}{6,626 \cdot 10^{-34} \cdot 3,06 \cdot 10^{14}} = 1,03 \cdot 10^{28}$$

$$\phi_s = \frac{I_s}{h \cdot V_s} = \frac{5,62 \cdot 10^5}{6,626 \cdot 10^{-34} \cdot 1,94 \cdot 10^{14}} = 2,80 \cdot 10^{24}$$

$$(N_2 - N_1)_5 = \frac{\phi_p \sigma_p - \Gamma_{21}}{\Gamma_{21} + 2\phi_s \sigma_s + \phi_p \sigma_p} N$$

$$(N_2 - N_1)_{10} = \frac{\phi_p \sigma_p - \Gamma_{21}}{\Gamma_{21} + 2\phi_s \sigma_s + \phi_p \sigma_p} N$$

$$(N_2 - N_1)_{15} = \frac{\phi_p \sigma_p - \Gamma_{21}}{\Gamma_{21} + 2\phi_s \sigma_s + \phi_p \sigma_p} N$$

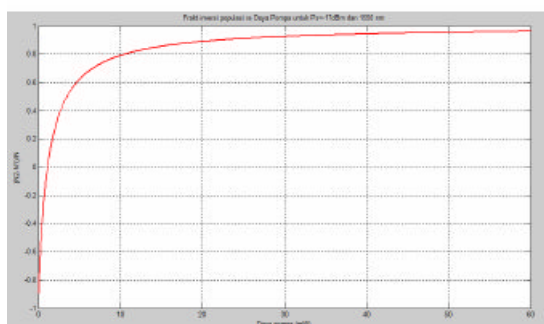
$$(N_2 - N_1)_{20} = \frac{\phi_p \sigma_p - \Gamma_{21}}{\Gamma_{21} + 2\phi_s \sigma_s + \phi_p \sigma_p} N$$

$$\left[\frac{N_2 - N_1}{N} \right]_5 = \frac{490,26 - 100}{100 + 3,7 + 490,26} = 0,66$$

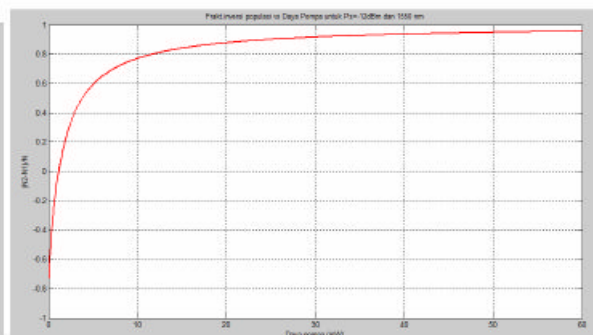
$$\left[\frac{N_2 - N_1}{N} \right]_{10} = \frac{980,4395 - 100}{100 + 3,7 + 980,4395} = 0,81$$

$$\left[\frac{N_2 - N_1}{N} \right]_{15} = \frac{1470,79 - 100}{100 + 3,7 + 1470,79} = 0,87$$

$$\left[\frac{N_2 - N_1}{N} \right]_{20} = \frac{1961,06 - 100}{100 + 3,7 + 1961,06} = 0,90$$



(a) Signal Power -17 dBm



(b) Power signal -12 dBm

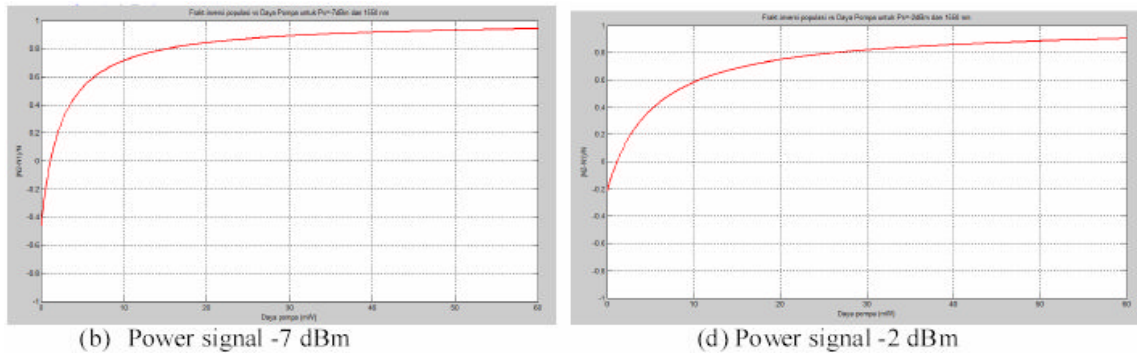


Figure 5: Fractional Inversion Population Characteristics On The Pump To Pump Wavelength 1,480 nm.

Figure 4 and 5 image shows the relationship between the fractional population inversion (N_2-N_1) / 2 on the pump power supplied to all signal powers with wavelength of 1550 nm. Signal powers perform on the same interval in order to investigate that the characteristic changes occur. Figure 4 performs population inversion of the pump power for wavelength 980 nm. It shows for the signal power -22 dBm, -17 dBm, -12 dBm, -7 dBm, and -2 dBm have the same threshold value, which occurs in about 1 mW pump power. Signal power of -22 dBm and -17 dBm population inversion values around -0.8. Signal power of -12 dBm around -0.6, -7 dBm signal power around -0.4, and -2 dBm signal power around -0.2.

While the figure 5 shows the population inversion of the power pump, for pump wavelengths of 1,480 nm. From the pictures turned out the threshold value for signal power -22 dBm, -17 dBm, -12 dBm, -7 dBm, and -2 dBm for 980 nm pump wavelength, equal to the threshold value for the pump wavelength of 1480 nm, which occurred on power pump about 1 mW. Similarly, for the value of population inversion, ie to signal power -22 dBm and -17 dBm at around -0.8, the signal power of -12 dBm at around -0.6, -7 dBm signal power around -0.4, and -2 dBm signal power around -0.2.

The example simulation calculation 1 which was done manually with the increase in pump power 5 mW shows that the greater power of the signal to be amplified by its threshold value, the greater the initial reinforcement. The absorption process by the Erbium ions cause increasing of the amplified signal power. A population inversion shows that the ions at the level of all the displaced ground state excited state level. Increasing in pump power linearly provides the population inversion due to increase a certain pump power limit exponentially. Furthermore, the approached saturation make the pump power become higher. Perfect population inversion occurs when the number of Erbium ions in level 1 is equal to zero ($N_1 = 0$), so that $N_2 = N$.

4.2 Population Inversion Fractional Calculation of Signal Power

This simulation aims to determine the value of population inversion of the existing signal power, using 20-60 mW pump power. The figure 6 shows the characteristics of the population inversion Fractional against the power of the amplified signal.

4.2.1 Simulation for Pump Wavelength 980 nm

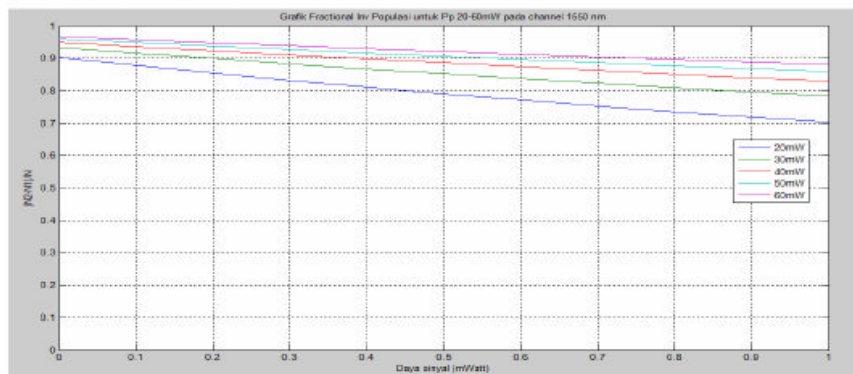


Figure 6: Fractional Inversion Population Characteristics of Input Signals Power On Wavelength 1550 nm to 980 nm Pump Wavelength.

4.2.2 Simulation for Pump Wavelength 1,480 nm

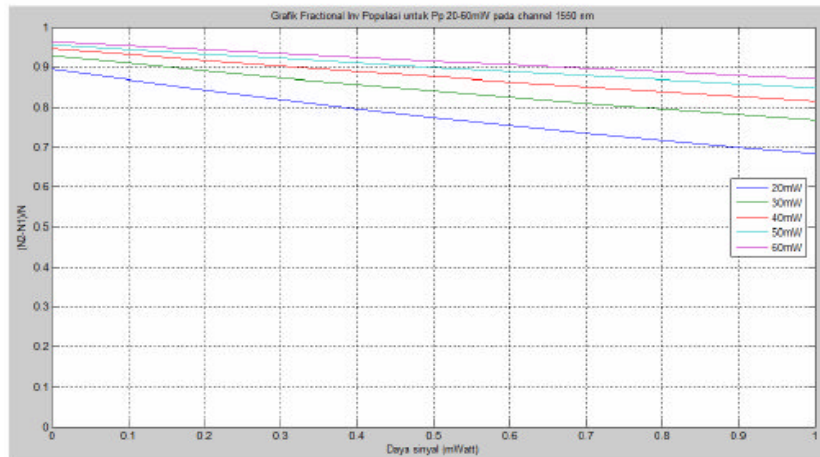


Figure 7: Fractional Inversion Population Characteristics of Input Signals Power On Wavelength 1550 nm to 1480 nm Pump Wavelength.

Figure 6 and 7 shows the relationship between the fractional population inversion $(N_2 - N_1) / N$ of the signal power, for 20-60 mW pump power, signal wavelength of 1550 nm. Figure IV.3 and IV.4 image is calculated by simulation using MATLAB programs. It presents that the greater power of the signal to be amplified by the EDFA produce fractional values, the smaller the population inversion for all the pump power. This fact occurs because the saturation effect on the population inversion process. A greater signal power will give increased influence on the saturation in the process of population inversion.

5. Conclusion

1. Threshold value for all signal power increases with increase of input signal power, which occurred at about 1 mW pump power. Similarly, the value of the population inversion increases with the increase of input signal power.
2. Cable length EDFA affect the gain is generated. Where the pump power 60 mW for 980 nm pump wavelength the maximum gain is obtained at 8-9 m long EDFA cable, and for 1,480 nm pump wavelength of maximum gain is obtained at 10-11 m.
3. The cable length EDFA generated by the EDFA gain will increase with increase of pump power. Where the pump power 20 mW for 980 nm pump wavelength obtained the maximum gain of ± 13 dB, while for 1480 nm pump wavelength obtained by the maximum gain ± 23 dB. And continued to increase until the pump power 60 mW for 980 nm pump wavelength of maximum gain is obtained at ± 45 dB, while for 1480 nm pump wavelength obtained by the maximum gain ± 61 dB. For the minimum pump power that can still produce the strengthening of the pump power 10 mW.
4. The amount of gain resulting decrease with increasing amount of power the signal to be amplified. Decrease the gain can reach $\pm 55\%$ for the signal power -22 dBm to -2 dBm signal power. While for each interval the signal power, gain reduction occurred, ie $\pm 15\%$.

References

- [1] "PL 1.1 - Dasar Sistem Komunikasi Optik, *OPTICAL ACCESS NETWORK*". P.T. Telekomunikasi Indonesia, Tbk. Bandung. 18 September 2004.
- [2] Sulisty, Meiyanto Eko. "Sistem Penjamakan Pada Sistem Komunikasi Serat Optik". AMIK Kartika Yani. Yogyakarta. 2006.
- [3] "Komunikasi Serat Optik (*Handout-1*)", Teknik Telekomunikasi, Fakultas Teknik Universitas Hasanuddin, Makassar.
- [4] "Teknologi WDM pada Serat Optik". Departemen Elektro Fakultas Teknik Universitas Indonesia. Depok. 2006.
- [5] Sunarto. "Pengenalan *Optical Amplifier* Di Dalam Sistem Komunikasi Optik". Jurusan Teknik Elektro-FTI, Universitas Trisakti. Jakarta. February 2005.

- [6] Yamashita, S, Okoshi, T. "Performance Improvement and Optimization of Fibre Amplifier with a Midway Isolator". *IEEE Photonic Technology Letters Volume 4* No. 11. November 1992.
- [7] Beker, P.C., Olsson, N.A., & Simpson, J.R. "Erbium-doped fiber amplifiers fundamentals and technology". *Academic Press*. USA. 1999.
- [8] Kaminow, Ivan P., Koci, Thomas L. "Optical Fiber Telecommunications IIIA". *Academic Press*. California. 1997.
- [9] Agrawal, Govin. P. "Fiber-optic communication systems". John Wiley & Sons, Inc. Canada. 1992.
- [10] Keigo Iizuka. "Elements of photonics volume II for Fiber and Integrated Optics". John Wiley & Sons, Inc. New York. 2002
- [11] Desurvire, Emmanuel. "Erbium Doped Fiber Amplifier : Principles and Applications". John Wiley & Sons, Inc. Canada. 1994.
- [12] Kang Liu, Max Ming. "Principles And Application of Optical Communication". Mc-Graw Hill. 1996.
- [13] Palais, Joseph C. "Fiber Optic Communications (Pengenalan Sistem Komunikasi Serat Optik". www.howstuffworks.com, www.tpub.com . Last accessed: March 2010.
- [14] Senior, John M. "Optical Fiber Communications". Prentice Hall International. 1985.
- [15] Hoss, Robert J. "Fiber Optic Communication Design Handbook". Prentice Hall. 1990.
- [16] Park, Y.K. "A 5 Gb/s Repeaterless Transmission System Using Erbium Doped Fiber Amplifier". *IEEE Photonic Technology Letters* Vol. 5 No. 2 February 1993

Digital Image Steganography Using Cipher Block Chaining Operation on AWGN Channel

#Ansar Suyuti¹, Sitti Wetenriajeng Sidehabi²

¹Electrical Engineering, Hasanuddin University
Kampus Tamalanrea Universitas Hasanuddin

²Akademi Teknik Industri Makassar

¹asuyuti@unhas.ac.id

²tenri_sidehabi@yahoo.com

Abstract

The purpose of steganography is to hide the very presence of communication as opposed to cryptography which aims to make communication unintelligible to those who do not possess the right keys. A digital steganography can convey classified information beneath a digital image, video, sound and other type of digital files. In this paper, a steganography is observed as a communication system where AWGN channel degrades the information. The system tested on several variance of AWGN and also observed in the influence of bit amount occupied by secret data. The experiment is validated by calculating the Mean Square Error (MSE) and Peak Signal to Noise Ratio (PSNR).

Keywords: steganography, cipher block chaining, noise recovery

1. Introduction

Steganography is the art and science of hiding information. The term "Information Hiding" relates to both watermarking and steganography. Watermarking usually refers to methods that hide information in a data object so that the information is robust to modifications. That means, it should be impossible to remove a watermark without degrading the quality of the data object. Essentially, the information-hiding process in steganographic system starts by identifying a cover medium's redundant bits. The embedding process creates a stego medium by replacing these redundant bits with data from the hidden message.

On the other hand, steganography refers to hidden information that is fragile. Modifications to the cover medium may destroy it [1]. In addition, it is stated that steganography strives for high security and capacity, which often entails that the hidden information is fragile. Even trivial modifications to the stego medium can destroy it [2]. From this point of view a question may rise of how well a steganography file can be recovered under several circumstances, e.g. noise, data manipulation, etc. Commonly research on steganography explores a better techniques in hiding information [3, 4, 5]. Some research tries to have countside of steganography by trying to identified information under a steganography files in handling national security threat [1, 6].

The paper is organized as follows. Section 2 gives an introduction to digital image and steganography. Section 3 explains the cipher-block chaining (CBC) used in the system. The overall block system and experimental results given in Section 4 ; and conclusion are drawn in Section 5.

2. Digital Images and Steganography

2.1 Digital Image Format

Digital Images are stored in a standard digital format known by computer operating system. Commonly format used by users are Bitmap (**BMP**), Joint Photographic Experts Group (**JPEG**), and Graphics Interchange Format (**GIF**). Currently BMP format is not as popular like JPG format since

BMP need a larger storage. However, bitmap has better quality in picture since it is not compressed like JPEG or GIF. Storage structure on the bitmap file is divided into three major sections as shown in Figure 1.



Figure 1: File Structure of Bitmap

The first section with size 54 bytes located at the beginning of the file used to store the header of the file bmp. The second section with size 1024 byte is filled by pallets information that that stores the composition of the RGB (Red, Green, Blue). The third part is allocated for BMP file that contains the information, in this case image information [7].

2.2. Steganography

In broadly definition, steganography is one of hiding techniques that insert a piece by piece of original information on a medium, so that information appears less dominant with a boarded media. In digital data, the techniques often used in modern steganography are:

A. Masking and Filtering

Masking and filtering techniques hide information by marking an image and is usually restricted to 24-bit and gray-scale images. Digital watermarks include information such as copyright, ownership, or license. While traditional steganography conceals information, watermarks extend information since it becomes an attribute of the cover image. Masking techniques hide information in such a way that the hidden message is more integral to the cover image than simply hiding data in the "noise" level. Masking adds redundancy to the hidden information. This makes the masking technique more suitable than LSB with lossy JPEG images. It may also help protect against some image processing such as cropping and rotating.

B. Transformation

Transformation is to hide data in a mathematical function called a compression algorithm. Two of these functions is the Discrete Cosine Transformation (DCT) and Wavelet Transformation, which is a technique that transform data information from one domain to other domain. The function of DCT and Wavelet transform data (spatial domain) into the field of frequency (frequency domain).

C. Least-Significant Bit Modification

This technique utilizing bits Least Significant Bit (LSB) of digital image, and replacing them with bits of secret data. The bits of secret data is going to change the color of each pixel component values given in the image of a container, as illustrated in Figure 2.

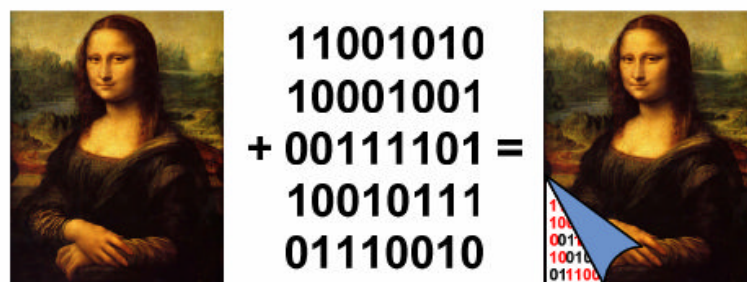


Figure 2. Effects of steganography

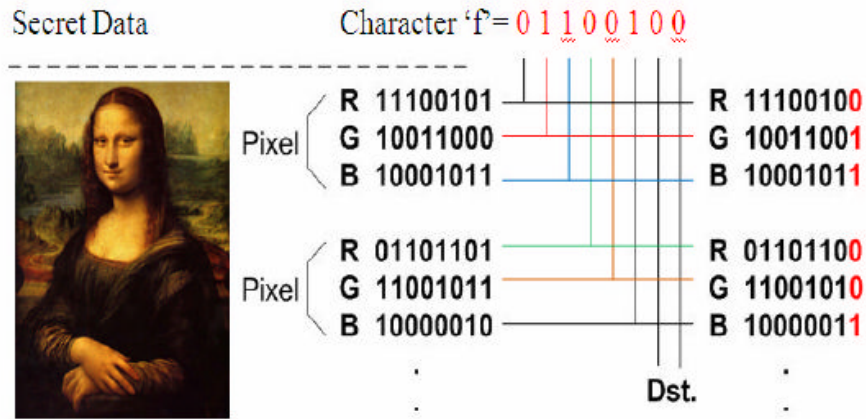


Figure 3: Replacing LSB bit on RGB Digital Image

Figure 3. illustrates the process of hiding secret data in the form of the character 'f' (binary: 01100100) into a digital image. The process of steganography conducted by replacing several bits of color components in each pixel of 24 bit color digital image with secret data bits. Bits that are modified are the LSB part, hence only differs to 1 value. Suppose a byte in a picture represent a certain color, then changes its LSB does not change color significantly. This the advantage of utilizing data hiding, since the human eye cannot distinguish small changes in color. This technique is used in this paper due to its simplicity.

3. Cipher-Block Chaining

Usually within 1 block Cipher Block consists of 64 bits or 128 bits, with all blocks are interconnected like a chain. In the process of encryption and decryption, CBC mode using XOR logic operation.

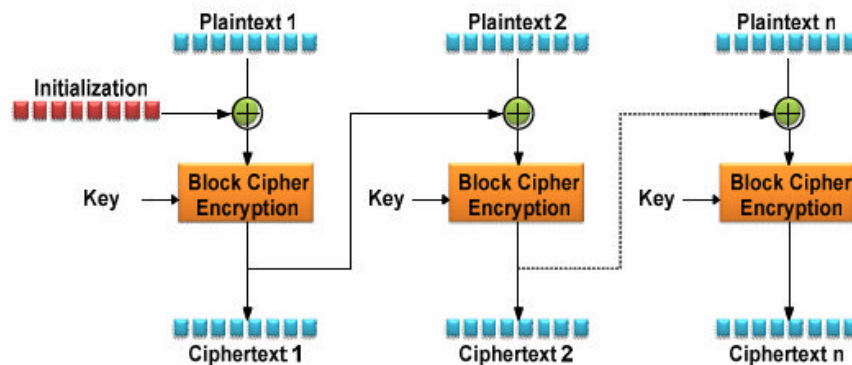


Figure 4: Block Diagram of CBC Encryption Mode [8]

Mathematically can be formulated as:

$$C_i = E_K(P_i \oplus C_{i-1}); C_0 = iv \quad (1)$$

In this mode, initial value (iv) as initial values used for the XOR with the plaintext block 1 (P_1) before entering the block encryption (E_K). The input for the next block is the XOR result between plaintext (P_i) with the previous ciphertext (C_{i-1}). Keys are used on each block encryption. The pattern in this mode is always repeated and is covered by the XOR operation, so that the attackers are more difficult to analyze the possibility of its plaintext.

Results of CBC data encryption (ciphertext) can be read through the decryption process, which is the reverse process of encryption.

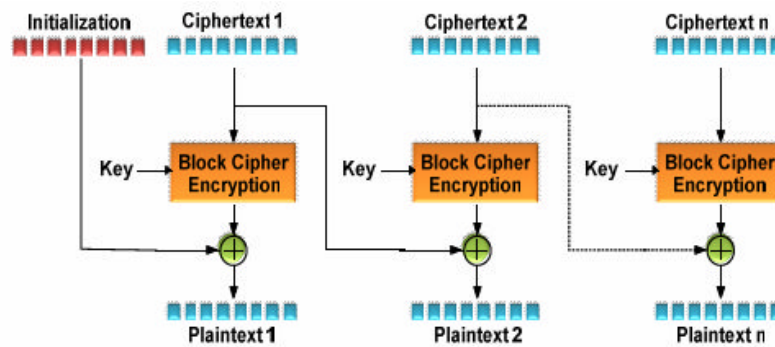


Figure 5: Block Diagram of CBC Decryption Mode [8]

Mathematicly can be formulated as:

$$P_i = D_K(C_i) \oplus C_{i-1}; C_0 = iv \quad (2)$$

In CBC decryption process, the initial value (iv) is known by the sender and receiver of messages for the XOR function with the decryption of the first block (C_i). Furthermore, the second block cipher (C_{i+1}) become initial value (iv) which is used for the XOR process with the second decryption block to obtain a block of plaintext (original data). The same process repeated till the last block cipher.

4. Experiment and Simulation Results

In writing this paper, the program created in a system consisting of several blocks with specific functions. General system block diagram is illustrated in Figure 6.

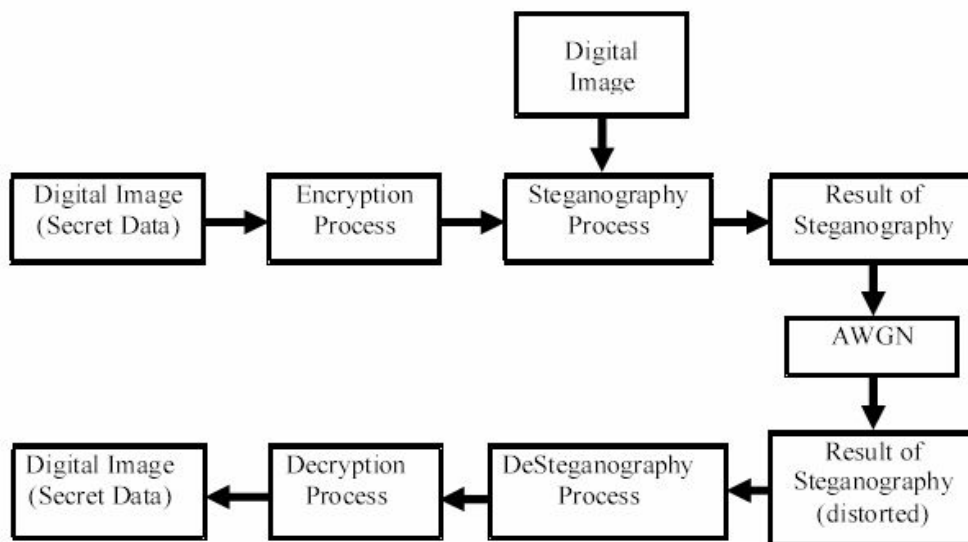


Figure 6: General Block System

In general the process describe in block diagram can be explain as follows:

1. Confidential data or so called the plaintext form of digital images, must first be encrypted to guarantee the integrity and confidentiality of information. The encryption method implemented in the system is the Cipher Block Chaining (CBC). The confidential/secret data or plaintext is first split into blocks of length 64 bits per block before the encryption process started. The result of encryption is called ciphertext.

2. The next process is steganography, the process of replacing the bits in the container file (in the form of 24 bit digital image bitmap format) with ciphertext. The output of this process is called as the results of steganography.
3. Steganography file then disturbed by gaussian noise as it passes through the block process Additive White Gaussian Noise (AWGN). Thus the results of steganography is contaminated with noise, the output from this process called steganography distorted.
4. The distorted steganography are next processed in destenography to recover the ciphertext contained in steganography distorted. The Ciphertext obtained will then be decrypted to have the plaintext or secret data.

Experiment Results

In the experiment, a picture of Monalisa in JPG format is used as container image. Several variance of noise are used to test the system. The initial parameters can be seen in Table 1.

Table 1: Setting Parameters

Container Image	Monalisa.jpg (1118 x 1500) pixel
Secret Data	Treasuremap.bmp (300 x 222) pixel
Initialisation	1234
Key	5678

Moreover, the steganography file is also observed with several insertion bit of LSB, that is from 1 to 8 bits names as stego level 1 to 8 consecutively. Table 2 shows the sample of RGB replacement.



Figure 7: Number of bits allocated for secret data
(a) Bit 1; (b) Bit 2; (c) Bit 3; (d) Bit 4; (e) Bit 5; (f) Bit 6; (g) Bit 7; (h) Bit 8

Table 2: RGB insertion from pixel (0,0)

LEVEL STEGO	Before Insertion			After Insertion		
	R	G	B	R	G	B
1	18	7	11	18	7	10
2	18	7	11	17	4	9
3	18	7	11	18	1	12
4	18	7	11	20	6	4
5	18	7	11	8	25	4
6	18	7	11	17	36	38
7	18	7	11	35	18	54
8	18	7	11	70	73	180

In stego level of 1 to 4, the change in RGB is not significant. The object starting to have significant difference when reach the stego level 5.

To have more view on the influence of bit inserted, the mean square error and PSNR can also be calculated and summarized in Table 3.

Table 3: Mean Square Error for Each Level

LEVEL STEGO	Image Monalisa.jpg	
	MSE	PSNR (dB)
1	4,80E-06	55,81
2	1,15E-05	52,02
3	3,20E-05	47,64
4	9,94E-05	42,83
5	2,70E-04	38,2
6	9,56E-04	33,12
7	3,87E-03	26,9
8	1,00E-02	20,58

As can be seen from Table 3, the number of bit inserted does degrade the quality of image. The PSNR is degrading from 4 to 6 dB for each level of stego.

The next test is experiment on how noise degrade the recovery process of stenography file. Variance of noise used are from 0,1 to 1.

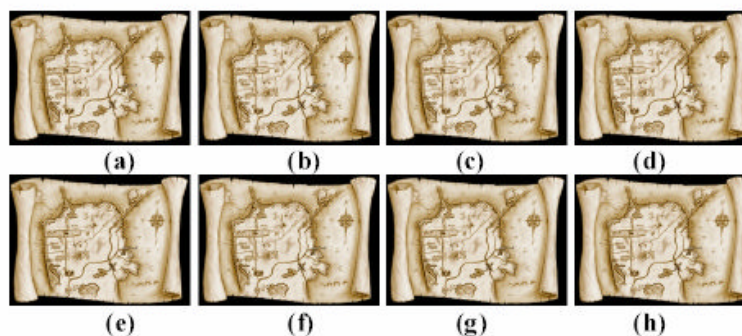


Fig. 8: Decoded Image Without Noise
 (a) Bit 1; (b) Bit 2; (c) Bit 3; (d) Bit 4; (e) Bit 5; (f) Bit 6; (g) Bit 7; (h) Bit 8

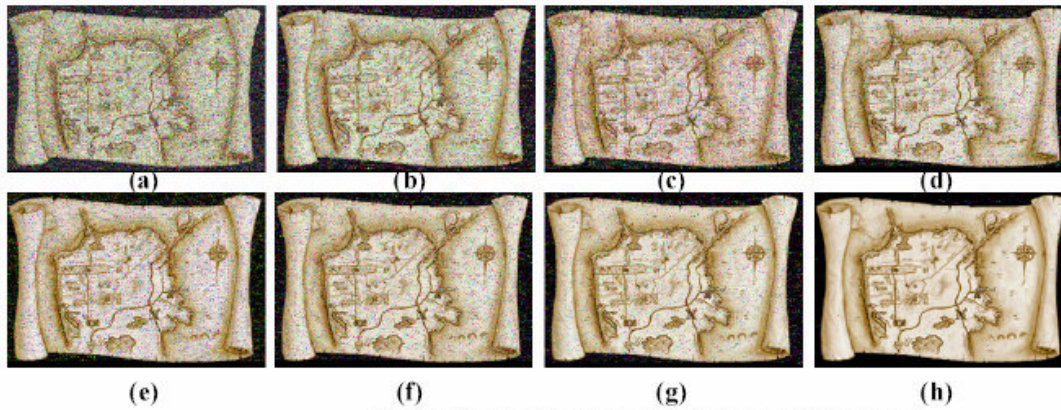


Figure 9: Decoded Image With Noise Variance 0.5
 (a) Bit 1; (b) Bit 2; (c) Bit 3; (d) Bit 4; (e) Bit 5; (f) Bit 6; (g) Bit 7; (h) Bit 8

From Figure 8 and 9 barely seen the degrading effects of noise to the decoded image. The overall result can be measured with the value of *Image Quality Measure* (MSE and PSNR).

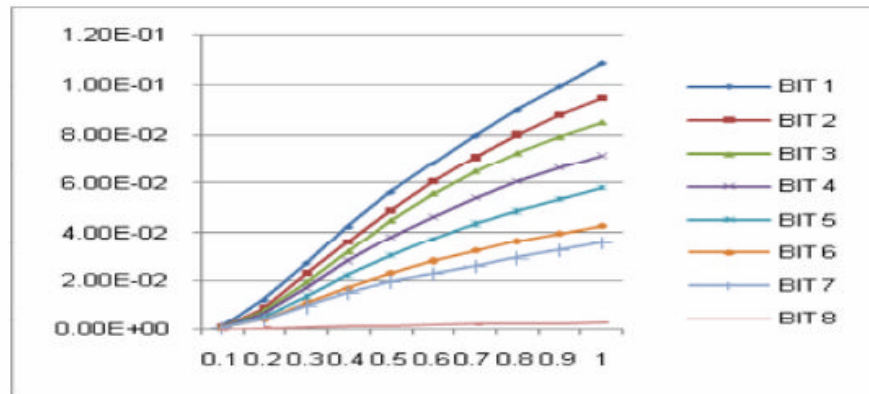


Figure 10: MSE to Noise Variance

The smallest MSE is $1,02 \times 10^{-4}$ and the maximum PSNR is 51,46 dB occur on noise variance 0,1 and *level stego* 8. While maximum MSE of 0,109 and minimum PSNR of 9,50 dB obtained in noise variance 1 and *level stego* 1.

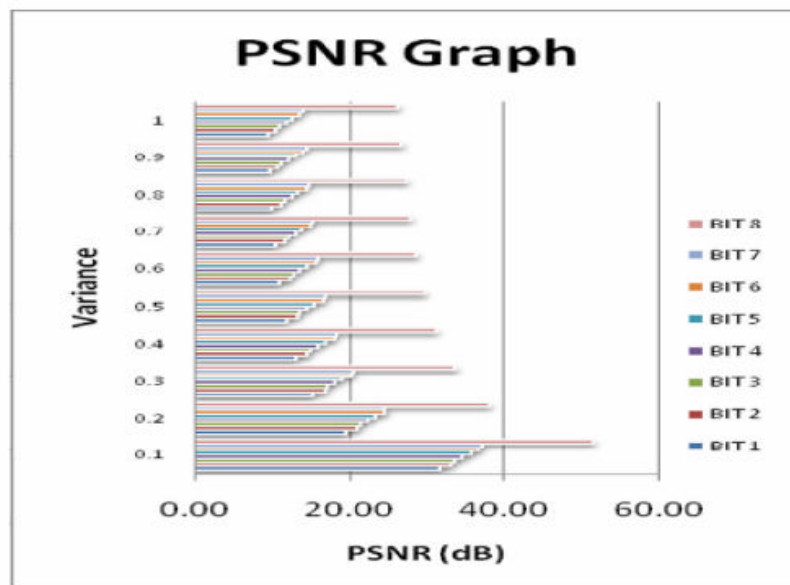


Figure 11: PSNR to Noise Variance

5. Conclusion

1. The amount of bits allocated for secret data does affect the quality of decoded image. The increasing number of bits allocated degrade the image consecutively. The MSE inclining and PSNR declining by adding the number of allocated bits.
2. By adding the variance value of noise gradually, the MSE degrade accordingly. The worst MSE obtained from simulation is 0,109 for noise variance 1.

References

- [1] N. Provos and P. Honeyman, "Detecting Steganographic Content on the Internet", ISOC NDSS'02, San Diego, CA, [August 2001, CITI Techreport], February 2002.
- [2] N. Provos and P. Honeyman, "Hide and Seek: An Introduction to Steganography", Security and Privacy, vol 1, IEEE Comp. Society, 2003.
- [3] X. Zhou, H. Pang, K.L. Tan, "Hiding Data Accesses in Steganographic File System", Proceedings of the 20th International Conference on Data Engineering, IEEE comp society, 2004.
- [4] A.D. Ker, Improved Detection of LSB Steganography in Grayscale Images, Volume 3200/2005, SpringerLink, 2005.
- [5] J. Fridrich, M. Goljan, "Reliable Detection of LSB Steganography in Color and Grayscale Images", IEEE Multimedia Trans., 2001.
- [6] H. Farid, Detecting Steganographic Messages in Digital Images, Technical Report, TR2001-412, Dartmouth College, Computer Science.
- [7] www.ukdw.ac.id/kuliah/si/ericblog/MatakuliahKomputerGrafis_10E92/citraDigital.pdf.
- [8] S.Kusumaningrum, T. Priadi, *Uji Steganography Dengan LSB Untuk Citra Digital*, Final Project, Electrical Engineering UNHAS, 2009.

MoPING – A Cellular Network Data Service Measurement Scheme

Ady Wahyudi Paundu¹⁾, Zahir Zainuddin²⁾, Zulfajri Basri Hasanuddin³⁾, Zaenab Muslimin⁴⁾

1) Department of Elektro, Hasanuddin University Makassar, email adywp@unhas.ac.id

2) Department of Elektro, Hasanuddin University Makassar, email zahir@unhas.ac.id

3) Department of Elektro, Hasanuddin University Makassar, email zulfajri@unhas.ac.id

4) Department of Elektro, Hasanuddin University Makassar, email zaenab@unhas.ac.id

This paper is aimed to propose a scheme for measuring cellular network data services in the perspective of end user. Since it works in a very much similar way with popular PING application, we named it MoPING (Mobile PING).

To capture clearer view of the network, system is designed to record network input parameter as much as possible, such as measurement time and location, user mobility, communication protocol, cellular technology being used, network provider identity, handset type and internet provider identity. The outputs of MoPING are time based parameters like latency, throughput, jitter, round-trip time and network time out. System consists of client and server component, with web based reporting method. Unlike other computer based client system, MoPING use smartphone-based client system.

To describe the features of MoPING, this system is given a set of test-case scenario, such as latency scenario, throughput scenario, mobility scenario and time-out scenario. Two other network measurement systems also being test as comparison object. First is PING as a default worldwide network monitoring program. The other is a web-based measurement testing.

The result of test-case scenarios reveals that MoPING is able to characterize time performance of its input cellular data network. Correlation test of MoPING output against PING output gives a Correlation Coefficient value 0.9982. That value shows that there is strong correlation between MoPING and PING output. Further it shows that both systems gives similar output trend and leads to a conclusion that MoPING output is valid.

Analysis of Sea Surface Temperature using MODIS Data

#Dodi Sudiana, Rifqi Annas

Department of Electrical Engineering, Universitas Indonesia
Kampus Baru UI Depok, 16424. Email: dodii@ee.ui.ac.id

1. Introduction

One of many technologies which can be used to overcome archipelago's problems such as violation of a territory, the determination of natural resources location, and the early warning of natural disaster, is Remote Sensing. This technology uses satellite's ability to capture cartographic image of wide area with its specification. One of satellites which has that ability is Moderate Resolution Imaging Spectroradiometer (MODIS) sensor carried by TERRA/AQUA satellite. Indonesia, which has spreaded over the equator line, has an unique characteristics. There is an interaction between water volume from Indian and Pacific Oceans through the archipelago, so it has a great potential in fishery and other aquatic resources. Fishing ground in the ocean depends on the condition or oceanography parameters, such as sea surface temperature, salinity, sea chlorophyll concentration, weather, etc. which are influenced by dynamic sea's mobility both horizontally and vertically. One of the sea parameters, the Sea Surface Temperature (SST), which could be implemented in fishing ground searching, could be derived from MODIS data. The data are processed using formulas derived from Algorithm Theoretical Basis Documents (ATBD) and implemented to obtain the SST of several sample area in Indonesian ocean.

2. Method

To detect the surface temperature, there are several narrow window in the infrared spectrum (3.5-13 μ m). MODIS sensor observes the Earth 1-2 times/day and has 36 channels, which three of them could be used to calculate the Sea Surface Temperature (SST), i.e.: channel 20, 31, and 32 (Table 1). The stage of data processing is based on the Algorithm Theoretical Basis Documents (ATBD)-MOD25 (Infrared Sea Surface Temperature) which could be downloaded from MODIS website [1].

Table 1. MODIS Channels for SST calculation

Kanal MODIS	Bandwidth (μ m)	Spectral Radiance
20	3.660 -3.840	0.45(300K)
31	10.780 -11.280	9.55 (300K)
32	11.770 -12.270	8.94 (300K)

To process the data, we use MODIS level 1b in HDF (Hierarchical Data Format) format from National Aeronautics and Aerospace Agency (LAPAN). The flowchart of data processing is illustrated in Fig. 1. As referred in the ATBD, channels 20, 31, and 32 and Layer Sensor Zenith (LSZ) data are derived from 1000 m resolution MODIS data and geo.hdf, respectively. In the pre-processing stage, bow-tie correction is implemented to overcome the overlapping images. This is caused by increasing Instantaneous Field of View (IFOV) from 1 \times 1 km at nadir into 2 \times 5 km at maximum scan angle (55 $^\circ$) [2]. To reduce the geometric distortion of the image because of the Earth curvature and other factors such as variation in satellite altitude, speed and position, geometric correction is applied [3]. The radiance value of MODIS data could be derived using equation (1).

$$L_i = \text{radiance_scales}(SI_i - \text{radiance_offsets}) \quad (1)$$

where: L_i = radiance of channel i ; SI_i = integer scale of channel i (Digital Number/DN); *radiance_scales* and *radiance_offsets* are derived from the attributes in the HDF file, depend on the calibrated channels.

The brightness temperature is calculated using the inverse Planck function (black body radiation), which assumes the Earth has a room temperature of 300K, as shown in Eq. (2).

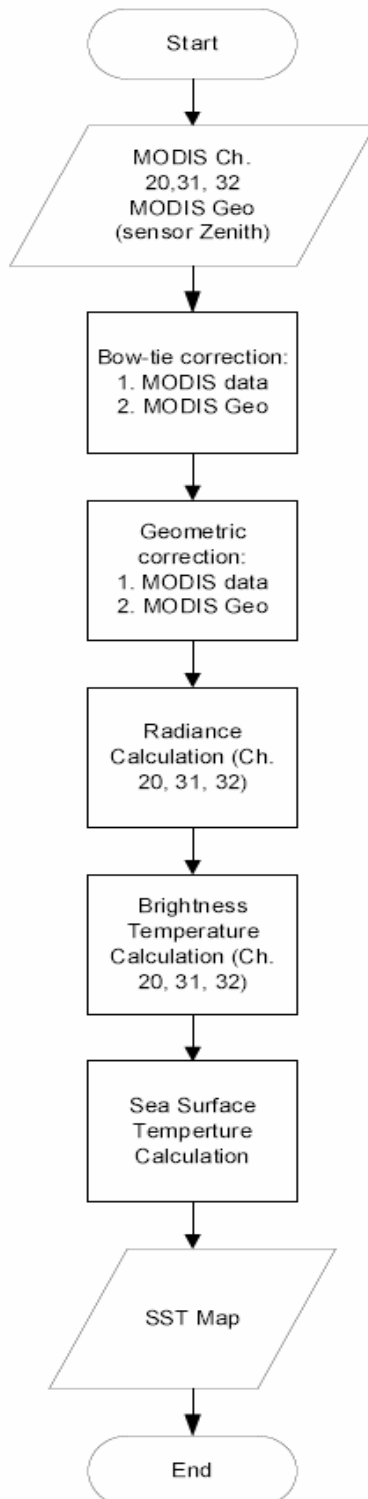


Fig. 1. Flowchart of SST calculation

$$T_b(\lambda) = \frac{C_2}{\lambda \ln \left[\frac{C_1}{\lambda^5 \pi L_\lambda} + 1 \right]} \quad (2)$$

where:

T_b = brightness temperature of channel b (K)

L_λ = spectral radiance ($\text{Wm}^{-2}\text{m}^{-1}\text{sr}^{-1}$)

λ = wavelength (m)

$C_1 = 1.1910659 \times 10^{-5}$ ($\text{m}^{-1} \text{Wsr}^{-1}\text{cm}^4$)

$C_2 = 1.438833$ (cmK)

Finally, the Sea Surface Temperature (SST) is calculated using the formula stated in the ATBD-MOD25 (Infrared Sea Surface Temperature) as shown in Eq. (3).

$$\text{modis_sst} = c_1 + c_2 \times T_{31} + c_3 \times T_{31,32} + c_4 \times (\sec(\theta) - 1) \times T_{31,32} \quad (3)$$

where:

T_{31} = brightness temperature of channel 31

$T_{31,32}$ = brightness temperature difference between channel 31 and 32 ($T_{31} - T_{32}$)

θ = solar zenith angle

c_1, c_2 and c_3 is non-linear SST coefficients which are shown in Table 2.

Table 2. Coefficients for SST calculation

Satellite	Time	Coefficients			
		c1	c2	c3	c4
Aqua	Day	1.152	0.960	0.151	2.021
	Night	2.133	0.926	0.125	1.198
Terra	Day	1.052	0.984	0.130	1.860
	Night	1.886	0.938	0.128	1.094

3. Experiment Results

Based on the above algorithm, we derive the SST for area northern of Java Island (Java Sea) which is cropped from the SST map of the whole scene. The SST results on Java Sea which are analyzed during year 2008 are shown in Table 3.

Table 3. SST in 2008 at location 4:30:2.27 S - 106:30:1.37 E and 5:29:58.67 S - 108:29:54.17 E

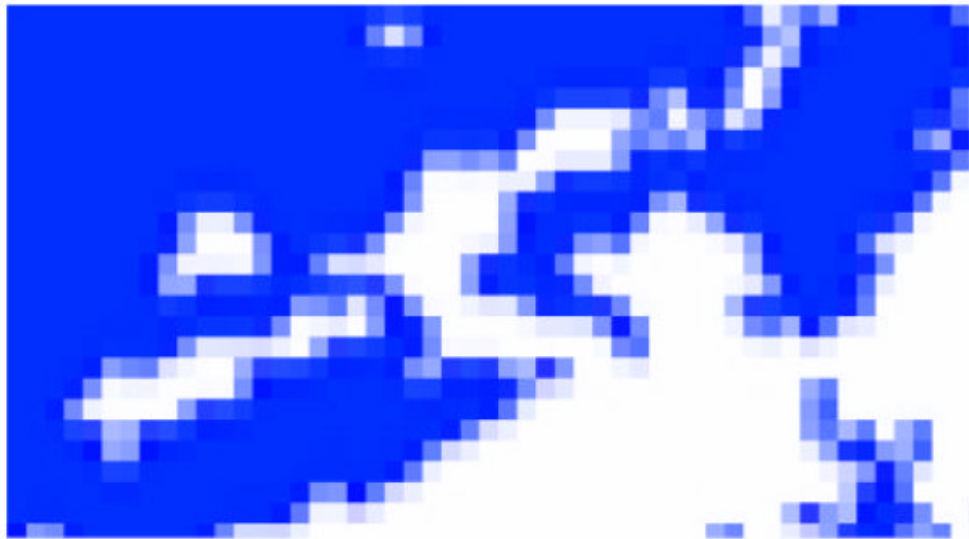
Date	Time	Min. SST (°C)	Max. SST (°C)
1 Jan. 2008	13.57	-57,925	26,523
4 Jan. 2008	13.29	-51,989	27,447
6 Jan. 2008	13.16	-66,296	29,820
16 Jan. 2008	13.53	-38,000	27,000

29 Jan. 2008	13.22	-84,073	-13,866
2 Feb. 2008	12.58	-62,812	28,673
17 Feb. 2008	13.55	-37,680	18,931
18 Apr. 2008	10.29	0,000	29,125
23 Apr. 2008	13.41	0,000	32,499
2 May 2008	13.35	0,000	30,244
8 May 2008	12.58	0,000	30,890
22 May 2008	13.11	-38,000	30,014
5 Jun. 2008	13.24	0,000	30,447
19 Jul. 2008	13.48	0,000	34,908
12 Aug. 2008	12.59	-5,352	32,582
24 Aug. 2008	13.24	0,000	29,532
2 Sept. 2008	13.19	0,000	32,821
18 Sept. 2008	13.18	0,000	29,417
25 Sept. 2008	13.24	0,000	29,504
9 Oct. 2008	13.37	0,000	30,081
23 Oct. 2008	13.49	0,000	32,015
9 Des. 2008	13.08	-76,273	-8,991
16 Des. 2008	13.13	-52,775	23,706
17 Des. 2008	13.56	0,000	28,788
28 Des. 2008	13.38	0,000	29,493
30 Des. 2008	13.26	-17,856	18,726

In Table 3, since some area of the image are covered by clouds, there are some data which have negative or zero values. Other disturbances in MODIS data, such as cloud coverage, striping errors, sunglint, etc. affect the accuracy of fishing ground mapping. As an example, Fig. 2(a) and (b) showed fishing ground's area of interests which has no cloud and cloud cover, respectively. In Fig. 2(a), which is cloud free imagery, the SST ranges from 21°C to 33°C. Meanwhile, in Fig. 2(b), the range is between -21°C to 28°C. High SST in July is due to East Monsoon which caused Java Island become more dryer. In fact, Asia has usually high temperature and low pressure during April-October when the Sun began to shift to Northern Hemisphere. The lowest SST in December is affected by Western Monsoon, in which high pressure is centered in Asia and caused high rainfall in Indonesia, including Java Sea [4].



(a)



(b)

Fig. 2. Example of cloud covered data. (a) Data without cloud cover; (b) Data with cloud cover

Therefore, the data on Jan. 29 and Dec. 9, 2008 could not be used since most of the area in the imageries are covered with cloud as shown in Fig. 3 and 4, respectively.

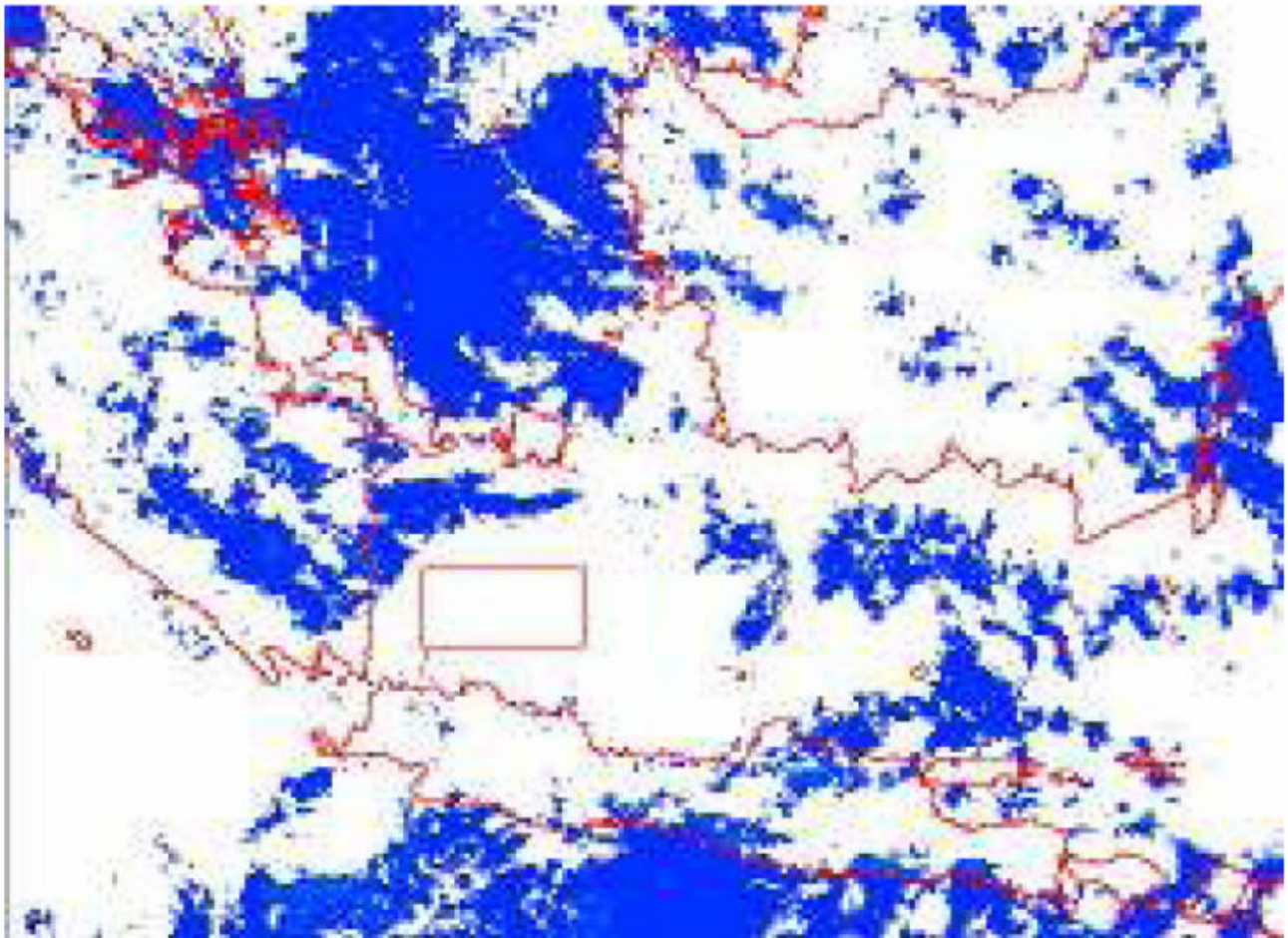


Fig. 3. SST mapping on Jan. 29, 2008

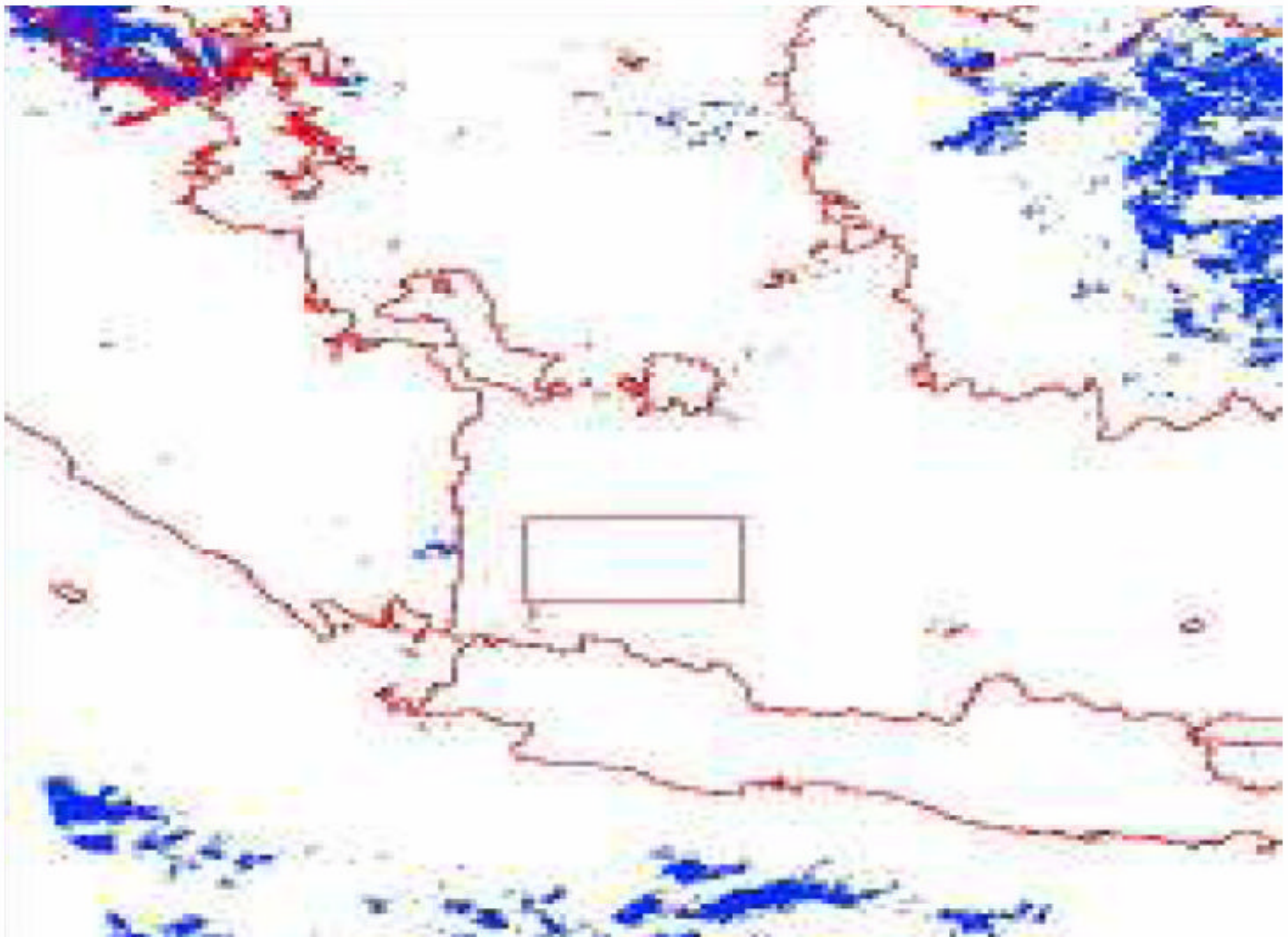


Fig. 4. SST mapping on Dec. 9, 2008

To minimize the effect of cloud cover, since the SST has negative values, only maximum SST will be considered as valid data, as shown in the rightmost column in Table 3. In average the SST in Java Sea during year 2008 is about 28.887°C, while the minimum and maximum SST is 34.908°C (on July 19), and 18.726°C (Dec. 30), respectively. Fig. 5 showed the graphical illustration of maximum SST during year 2008. In the Figure, high SST on Jan.-Feb., May-Jun., and Aug.-Nov. proved that the SST has strong correlation to the weather and climatological changes in Java Sea during the dry and rainy seasons. Other factors which have relationship to this changes are the Monsoon, wind direction, wave height, and other oceanographic factors.

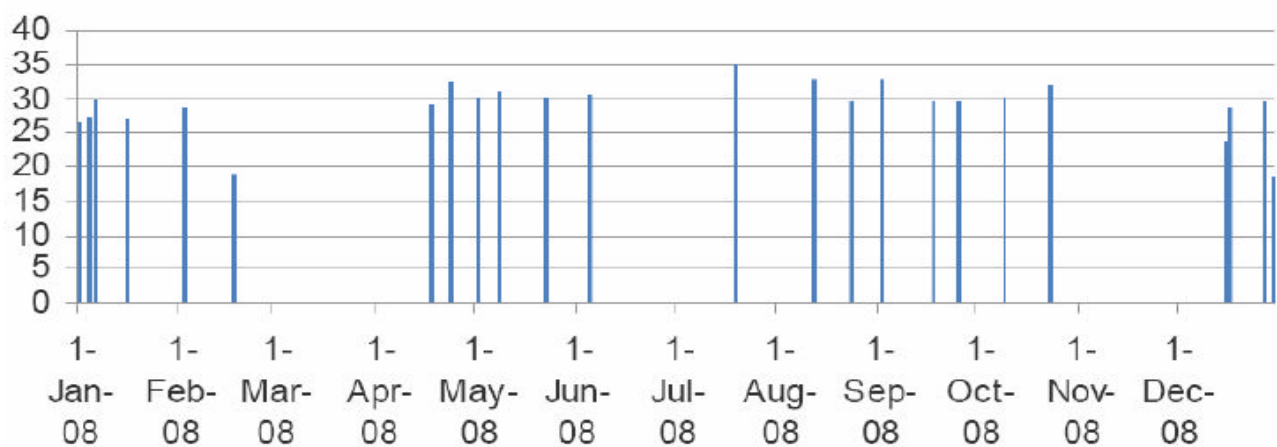


Fig. 5. SST of Java Sea area from Jan.-Dec. 2008

4. Conclusions

A method to retrieve the SST from MODIS data using ATBD-MOD25 has been proposed. The results showed a dynamic temperatures during dry and rainy seasons and in Java Sea (location: 4:30:2.27 S - 106:30:1.37 E and 5:29:58.67 S - 108:29:54.17 E) during year 2008, the average, minimum and maximum SST are 28.887°C, 34.908°C (on July 19), and 18.726°C (on Dec. 30), respectively. Several disturbances such as cloud cover, striping error, sunglint, and other oceanographic factors caused a failure in deriving accurate SST.

References

- [1] O.B. Brown and P.J. Minnett, with contributions from R. Evans, E. Kearns, K. Kilpatrick, A. Kumar, R. Sikorski and A. Zavody, "MODIS Infrared Sea Surface Temperature Algorithm", Algorithm Theoretical Basis Document, Version 2.0, University of Miami, April 30, 1999
- [2] Miftahuraifah Quratun Aini, S.Si, "Kajian Distribusi Potensi Fitoplankton di sebagian Laut Utara Jawa menggunakan Citra MODIS", Proceeding Geo-Marine Research Forum, 2007.
- [3] T.M Lillesand, and R.W. Kiefer, "Remote Sensing and Image Interpretation", New York: John Wiley & Sons Inc., 1979.
- [4] N.M. Short, Sr., "Remote Sensing Tutorial", <http://rst.gsfc.nasa.gov/>, 2008. Last access on July 10, 2010.

The Design and Development of Facebook Based Agenda Application With BlackBerry Integration

Ibnu Gunawan, Yulia Kendengis, Deny Hendrata
Informatic Engineering Department, Petra Christian University
Siwalankerto 121 – 131 Surabaya 60236 Indonesia
ibnu@petra.ac.id, yulia@petra.ac.id, m26406140@petra.ac.id

ABSTRACT

BlackBerry users need a BlackBerry application to inform as well as promote the events which he had built from the BlackBerry to his Facebook friends. Users also want a Facebook Application that utilizes the advantages of the features possessed by the Facebook event and integrate it with the BlackBerry event.

This mobile application for BlackBerry is made with the BlackBerry Java Development Environment (JDE), while the Agenda application is made on the Facebook Platform with the PHP Client Library provided by Facebook. The data storage is built uses the MySQL Database. And then we test the application to meet the objectives in the first paragraph.

Based on test results, it can be concluded that the application integrates well with the BlackBerry Event in terms of Event features possessed by Facebook, such as the Create Event, Edit Event, Invite, Cancel Event, Sharing / Publishing feature and synchronizes the Events. The agenda application also handles the other two types of PIM in BlackBerry handset, To Do List and Contact.

Key words: Facebook, BlackBerry, Agenda, Event, Synchronization.

1. Introduction

In Indonesia, the total number of Blackberry user is going higher and higher as the advance of cellular technology. According to survey that has been launched by www.detik.com, the total number of Blackberry user on Indonesia per July 2009 is about 300 – 400 person. It is the highest number in the world, and rising about 500% last year.

One of the cause is the social networking site called Facebook. Even now, facebook is trend in our lifestyle, Every one loves facebook. They use it to socialized with other. And, one of the most important thing is, we can access facebook from our blackberry.

Most Blackberry user is business man / woman that very very busy with their activity. So, there is agenda application build in on blackberry handset. These agenda application is equipped with reminder that can ring blackberry whenever event is coming. The problem is arise when the blackberry user want to used his/her blackberry to open facebook. There is no application on facebook that can get blackberry personal data like PIM or event and/or agenda to sychronized it with facebook.

So there is three factor that push us to make these facebook based agenda application with blackberry integration. First and the most important is there is no application like this on facebook, the second is there is huge blackberry user and the third is most of them are business man / woman that used facebook too. In the next section we will describe the technology to make this application.

2. Background

To make this agenda application, we used the development technology from both facebook and blackberry, and because the blackberry is java based, then we used the java micro edition too.

2.1 Blackberry

BlackBerry is a mobile device made by Research In Motion (RIM). The BlackBerry have a full capability as a smartphone i.e an Address Book, Calendar, To Do List and push mail through gsm or

cdma carrier. BlackBerry is also a name from OS that come with the Blackberry devices. The Blackberry OS is fully support MIDP 1.0 and WAP 1.2, the Blackberry OS 4 have a fully support of MIDP 2.0 subset.

BlackBerry is a backward compatible devices, it's mean that the application that can run smoothly on OS 4.2 will run on higher version OS. Actually, the compatibility of the application is defined by the API that used to compiled the application. For example, when the application is used API 4.2, although it compiled by JDE 4.5, it will run smoothly on OS 4.2 (King, 2009).

2.1.1 Blackberry PIM

PIM is a application that defined the personal information group. There are three group of personal information on Java ME devices include the BlackBerry : Calendar, Address Book (Contacts), dan Tasks (To Do List) (King, 2009). This three group is showed on fig 2.1

PIM in the BlackBerry is saved on a PIMList, an entry (for example is Calendar) is called PIMItem that consist of data fields. In other word, there is some PIMItem that grouped on a PIMList (PIMItem is an element of a PIMList). A Data Field that lay on a PIMItem can consist of many data field. Such as String, Date, Integer, etc. There is two main class that can be used to manipulate the PIM data, ie:

- `javax.microedition.pim`
is a standard class that consist of PIM basic feature.

- `net.blackberry.api.pdap`

This is a specific class made for blackberry. This class has a new feature that only can be used on blackberry handset if the application is verified by sign in using special code from RIM.

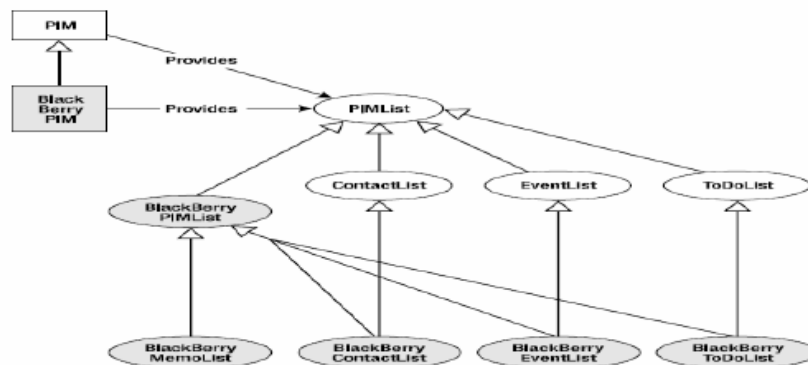


Figure 2.1 : PIM Structure

2.2 Facebook

In order to develop a facebook application, on 24 May 2007 The facebook has launched a facebook platform. This platform provide a framework for the facebook software developer (Wagner, 2008). They used a special mark up language called FBML (Facebook Markup Language) and FQL (Facebook Query Language) to query data from it. In the next section we will digg more depper to canvas. Canvas is a UI for facebook application.

2.2.1 Canvas

Canvas can be accesed from the url : http://apps.facebook.com/application_name. Canvas application is consist of FBML and iFrame. one thing to consider to choose a a canvas is a component that build it. FBML is a kind of *Canvas* that can be used a FMBL *tag* to built the UI, because of that, this canvas is like a parser, they parse the FBML tag first on the server before they give us the whole UI picture. In another word, iFrame did not need Facebook server to give the whole UI picture, because they use a HTML that come from the developer application server. The detail picture of FBML and iFrame is on Fig 2.2.

2.2.2 Facebook API

Facebook API is a REST (Representational State Transfer) based interface. REST is an architecture that used HTTP. Facebook provide an REST like implementation for their API. It is not pure REST because they did not give an URI for an individual resource (methods, object). This API interface is implemented using single end point, which is followed by all data for requesting something, on POST or GET parameter. This is like a RPC or known as Remote Procedure Call through interface that look a like

HTTP. This is the rule from facebook for their API: Each API Call must have their own parameter, and each application must have their own information and security hash to make sure the API Call is valid (Maver & Popp, 2009). For example, to manually call an API function named `friends.getAppUsers()`, we can use a URL like this:

```
http://api.facebook.com/restserver.php?method=facebook.friends.getAppUsers&session_key=XXXXXXXXXXXXXXXXXX&api_key=XXXXXXXXXXXXXXXXXX&call_id=1234557716.362&v=1.0&sig=XXXXXXXXXXXXXXXXXXXX
```

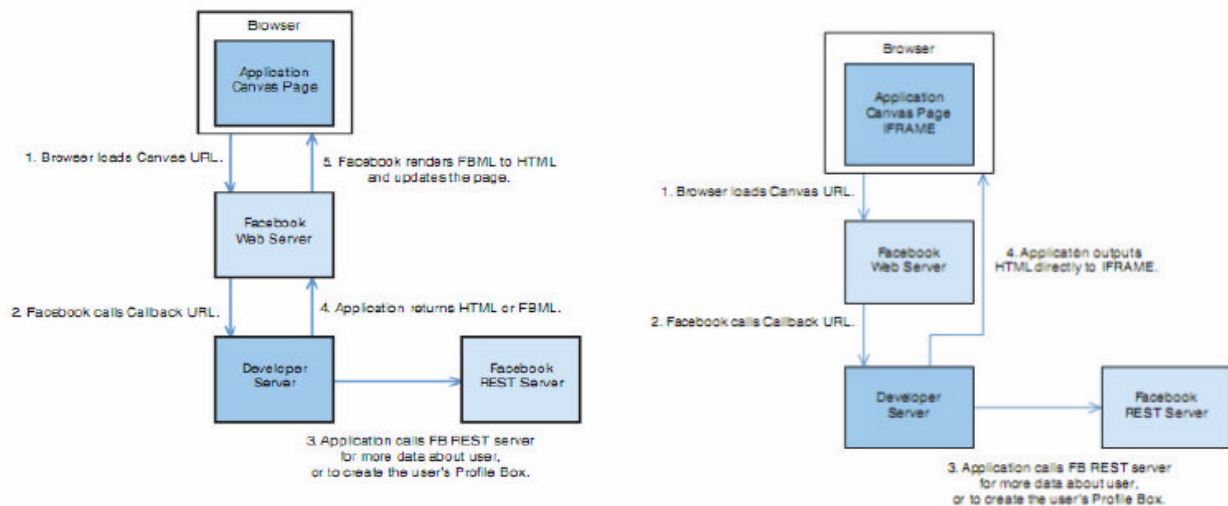


Figure 2.2: FBML and iFrame

It would be so difficult for programmer to call an API function manually, fortunately Facebook provide a multilanguage wrapper like PHP to adhere this problem. For example to make a facebook API Call from PHP, the listing program may look like this:

```
$facebook = new Facebook($app_apikey, $app_secretkey);
$result = $facebook->api_client->friends_getAppUsers();
```

So there, it can be conclude that PHP Client Library just consist a method / function wrapper to make an API Call for REST Server (wagner, 2008). For more detail we can look to Figure 2.4. Officially, facebook has fully support PHP 4 and 5 client library, and Java too. Using PHP, all API Call is provide on object `$facebook->api_client`. To instantiate a facebook object, the listing program my look like this:

```
<?php
Require_once 'facebook.php';
Require_once 'facebookapi_php5_restlib.php';
$appapikey = 'api_key'; //api key aplikasi
$appsecret = 'secret_key'; //secret key aplikasi
$facebook = new Facebook($appapikey, $appsecret);
$friends = $facebook->api_client->friends_get(); // API call
?>
```

In the next chapter we will describe how to use these technology to make our Agenda application.

3. System Design

Basically, our agenda application that make on facebook platform standard would be host on a web server, and then, the mobile application is a blackberry application that made on Java ME platform. So we have two application, and there is one database for agenda application that hosted on a web server. Our agenda application will made by PHP 5 client library and hosted on apache web server with My SQL database.

3.1 Requirement analysis

As stated before, a good agenda application must have 3 main activity ie: manage event (for eg an appointment or other agenda), manage to do list, manage contact. Beside that, user may want to share a picture from an event, or a movie to promote an event. Because of that need, facebook platform can enabling an application to integrate itself with event on facebook, so the user can share something to the facebook's news feed and wall.

On the other side, in mobile Blackberry application, it must have capabilities to send user data from Blackberry device's Calendar, Task and Phonebook to our agenda. And the most important is that this mobile application can synchronize the data from the Blackberry to our agenda and vice versa. So it would be maintain the consistency data between facebook and blackberry. To make it a good design we used an uml shown in Figure 3.1.

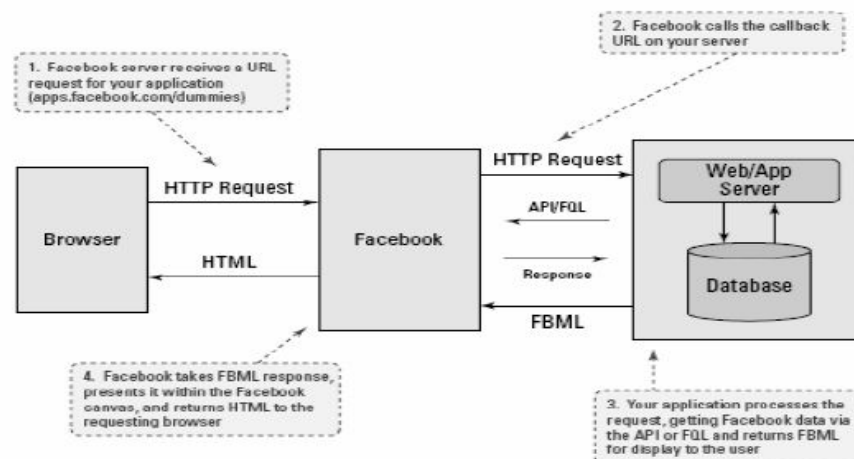


Figure 2.4: An API Call

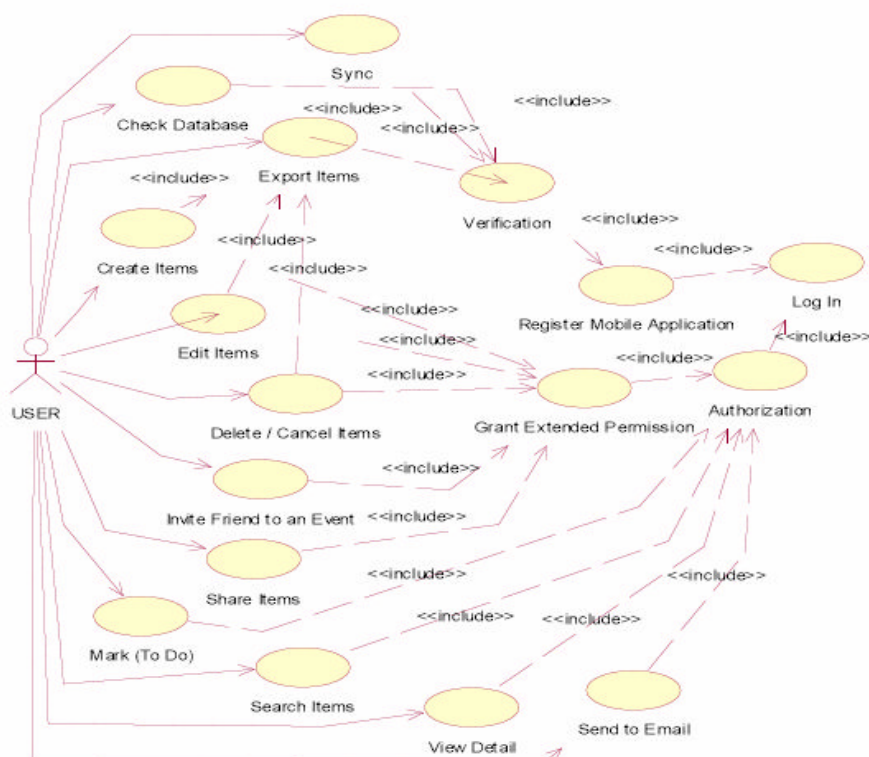


Figure 3.1: Agenda app UML use case diagram

From an use case diagram in Figure 3.1 we can built a class diagram for our agenda application. It is shown in Figure 3.2. And finally the E-R diagram is shown in Figure 3.3

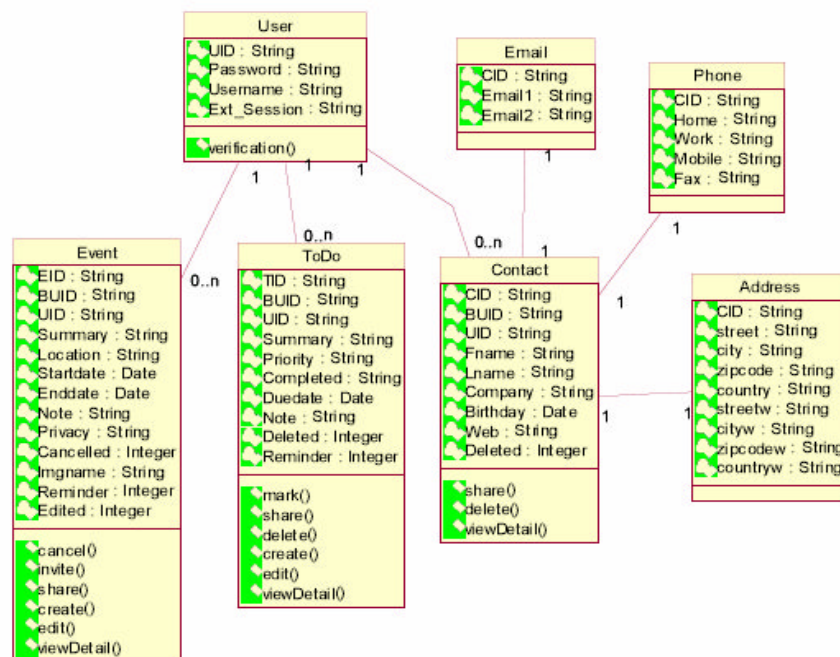


Figure 3.2: Class Diagram

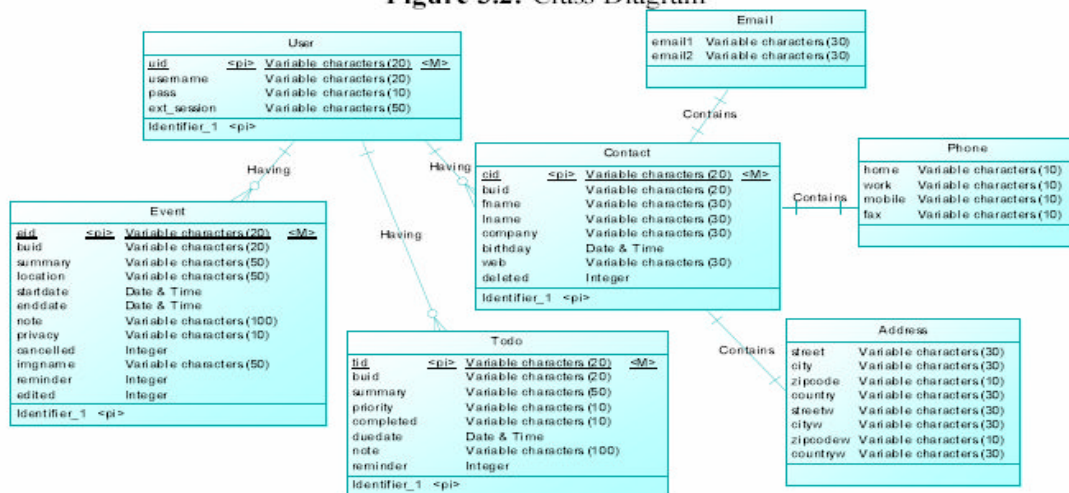


Figure 3.3: E-R Diagram

From the three diagram above, we can prepare to implement this to blackberry mobile device and facebook development platform. In the next chapter we will describe the implementation of the design of our facebook based agenda application.

4. System Implementation

We will built our application on few steps. Begin with developing the blackberry mobile application and we will continue with development of facebook application platform.

4.1 Blackberry Application

On Blackberry application development, first we begin with setting the workspace of blackberry JDE 4.7.0. we can see the illustration in Figure 4.1. after setting the workspace we can continue with create a new project like illustration in Figure 4.2.

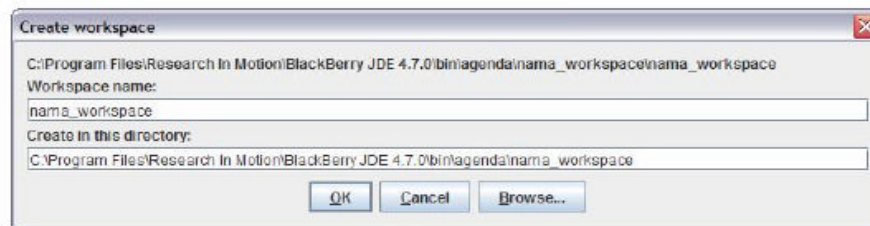


Figure 4.1: Setting workspace

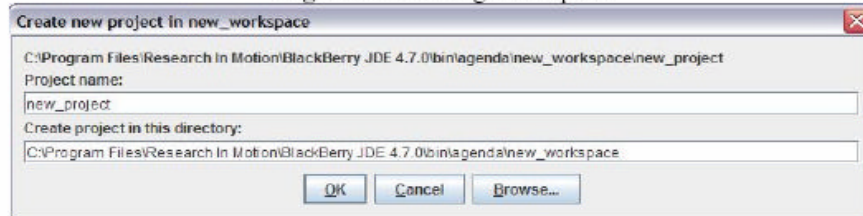


Figure 4.2: Create a new project

After that we will continue with coding, and if its finished, we can compile it and the blackberry JDE will show his simulator like Figure 4.3



Figure 4.3: Blackberry JDE 4.7.0

4.2 Facebook Application

Same as Blackberry application, we must setting the facebook environment first. But before we set the facebook environment, we must have a facebook account and has registered in www.facebook.com/developers. Then we can follow the instruction on screen, begin shown as Figure 4.4.



Figure 4.4: The facebook developer site

After we finish develop, we can testing the application and it would be shown in next chapter.

5. System Testing

In this chapter we will review our system. We begin with the facebook first and then continued with the blackberry application. Figure 5.1 show the UI for our agenda application and blackberry mobile application.

6. Conclusion

This is our conclusion based on our testing, first, there is a way to synchronized the agenda from blackberry to event on facebook. Second, these synchronized application is very sensitive in latency especially in API latency. It is caused by slow respond or time out on facebook server when our application make an API request. But afterall is very usefull application.

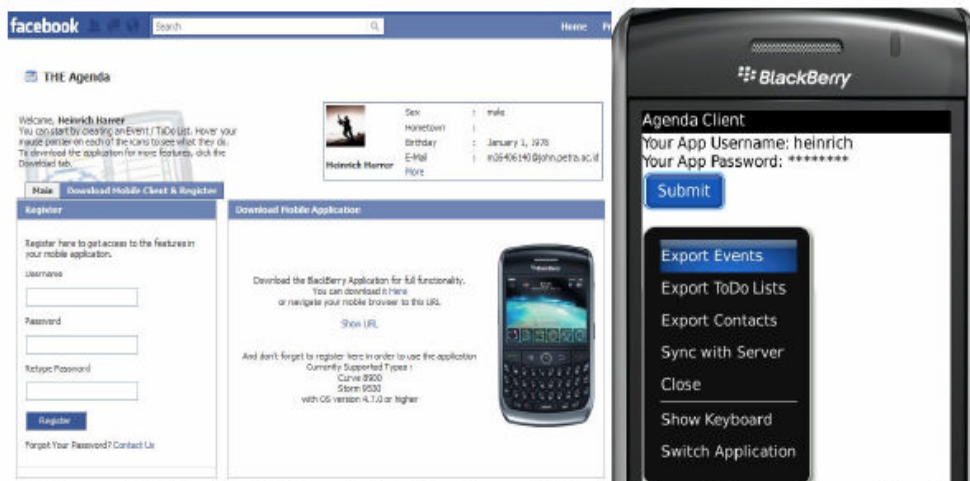


Figure 5.1: Facebook Agenda Application and blackberry mobile agenda application

And then how to synchronized it shown in Figure 5.2 and we see that it work well.

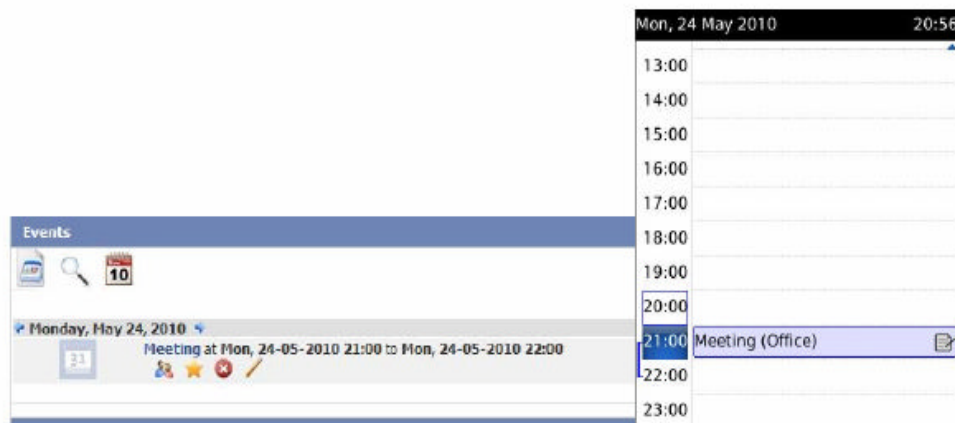


Figure 5.2: Mobile Application

7. References

- Agnes, M. (2002). *Websters new world college dictionary and thesaurus* (2nd ed.). New York : Hungry Minds, Inc.
- King, C. (2009). *Advanced BlackBerry development*. New York : Apress
- Maver, J., & Popp, C. (2009). *Essential Facebook development : Build successful applications for the Facebook platform*. Boston : Pearson Education, Inc.
- Noor, R.C. (2009, July 31). *Indonesia akan jadi pengguna BlackBerry terbesar dunia*. Detikinet. Retrieved November 12, 2009, from <http://www.detikinet.com/read/2009/07/31/115338/1175020/328/indonesia-akan-jadi-pengguna-blackberry-terbesar-dunia>.
- Research In Motion. (2009). *BlackBerry device application development : Getting started guide*. Waterloo : Research In Motion Limited. http://docs.blackberry.com/en/developers/deliverables/5783/BlackBerry_Java_Development_Environment_getting_started.pdf
- Topley, K. (2002). *J2ME in a Nutshell*. New York : O'Reilly.
- Wagner, R. (2008). *Building Facebook application for dummies*. Hoboken : Wiley Publishing, Inc.

Performance Analysis of Dijkstra, A* and Ant Algorithm for Finding Optimal Path Case Study: Surabaya City Map

Leo Willyanto Santoso, Alexander Setiawan, Andre K. Prajogo
Informatics Department, Faculty of Industrial Engineering
Petra Christian University
Jl. Siwalankerto 121-131 Surabaya, 60236
leow@petra.ac.id

1. Introduction

In the programming world there are so many algorithms that can be used to do an optimal path finding, for example Dijkstra, Ant and A* algorithm. However, there has been little work on the benchmarking in terms of the performance analysis of these algorithms [3, 7]. In this paper, we compare the performance of Dijkstra, Ant and A* algorithm to better know the characteristic of each algorithm when finding optimal path of certain route.

It would need the appropriate algorithm to search the optimal route, therefore, the purpose of this research is to explore what a good routing algorithm by comparing the 3 types of algorithms that can be used to solve the problem route search is: Ant algorithm, Dijkstra and A* in hopes of finding the best algorithm for searching a route.

The problems to be solved in this research are as follows:

1. How to implement an optimal routing algorithm in this application.
2. How to create a user friendly and easily understandable application.
3. How to set the constraints in this application.
4. How to implement an optimal routing algorithm on several goals at once.

The purpose of this research is to make an application to compare search algorithm routes between the three algorithms used in the search for optimal route so that the results of the third comparison of these algorithms can be determined which algorithms are suitable for searching the optimal route.

The remaining part of this paper is organized as follows. Section 2 presents an overview of current proposal for dealing with routing algorithm. Section 3 depicts the approach that we have delineated to solve the proposed problems. Moreover, the performance of proposed methods were discussed. Finally, section 4 concludes the paper.

2. Background

In graph theory, the shortest path problem is the problem of finding a path between two vertices (or nodes) such that the sum of the weights of its constituent edges is minimized. An example is finding the quickest way to get from one location to another on a road map; in this case, the vertices represent locations and the edges represent segments of road and are weighted by the time needed to travel that segment [2, 6].

Multiple destination path finding problem is problem to find a solution path which must pass through several places at once. This problem can be solved by two approaches, brute force and heuristic [1].

2.1 Ant Colony Algorithm

This algorithm is aiming to search for an optimal path in a graph, based on the behavior of ants seeking a path between their colony and a source of food.

The original idea comes from observing the exploitation of food resources among ants, in which ants' individually limited cognitive abilities have collectively been able to find the shortest path between a food source and the nest. The first ant finds the food source (F), via any way (a), then returns to the nest (N), leaving behind a trail pheromone (b). Ants indiscriminately follow four possible ways, but the

strengthening of the runway makes it more attractive as the shortest route. Ants take the shortest route; long portions of other ways lose their trail pheromones [5].

- An ant will move from node i to node j with probability:

$$P_{i,j} = \frac{(\tau_{i,j}^\alpha)(\eta_{i,j}^\beta)}{\sum (\tau_{i,j}^\alpha)(\eta_{i,j}^\beta)} \quad (1)$$

where,

$\tau_{i,j}$ is the amount of pheromone on edge ij

α is a parameter to control the influence of $\tau_{i,j}$

$\eta_{i,j}$ is the desirability of edge ij (a priori knowledge, typically $1/d_{ij}$, where d is the distance)

β is a parameter to control the influence of $\eta_{i,j}$

- It must visit each city exactly once.

- Pheromone Update:

$$\tau_{i,j} = (1 - \rho)\tau_{i,j} + \Delta\tau_{i,j}$$

where

$\tau_{i,j}$ is the amount of pheromone on a given edge ij

ρ is the rate of pheromone evaporation

$\Delta\tau_{i,j}$ is the amount of pheromone deposited, typically given by

$$\Delta\tau_{i,j}^k = \begin{cases} 1/L_k & \text{if ant } k \text{ travels on edge } i, j \\ 0 & \text{otherwise} \end{cases} \quad (2)$$

where L_k is the cost of the k th ant's tour (typically length).

2.2 Dijkstra Algorithm

Dijkstra's algorithm is a graph search algorithm that solves the single-source shortest path problem for a graph with nonnegative edge path costs, producing a shortest path tree.

In the following algorithm [4], the code $u := \text{vertex in } Q \text{ with smallest dist}[\]$, searches for the vertex u in the vertex set Q that has the least $\text{dist}[u]$ value. That vertex is removed from the set Q and returned to the user. $\text{dist_between}(u, v)$ calculates the length between the two neighbor-nodes u and v . The variable alt on line 13 is the length of the path from the root node to the neighbor node v if it were to go through u . If this path is shorter than the current shortest path recorded for v , that current path is replaced with this alt path. The previous array is populated with a pointer to the "next-hop" node on the source graph to get the shortest route to the source.

```

1 function Dijkstra(Graph, source):
2   for each vertex v in Graph:           // Initializations
3     dist[v] := infinity                 // Unknown distance function from source to v
4     previous[v] := undefined           // Previous node in optimal path from source
5   dist[source] := 0                    // Distance from source to source
6   Q := the set of all nodes in Graph   // All nodes in the graph are unoptimized - thus are in Q
7   while Q is not empty:                // The main loop
8     u := vertex in Q with smallest dist[]
9     if dist[u] = infinity:
10      break
11    // all remaining vertices are inaccessible from source
12    remove u from Q
13    for each neighbor v of u:           // where v has not yet been removed from Q.
14      alt := dist[u] + dist_between(u, v)
15      if alt < dist[v]:                 // Relax (u,v,a)
16        dist[v] := alt
17        previous[v] := u
18  return dist[]

```

An upper bound of the running time of Dijkstra's algorithm on a graph with edges E and vertices V can be expressed as a function of $|E|$ and $|V|$ using the Big-O notation.

For any implementation of set Q the running time is $O(|E| \cdot dk_Q + |V| \cdot em_Q)$, where dk_Q and em_Q are times needed to perform decrease key and extract minimum operations in set Q , respectively.

The simplest implementation of the Dijkstra's algorithm stores vertices of set Q in an ordinary linked list or array, and extract minimum from Q is simply a linear search through all vertices in Q . In this

case, the running time is $O(|V|^2 + |E|) = O(|V|^2)$. For sparse graphs, that is, graphs with far fewer than $O(|V|^2)$ edges, Dijkstra's algorithm can be implemented more efficiently by storing the graph in the form of adjacency lists and using a binary heap, pairing heap, or Fibonacci heap as a priority queue to implement extracting minimum efficiently. With a binary heap, the algorithm requires $O((|E| + |V|)\log |V|)$ time (which is dominated by $O(|E| \log |V|)$, assuming the graph is connected), and the Fibonacci heap improves this to $O(|E| + |V| \log |V|)$.

2.3 Algoritma A* (A Star)

A* (pronounced "A star") is a computer algorithm that is widely used in path finding and graph traversal, the process of plotting an efficiently traversable path between points, called nodes. As A* traverses the graph, it follows a path of the lowest *known* path, keeping a sorted priority queue of alternate path segments along the way. If, at any point, a segment of the path being traversed has a higher cost than another encountered path segment, it abandons the higher-cost path segment and traverses the lower-cost path segment instead. This process continues until the goal is reached [8, 9].

The time complexity of A* depends on the heuristic. In the worst case, the number of nodes expanded is exponential in the length of the solution (the shortest path), but it is polynomial when the search space is a tree, there is a single goal state, and the heuristic function h meets the following condition:

$$|h(x) - h^*(x)| = O(\log h^*(x))$$

where h^* is the optimal heuristic, the exact cost to get from x to the goal. In other words, the error of h will not grow faster than the logarithm of the "perfect heuristic" h^* that returns the true distance from x to the goal

3. Implementation and Testing

In this section, discussed the use and testing of application. Testing process conducted by performing the test route search using three existing path finding algorithms with multiple destinations at once and by providing constraints. Applications have been tested on computers with Intel® Core2Duo processor specifications™ T5550@1.83 GHz with 2 GB of memory.

Using this application, users can directly search the route because the application has been entered the point - the crossing point and the points are already connected, however, the user must enter a first starting point and desired point to do a search and choosing one among the three algorithms that have been provided. Figure 1 shows entering the destination and choosing the algorithm.

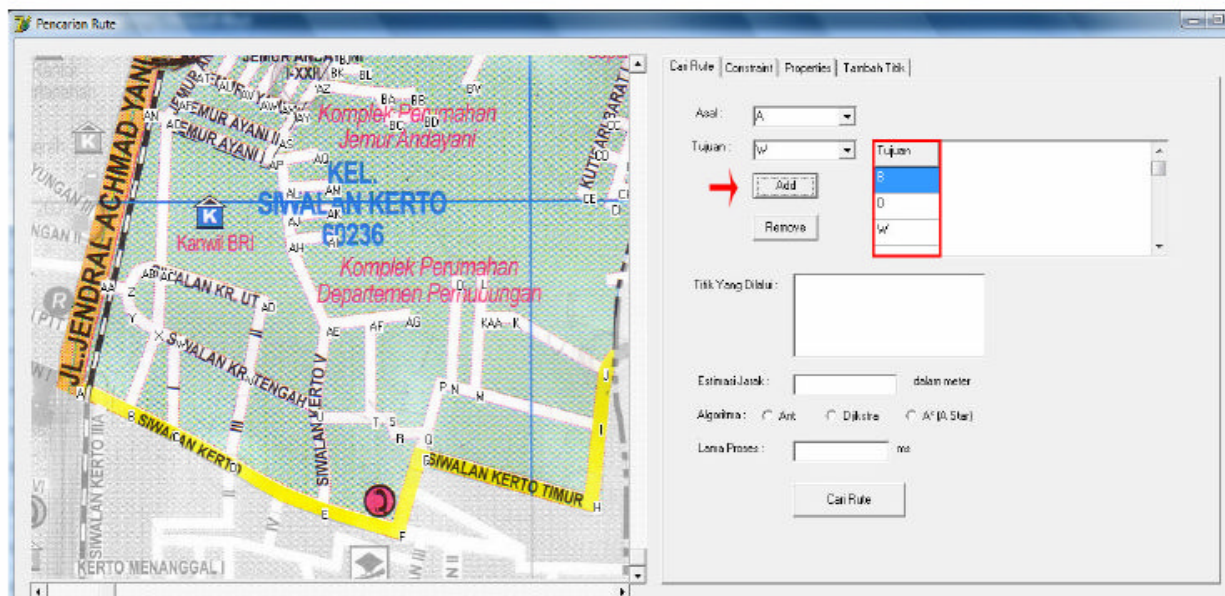


Figure 1: Entering Destination and Choosing Algorithm on Application

After entering the destination and choose the algorithm that is used then the user can press the search button after that will show the route, mileage and duration of the search process route. This can be seen in Figure 2.

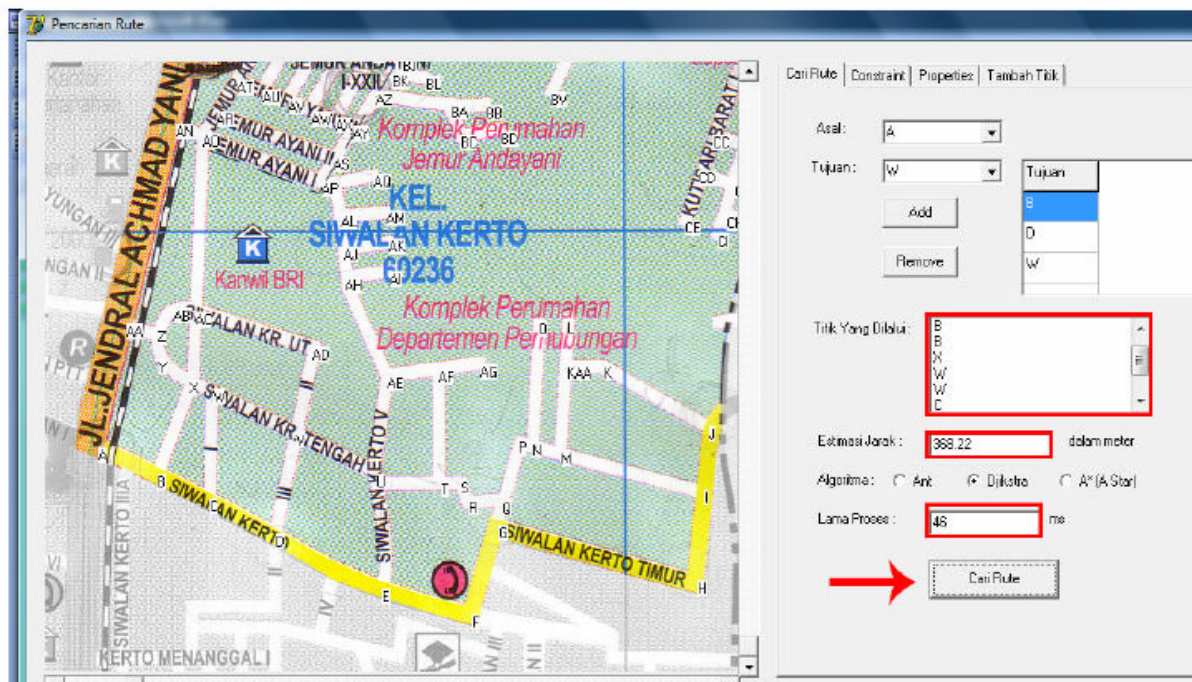


Figure 2: Route Search Result

Testing the application carried out by comparing the results of the 3 existing algorithms, the testing conducted are as follows:

- Testing the running time of algorithm
- Testing the correctness of the calculation in the program
- Testing mileage generated by the algorithm

There are two kinds of testing method of multiple destination on this application, heuristic methods and the Traveling Salesman Problem (TSP) where the heuristic method has better speed but with less accuracy. The test is done with destination "AE - U - E - G - BJ - AP". Here are the test results and TSP heuristic method:

Table 1: Testing Dijkstra's algorithm with heuristic methods

No.	Point passed (with destination AE - U - E - G - BJ - AP)	Distance traveled (meter)	Time (ms)
1.	A-B-C-D-E-U-AE-AH-AJ-AL-AP-AS-AY-AZ-BK-BJ-BK-AZ-AY-AS-AP-AL-AJ-AH-AE-AF-T-S-R-Q-G	3007.61	140
2.	A-B-C-D-E-U-AE-AH-AJ-AL-AP-AS-AY-AZ-BK-BJ-BK-AZ-AY-AS-AP-AL-AJ-AH-AE-AF-T-S-R-Q-G	3007.61	141
3.	A-B-C-D-E-U-AE-AH-AJ-AL-AP-AS-AY-AZ-BK-BJ-BK-AZ-AY-AS-AP-AL-AJ-AH-AE-AF-T-S-R-Q-G	3007.61	141
4.	A-B-C-D-E-U-AE-AH-AJ-AL-AP-AS-AY-AZ-BK-BJ-BK-AZ-AY-AS-AP-AL-AJ-AH-AE-AF-T-S-R-Q-G	3007.61	140
5.	A-B-C-D-E-U-AE-AH-AJ-AL-AP-AS-AY-AZ-BK-BJ-BK-AZ-AY-AS-AP-AL-AJ-AH-AE-AF-T-S-R-Q-G	3007.61	140

Table 2: Testing A* Algorithm with Heuristic methods

No.	Point passed (with destination AE – U – E – G – BJ – AP)	Distance traveled (meter)	Time (ms)
1.	A-B-C-D- <u>E</u> - <u>U</u> - <u>AE</u> -AH-AJ-AL- <u>AP</u> -AS-AY-AZ- BK- <u>BJ</u> -BK-AZ-AY-AS-AP-AL-AJ-AH-AE- AF-T-S-R-Q- <u>G</u>	3007.61	109
2.	A-B-C-D- <u>E</u> - <u>U</u> - <u>AE</u> -AH-AJ-AL- <u>AP</u> -AS-AY-AZ- BK- <u>BJ</u> -BK-AZ-AY-AS-AP-AL-AJ-AH-AE- AF-T-S-R-Q- <u>G</u>	3007.61	109
3.	A-B-C-D- <u>E</u> - <u>U</u> - <u>AE</u> -AH-AJ-AL- <u>AP</u> -AS-AY-AZ- BK- <u>BJ</u> -BK-AZ-AY-AS-AP-AL-AJ-AH-AE- AF-T-S-R-Q- <u>G</u>	3007.61	109
4.	A-B-C-D- <u>E</u> - <u>U</u> - <u>AE</u> -AH-AJ-AL- <u>AP</u> -AS-AY-AZ- BK- <u>BJ</u> -BK-AZ-AY-AS-AP-AL-AJ-AH-AE- AF-T-S-R-Q- <u>G</u>	3007.61	124
5.	A-B-C-D- <u>E</u> - <u>U</u> - <u>AE</u> -AH-AJ-AL- <u>AP</u> -AS-AY-AZ- BK- <u>BJ</u> -BK-AZ-AY-AS-AP-AL-AJ-AH-AE- AF-T-S-R-Q- <u>G</u>	3007.61	94

Table 3: Testing Ant Algorithm Ant with Heuristic methods

No.	Point passed (with destination AE – U – E – G – BJ – AP)	Distance traveled (meter)	Time (ms)
1.	A-B-C-D- <u>E</u> - <u>U</u> - <u>AE</u> -AH-AJ-AL- <u>AP</u> -AS-AY-AZ- BK- <u>BJ</u> -BK-AZ-AY-AS-AP-AL-AJ-AH-AE- AF-T-S-R-Q- <u>G</u>	3007.61	14133
2.	A-B-C-D- <u>E</u> - <u>U</u> - <u>AE</u> -AH-AJ-AL- <u>AP</u> -AS-AY-AZ- BK- <u>BJ</u> -BK-AZ-AY-AS-AP-AL-AJ-AH-AE- AF-T-S-R-Q- <u>G</u>	3007.61	13946
3.	A-B-C-D- <u>E</u> - <u>U</u> - <u>AE</u> -AH-AJ-AL- <u>AP</u> -AS-AY-AZ- BK- <u>BJ</u> -BK-AZ-AY-AS-AP-AL-AJ-AH-AE- AF-T-S-R-Q- <u>G</u>	3007.61	13884
4.	A-B-C-D- <u>E</u> - <u>U</u> - <u>AE</u> -AH-AJ-AL- <u>AP</u> -AS-AY-AZ- BK- <u>BJ</u> -BK-AZ-AY-AS-AP-AL-AJ-AH-AE- AF-T-S-R-Q- <u>G</u>	3007.61	13604
5.	A-B-C-D- <u>E</u> - <u>U</u> - <u>AE</u> -AH-AJ-AL- <u>AP</u> -AS-AY-AZ- BK- <u>BJ</u> -BK-AZ-AY-AS-AP-AL-AJ-AH-AE- AF-T-S-R-Q- <u>G</u>	3007.61	13993

**Figure 3:** The output of Heuristic Method Testing

Table 4: The testing of *Dijkstra* Algorithm with TSP Method

No.	Point passed (with destination AE – U – E – G – BJ – AP)	Distance traveled (meter)	Time (ms)
1.	A-B-C-D- <u>E</u> -F- <u>G</u> -Q-R-S-T- <u>U</u> -AH-AJ-AL- <u>AP</u> -AS- AY-AZ-BK- <u>BJ</u>	2260.96	9454
2.	A-B-C-D- <u>E</u> -F- <u>G</u> -Q-R-S-T- <u>U</u> -AH-AJ-AL- <u>AP</u> -AS- AY-AZ-BK- <u>BJ</u>	2260.96	9485
3.	A-B-C-D- <u>E</u> -F- <u>G</u> -Q-R-S-T- <u>U</u> -AH-AJ-AL- <u>AP</u> -AS- AY-AZ-BK- <u>BJ</u>	2260.96	9453
4.	A-B-C-D- <u>E</u> -F- <u>G</u> -Q-R-S-T- <u>U</u> -AH-AJ-AL- <u>AP</u> -AS- AY-AZ-BK- <u>BJ</u>	2260.96	9484
5.	A A-B-C-D- <u>E</u> -F- <u>G</u> -Q-R-S-T- <u>U</u> -AH-AJ-AL- <u>AP</u> -AS- AY-AZ-BK- <u>BJ</u>	2260.96	9438

Table 5: Testing of A* Algorithm with TSP Method

No.	Point passed (with destination AE – U – E – G – BJ – AP)	Distance traveled (meter)	Time (ms)
1.	A-B-C-D- <u>E</u> -F- <u>G</u> -Q-R-S-T- <u>U</u> -AH-AJ-AL- <u>AP</u> -AS- AY-AZ-BK- <u>BJ</u>	2260.96	9313
2.	A-B-C-D- <u>E</u> -F- <u>G</u> -Q-R-S-T- <u>U</u> -AH-AJ-AL- <u>AP</u> -AS- AY-AZ-BK- <u>BJ</u>	2260.96	9328
3.	A-B-C-D- <u>E</u> -F- <u>G</u> -Q-R-S-T- <u>U</u> -AH-AJ-AL- <u>AP</u> -AS- AY-AZ-BK- <u>BJ</u>	2260.96	9298
4.	A-B-C-D- <u>E</u> -F- <u>G</u> -Q-R-S-T- <u>U</u> -AH-AJ-AL- <u>AP</u> -AS- AY-AZ-BK- <u>BJ</u>	2260.96	9327
5.	A-B-C-D- <u>E</u> -F- <u>G</u> -Q-R-S-T- <u>U</u> -AH-AJ-AL- <u>AP</u> -AS- AY-AZ-BK- <u>BJ</u>	2260.96	9422

Table 6: Testing of Ant Algorithm with TSP Method

No.	Point passed (with destination AE – U – E – G – BJ – AP)	Distance traveled (meter)	Time (ms)
1.	A-B-C-D- <u>E</u> -F- <u>G</u> -Q-R-S-T- <u>U</u> -AH-AJ-AL- <u>AP</u> -AS- AY-AZ-BK- <u>BJ</u>	2260.96	25155
2.	A-B-C-D- <u>E</u> -F- <u>G</u> -Q-R-S-T- <u>U</u> -AH-AJ-AL- <u>AP</u> -AS- AY-AZ-BK- <u>BJ</u>	2260.96	26005
3.	A-B-C-D- <u>E</u> -F- <u>G</u> -Q-R-S-T- <u>U</u> -AH-AJ-AL- <u>AP</u> -AS- AY-AZ-BK- <u>BJ</u>	2260.96	25990
4.	A-B-C-D- <u>E</u> -F- <u>G</u> -Q-R-S-T- <u>U</u> -AH-AJ-AL- <u>AP</u> -AS- AY-AZ-BK- <u>BJ</u>	2260.96	25600
5.	A-B-C-D- <u>E</u> -F- <u>G</u> -Q-R-S-T- <u>U</u> -AH-AJ-AL- <u>AP</u> -AS- AY-AZ-BK- <u>BJ</u>	2260.96	26083



Figure 4: The output of TSP Method

From the test results can be concluded that the route search with heuristic methods can provide results faster but produces a much longer route, whereas when using the TSP method the time required to perform the search requires more time than the heuristic method, but produces a shorter route. However, there is also a condition in which the two methods produce similar results.

Our simulation show that the ant algorithm is not good enough to be used for path finding if compared to the Dijkstra and A* algorithm because lack of accuracy and stability and the duration for the process is far slower. However, under varying traffic conditions, Ant algorithm could adapt to the changing traffic and performs better than other shortest path algorithm. Moreover, the Dijkstra and A* algorithm could be developed more because the duration is still fast enough.

4. Conclusions

Based on the results of the implementation and testing program that has been done, it can be concluded that:

- Ant algorithm is not suitable for path finding algorithm because it is less stable and requires a long time to do a search.
- Dijkstra's algorithm and the algorithm A* provide optimal results in a fairly quick time.
- The more destinations you are looking for the longer process is needed.
- The constraint on the road does not affect the long process required. The constraint could affect the result of the search route depending on some conditions.
- Heuristic methods have a faster running time but sometimes gives a longer route, while the TSP method has a little longer running time but produces a much shorter routes than heuristic methods.
- Heuristic methods and TSP could provide the same results under certain conditions.

The emphasis of this paper was on feasibility – identification of possible approaches and development of methods to put them into practices. The evaluation of performance and the reliability of methods was proposed in this paper. Firstly, benchmarking for performance evaluation indicates for which method is

the most efficient and effective from response time point of view. The next concern is the quality of the result.

References

- [1] Champandard, Alex J. *How to Calculate Paths to Multiple Destinations*. Retrieved September 10, 2009 from <http://www.aigamedev.com>, 2003.
- [2] Cormen, T.H., Leiserson, C.E., Rivest, R.L., & Stein, C. *Introduction to algorithms* (2nd ed.). Massachusetts: The MIT Press. 2001.
- [3] Dariusz Król , Łukasz Popiela, Modelling Shortest Path Search Techniques by Colonies of Cooperating Agents, Proceedings of the 1st International Conference on Computational Collective Intelligence. Semantic Web, Social Networks and Multiagent Systems, October 05-07, 2009, WrocBaw, Poland, 2009.
- [4] Dijkstra, E. W. "A note on two problems in connexion with graphs". *Numerische Mathematik* 1: 269–271, 1959.
- [5] Dorigo, M., Maniezzo, V. & Colomi, A., Ant System: Optimization by a Colony of Cooperating Agents. *IEEE Transactions on Systems, Man, and Cybernetics–Part B*, 26, 1-13, 1996.
- [6] Khan, Md. Mujibur Rahman. *Ant System to find the shortest path*. Paper presented at the 3rd International Conference on Electrical & Computer Engineering. Dhaka, Bangladesh, 2004.
- [7] Lin Zhang , Li Xiaoping, The research and improvement of AntNet algorithm, Proceedings of the 2nd international Asia conference on Informatics in control, automation and robotics, p.505-508, March 06-07, 2010, Wuhan, China, 2010.
- [8] Nillson, N.J. *Artificial intelligence: A new synthesis*. San Fransisco: Morgan Kauffman Publishers, 1998.
- [9] Russel, S. & Norvig, P. (2003). *Artificial Intelligence: A modern approach* (2nd ed.). New Jersey: Prentice Hall, 2003.

A Novel of Hybrid Maintenance Management Models for Industrial Applications

Zulkifli Tahir¹, M.A. Burhanuddin², and Anton Satria Prabuwno³

¹ Faculty of Engineering, Department of Electrical Engineering, Universitas Hasanuddin Makassar, Indonesia, Email: zulkifli@unhas.ac.id;

² Faculty of Information and Communication Technology, Department of Industrial Computing, Universiti Teknikal Malaysia Melaka, Melaka, Malaysia, Email: burhanuddin@utem.edu.my

³ Faculty of Information Science and Technology, Universiti Kebangsaan Malaysia Bangi, Selangor D.E., Malaysia, Email: antonsatria@ftsm.ukm.my

Abstract— It is observed through empirical studies that the effectiveness of industrial process have been increased by a well organized of machines maintenance structure. In current research, a novel of maintenance concept has been designed by hybrid several maintenance management models with Decision Making Grid (*DMG*), Analytic Hierarchy Process (*AHP*) and Fuzzy Logic. The concept is designed for maintenance personnel to evaluate and benchmark the maintenance operations and to reveal important maintenance strategies such as Condition Based Maintenance, Design-out Maintenance, Operate to Failure, Service Level Upgrade, Fix Time Maintenance etc. The experimental maintenance data are collected from one of food processing industries in Malaysia for the whole period 2004-2008. The result shows that a novel of hybrid maintenance management models is suitable to be applied as industrial applications for machines maintenance in industries.

I. INTRODUCTION

The importance of maintenance functions for maintenance management in commonly industries has growing rapidly [1]. Recently problem has found that the industries usually just follow the maintenance advices provided by contractors to perform maintenance processes. This dependency on outside contractor will surely increase maintenance cost [2]. To overcome this problem, Information Technology (*IT*) is indeed the best solution by mining historical data and predicts future maintenance strategies [3].

There is lots of *IT* models with varieties of optimizations and techniques that have been proposed to improve the effectiveness of the industrial processes ([4], [5], [6], [7]). In order to increase the effectiveness of the machines, an appropriate concept with decision making capability is extremely needed [8]. This research advocates the hybrid maintenance models to analyze industrial data to support industrial maintenance process. Decision Making Grid (*DMG*) by [9], Fuzzy Logic by [10] and Analytic Hierarchy Process (*AHP*) by [11] are the maintenance optimization models and techniques that have been used.

II. BACKGROUND OF STUDY

This section describes the brief explanation about maintenance models that have been used to develop the concept as follows:

1) Decision Making Grid

Reference [9] has developed an intelligent maintenance system and proposed a Decision Making Grid (*DMG*) model based on multiple criteria and rule-based system, which has been successfully implemented in the automotive sector producing roof systems industry. *DMG* is a control chart in two dimensional matrix forms. A better maintenance model for quality management can be formed by handling both row and columns

respectively. The matrix offers an opportunity to decide what maintenance strategies are needed for decision making.

Reference [12] modified *DMG* proposed by [9] as one of the decision support module in computerized system. They extended the theory of maturity grid and implemented it into a disk brake part manufacturing company in England. Later, reference [13] comprehended the model and demonstrated the hybrid intelligent approach using the *DMG* and fuzzy rule based techniques. Then [14] applied the formalized *DMG* in computerized system in one of the food processing factories in Malaysia. Reference [15] improved the *DMG* by introducing a tri-quadrant approach to cluster and categorize the variables. Reference [16] described the maintenance strategies for changeable manufacturing using *DMG* and Fuzzy Logic for failure prone manufacturing system.

2) Fuzzy Logic

Fuzzy Linguistic was introduced by [17] as a superset of conventional or Boolean logic that has been extended to handle the concepts of partial truth that is truth values between “completely true” and “completely false”. It was described as a means to model the uncertainty of natural language. Reference [17] stated that rather than regarding fuzzy theory as a single theory, we should regard the process of “fuzzyfication” as a methodology to generalize any specific theory from crisp or discrete to a continuous or fuzzy form [10]. By the term “fuzziness” Zadeh meant classes in which there is no sharp transition from membership [18].

3) Analytic Hierarchy Process

Analytic Hierarchy Process (*AHP*) was developed by [11] as mathematical decision making model to solve complex decision making problems when there are multiple objectives or criteria considered. It requires the decision makers to provide judgments about the relative importance criterion for each decision alternative [19].

AHP has been used to solve the maintenance problem in many industrial areas. For instance, [20] have used *AHP* to justify the Total Productive Maintenance (*TPM*) in Indian industries. While [21] have described the application of *AHP* to selecting the best maintenance strategies for an important Italian oil refinery. Reference [22] described the selection of optimum maintenance strategies based on fuzzy *AHP* for thermal power plant in China. Reference [23] has been evaluated the information service quality of ten primary high tech industry information center web portals in China using *AHP*.

III. MAINTENANCE CONCEPT

In brief, maintenance concept has been designed as shown in fig. 1 below:

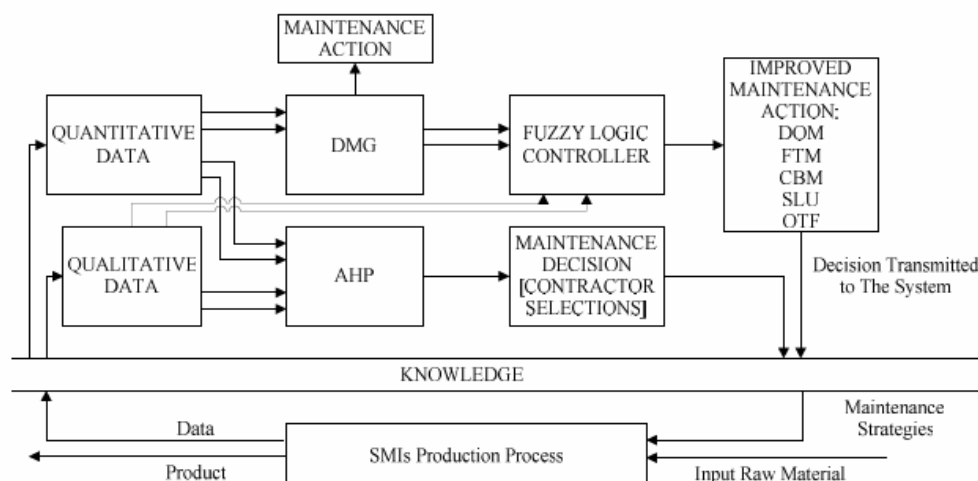


Figure 1 Hybrid Maintenance Concept Design

This design shows the continuous process for the effectiveness of maintenance management in *SMIs*. The design is an iterative process of recoding, extracting, and studying the data, analyzes the data based on decision making models, and the results are applied in the in manufacturing system. Each of them is described as follows:

1. *Recording the data.* Maintenance data are always recorded by maintenance personnel as tracery history. The data can be recorded in several ways, it can be written manually in maintenance data form or by writing using computerized system. Some machines have automatic writing systems embedded in them. Data in this framework are inserted into the database system for further analysis. These data are very useful for analysis as well as for improving the effectiveness of maintenance management in industries.
2. *Extract and studying the data.* The maintenance data which is recorded in the database is very useful for maintenance experts as it helps in taking maintenance decision and in maintenance management. The problems and factors that influence machine breakdowns can be selected and analyzed from that raw maintenance data. The quantitative data can be selected and collected from database to embed with decision making models. The qualitative data from the maintenance experts can also be used and inserted in the database to be embedded with decision making models.
3. *Analyze the data with decision making models.* All selected data is analyzed using decision making models, both in *DMG* and in *AHP*, to get an appropriate maintenance strategies and maintenance decisions for each machine.
4. *Producing the decisions results.* The *DMG* can produce the appropriate maintenance strategy by embedding the machines downtime and frequency of machine failures. The qualitative data from maintenance experts, such as maintenance manager, technician, or machine operator, can be submitted in Fuzzy *DMG* to provide the better results in decision making. The *AHP* models can be used to produce the best maintenance decision from multiple criteria and multiple alternatives in maintenance management, such as selecting the best contractors to conduct maintenance operation. Both *DMG* and *AHP* are used in the Decision Support System (*DSS*) to simplify the analyzing process and to reduce time needed in making maintenance decisions. With these maintenance decisions, the maintenance knowledge can be attempted and can provide suggestions for better maintenance action in industrial maintenance processes.
5. *Apply the suggested maintenance strategies and maintenance decisions into the industrial process.* The results from decision support system should be applied in manufacturing process. It leads to better maintenance action for each machine based on the calculation of the data from *DMG*. *OTF*, *FTM*, *CBM*, *SLU*, *DOM* are examples of maintenance strategies that are suggested in each machine. These maintenance strategies are explained in detail as follows:
 - a) *Operate to Failure (OTF):* This strategy is implemented when the machine seldom fails, and once failed the downtime is short, Failure Based Maintenance (*FBM*) is suitable for the machines in this group;
 - b) *Fixed Time Maintenance (FTM):* This strategy use Preventive Maintenance (*PM*) schedule, implemented when failure frequency and downtime are almost at the moderate cases;
 - c) *Skill Level Upgrade (SLU):* Machine always failed but it can be fixed very fast. Maintaining the machines in this group is relatively easy. Upgrading the skill level of the operator, because machine has been visited many times (high frequency) and for limited period (low downtime);
 - d) *Condition-Based Maintenance (CBM):* This used to analyze the breakdown event and closely monitor its condition when the machine does not breakdown often but take a long time to fix;
 - e) *Design Out maintenance (DOM):* Machine is always fails. Once failed, it takes a long time to bring it back to the normal operation. This is the most problematic group of machines and major design out projects need to be considered. Sometimes, machines need to be structurally modified.

The best maintenance goal from multiple criteria and alternative can also be reached based on the calculation in the *AHP* model. This *AHP* model provide the best maintenance goal based on the pair to pair weight calculation from each maintenance criterion and maintenance alternative that is analyzed from the data recorded.

After the maintenance strategy is applied to each machine, the next step is to record data on *DSS* design like extracting and studying the data, analyzing the data with decision making models and producing the decision results, until a new maintenance strategy is suggested for each machine and in time this will increase the effectiveness of the process of maintenance management in industries.

IV. DATA COLLECTIONS

In this study, the real data in the maintenance management from industries is indispensable for analysis of decision making and to justify the research purpose. Several industries in Malaysia were visited for case study and analysis. Data gathered from the Small and Medium Industry (*SMI*) in the field of food processing brings

to evidence that they possess the International Standard Organization (*ISO*) in quality, prize and delivery schedules. Two types of data, namely qualitative and quantitative data are collected.

The qualitative data is obtained by observing the production floor process during peak hours and via interview with the factory managers, technicians, operators and maintenance staff in *SMI*. The issues of machine breakdown and maintenance management is gathered for further analysis and to provide better maintenance strategies in the implementation of decision making models in *DSS*. In this research, secondary qualitative data from [2] has been used for conducting the analysis. They have distributed questionnaires to respondents who operate, maintain and manage the machines in *SMIs*.

The quantitative data on machine specification, machine breakdown, maintenance management and repair report are collected with copies of the original maintenance forms from *SMI*. The data are collected within a period of the year 2004-2008 in the machines that are currently being used to produce *ground fried cocomit*, *kaya madu*, *roselle cordial juice*, *pineapple jam*, *roselle jam* and *starfruit jam*. The secondary data from machine operations, maintenance outsourcing, and other sources are taken from a brake pad manufacturing company, as posited by [12] and food processing company by [2].

V. TESTING AND ANALYSIS

The testing of maintenance concept is done using qualitative and quantitative data on machine records from food processing industries. The raw data is keyed into Microsoft Excel software for analysis. The data analysis with maintenance concept is provided to obtain the maintenance strategy in each machine. The result and solutions are given to the maintenance department to implement the suggested strategies in twice, the first in 2006 and the second in 2007. Then a comparison study is conducted to see the improvement of the experiment. Fig. 2 below shows the graph of the implementation of maintenance concept to show the improvement base on the data recorded in 2004 until 2008.

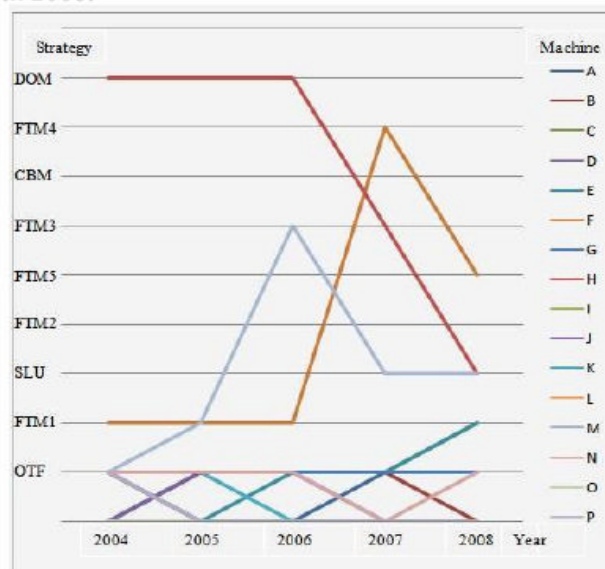


Figure 2: The Implementation of the Maintenance Concept

After implementation of strategies in 2006 and 2007, some improvements have been observed, especially for machine *H* (filling machine), machine *F* (backup cooker) and machine *M* (machine labels and jet printer) as shown in fig. 2. There is a rapid downtime reduction for machine *H* in the period 2006 until 2008. It is because the *SMIs* has installed new filling machine (machine *H*) to replace the worst performing equipment in 2006. Thus, that machine has given well *FTM3* strategies with preventive maintenance and monitored by trained and experienced operator in 2007. As consequences, less downtime occurs in Machine *H* and therefore the preventive maintenance has been removed for suggestion strategies in 2008. Machine *H* is just given the right trained experienced operator to solve its problem with still high frequency of failure but easy to solve. Machine *F* has shown worse in 2006, but reflects some improvement in 2007. Machine *F* is given *DOM* strategy that suggested installing new devices in the production line based on the query selection method by [13]. But it is not enough to solve the maintenance problem. In 2007, the maintenance strategies of this machine has been improved with hard *FTM4* based on tri-quadrant clustering method by [2] with more frequent tasks given to maintain the machines using preventive maintenance strategy. This hard *FTM4* strategy is suitable for machine

F with decreasing machine downtime from 2007 until 2008. In 2008, the maintenance strategy suggestion of machine F is middle $FTM5$, which reduces the task to maintain the machine in each period of time in comparison to hard $FTM4$ strategy in 2007. Machine M also show the improvement in 2007. It is because the operator has more experience in solving the problems that always occur as they are given ample training by the vendors of the machine. The machine is given SLU strategy in 2007 and 2008. Machine M is not given many tasks for maintenance because it automatically maintain when it seem to be failed by the hands of an experienced operator. Other machines are provided with usual maintenance strategies in $SIMs$ such as OTF and easy $FTM1$ because these machines have low frequency of failures and low downtime which consequently results low in costs for the maintenance of the machines.

VI. CONCLUSIONS

The maintenance concept is proposed based on the fact that the system of decision-making needs to be improved for the effectiveness of the maintenance management system in industries. This maintenance concept is designed with an appropriate maintenance strategy in each machine based on the selected decision making model. The decision making models with the extension of mathematical and artificial intelligence have been formulated for some specific situations. This maintenance design is useful in measuring and suggesting the maintenance strategies on the machines, and consequently provides the guidelines to implement the maintenance activities in the industries.

ACKNOWLEDGMENT

The authors would like to thank Faculty of Information & Communication Technology, Technical University of Malaysia Melaka for providing facilities.

REFERENCES

- [1] Latif, A. A. (2000). Relocation of Small and Medium Industries (SMIs) Manufacturing to Non Metropolitan Areas: A Lesson from USA and Canada, *Utara Management Review*, Vol 1 (1), pp. 19-31.
- [2] Burhanuddin, M. A. (2009). Decision Support Model in Failure-Based Computerized Maintenance Management System for Small and Medium Industries, Thesis of Doctor of Philosophy in Computer Science, Universiti Teknologi Malaysia, UTM.
- [3] Kittipong, S. (2008). A Comprehensive Framework for Adoption of Techno-Relationship Innovations. Empirical Evidence from eCRM in Manufacturing Small and Medium Industries. Thesis of the Doctorate in Philosophy. Sweden: Umea University.
- [4] Boznos, D. (1998). The use of CMMSs to support team-based maintenance. Thesis of the Master in Philosophy. Cranfield University.
- [5] Ben-Daya, M. & Alghamdi, A. S. (2000). On an imperfect preventive maintenance model, *International Journal of Quality & Reliability Management*, vol. 17, no. 6, pp. 661-70.
- [6] Sherwin, D. (2000). Review overall model for maintenance management, *Reliability Engineering and System Safety*, vol. 6, no. 4, pp. 138-64.
- [7] Garg, A. & Deshmukh, S. G. (2006). Application and Case Studies: Maintenance management-literature review and directions. *Journal in Quality in Maintenance Engineering*. Vol 12, No. 3, pp. 205-238.
- [8] Junaidah, H. (2007). Information and Communication Technology Adoption among Small and Medium Industries in Malaysia. *International Journal in Business and Information*. Vol. 12, No. 2, pp. 221-240.
- [9] Labib, A. W. (1998). World class maintenance using a computerized maintenance management system, *Journal of Quality in Maintenance Engineering*, Vol. 4, No. 1, pp. 66-75.
- [10] Zadeh, L. A. (1988). *Fuzzy Logic*, IEEE Computer Society, Vol. 21, pp. 83-93.
- [11] Saaty, T.L. (1980). *The Analytic Hierarchy Process*, McGraw-Hill, New York.
- [12] Fernandes, O, Labib, A. W., Walmisley, R. & Petty, D. J. (2003). A decision support maintenance management system: development and implementation, *International Journal of Quality & Reliability Management*, vol. 20, no. 8, pp. 965-79.
- [13] Labib, A.W. (2004). A Decision Analysis Model for Maintenance Policy Selection Using a CMMS, *Journal of Quality in Maintenance Engineering*, Emerald, pp. 191-202.
- [14] Burhanuddin, M. A., Ahmad, A. R. & Desa, M. I. (2007). An Application of Decision Making Grid to Improve Maintenance Strategies in Small and Medium Industries, *Proc. the 2nd IEEE Conference on Industrial Electronic & Application*, pp. 455-60.

- [15] Burhanuddin, M. A., Ahmad, A. R., Desa, M. I. & Prabuwo, A. S. (2008). An improved Decision Making Grid Model to Identify Maintenance Strategies, International Conference on Plant Equipment and Reliability, Technical University of Petronas, pp. 81-86.
- [16] Labib, A. W. & Yuniarto, M. N. (2009). Maintenance strategies for Changeable Manufacturing. New York: Springer-Verlag Inc. Chapter 19, pp. 337-351.
- [17] Zadeh, L. A. (1965). Fuzzy sets, Information and Control, 8(3), 338-353.
- [18] Mechefske, C. K. & Wang, Z. (2001). Using fuzzy linguistic to select optimum maintenance and condition monitoring strategies, Mechanical Systems and Signal Processing, vol. 15, no. 6, pp. 1129-1140.
- [19] Kodali, R. (2001). Qualification of TPM benefits through AHP model, Productivity, vol. 42, no. 2, pp. 265-73.
- [20] Kodali, R. & Chandra, S. (2001). Analytic hierarchy process of justification of total productive maintenance, Production Planning and Control, vol. 12, no. 7, pp. 695-705.
- [21] Bevilacqua, M. & Braglia, M. (2000). The analytic hierarchy process applied to maintenance strategy selection, Reliability Engineering and System Safety, vol. 70, no. 1, pp. 71-83.
- [22] Wang, L, Chu, J. & Wu, J. (2007). Selection of optimum maintenance strategies based on a fuzzy analytic hierarchy process. International Journal of Production Economics. Vol. 107, pp. 151-163.
- [23] Guo, M. & Zhao, Y. (2009). AHP based evaluation of information service quality of information center web portals in high-tech industries, IEEE on management and service science, MASS 09, pp. 1-4.

THE APPLICATION of MAXIMUM LIKELIHOOD ESTIMATION FOR UNBALANCED DATA TO DETERMINE OF CLEAN WATER DEBITS FROM PDAM MAKASSAR

Georgina M. Tinungki
 Department of Mathematics,
 Faculty of Mathematics and Natural Science
 Hasanuddin University Makassar Indonesia
 e-mail: ina_matematika@yahoo.co.id

Abstract— Classification model in one way or sometimes also named design random complete, this planning usually is used when the design is homogeny means the homogeneity of the design is small and clustering into cluster that doesn't give any use. How to overcome the estimation of variance component with negative value on one way classification for balanced data and unbalanced data.

The data that used is balanced data and unbalanced data on one way classification. For knowing what factors that caused the variance component is negative value and what's the solution. Variance component always positive because it is assumption to represent variance from random variable. But the method as Analysis of Variance causes negative estimation. Negative estimation maybe appears with some causes namely : variable in data maybe enough big, the data consist of outlier data, change and using the wrong model, value indication from variance each treatment is zero.

Negative estimation is an indication that observation in negative correlation data. As theoretic the value estimation for component variance can has negative value when mean square error (MSE) more than mean square treatment (MST) or $MSE > MST$. In certain case $\hat{\sigma}_\tau^2$ has negative value while the value from σ_τ^2 is $0 \leq \sigma_\tau^2 < \infty$. Maximum Likelihood Method can gives solution for overcome the case like this, for balanced data. For facilitating the process of data processing, using some software namely Microsoft Excel and SPSS 14.

Keywords- variance component, design random complete, well-balanced data and do not well-balanced. Maximum Likelihood Method

I. INTRODUCTION

Statistical variance is the value that shows the measure of data distribution. The more distribution of data's the more the variance. The more the data's does not distribute the variance getting less. The data that do not distribute the variance is zero.

Analysis of variance (ANOVA) is a method that analyze statistical which include statistical inference. In Indonesian literature this method is known with many names. The first time the analysis of variance the introduced by Sir Ronald Fisher the father of modern statistic. In practice analysis can be a test and estimation. Especially applied mathematics.

In general, analyze of variance test two variances based on null hypothesis where two variances are same. The first variance is among sample and the second one is *within samples*. In idea like this the analysis of variance with two samples will give a same result with t-test for two means.

In order valid in estimate the result must have four assumptions that must be experiment design:

1. Data has normal Distribution, because the test using F-test Snedecor,
2. Variance must homogeny, that is known as homoscedastisitas, because only used in one estimation for variance in sample,
3. Each sample is independent, and must be arranged with appropriate design experiment.
4. The components in the model is additive.

Elementary assumptions above is absolute matter which must be fulfill in usage of analysis of variance. Do not be fulfilled one of them can deviation level of significance sensitivity F-test or t-test to real from null

hypothesis. Because this elementary assumptions have the character of absolutely, after the data is found from research result than early hence step is first what the data is to test the data fulfill existing assumptions. Nowadays, a lot of statistical software available in helping the researchers doing assumption test. When the assumption after test does not fulfill, the only way is transformation of data.

II. AR (1) MODEL

The Autoregressive model for the first order is:

$$Z_t = \beta_1 Z_{t-1} + \varepsilon_t \quad (5)$$

In order to stationer, the formula must be $|\beta_1| < 1$

Auto covariance for variable that contains in autoregressive model AR(1) is:

$$E(Z_{t-k} Z_t) = E(\beta_1 Z_{t-k} Z_{t-1}) + E(Z_{t-k} \varepsilon_t) \quad (6)$$

$$\gamma_k = \beta_1 \gamma_{k-1} \quad k \geq 1$$

while autocorrelation function – ACF is:

$$\rho_k = \beta_1 \rho_{k-1} = \beta_1^k \quad k \geq 1 \quad (7)$$

where $\rho_0 = 1$. Therefore, ACF descend exponentially according to one or two form that depends on the sign of β_1 . If $0 < \beta_1 < 1$, all of autocorrelation is positive; if $-1 < \beta_1 < 0$, the sign of autocorrelation show a change pattern which is begin with negative value of autocorrelation. The level of autocorrelation value decreases exponentially in both cases.

For AR(1) model, partial autocorrelation function – PACF is:

$$\phi_{kk} = \begin{cases} \rho_1 = \beta_1, & k = 1 \\ 0, & k \geq 2 \end{cases} \quad (8)$$

Because PACF from AR(1) model show a positive spike or negative at lag 1 that is depend on β_1 , and then break.

The approximation parametric of AR(1), β by using OLS method is:

$$\hat{\beta} = \frac{\sum_{t=2}^n Z_t Z_{t-1}}{\sum_{t=2}^n Z_{t-1}^2}$$

III. ADDITIVE LINEAR MODEL

Observation can be elaborated into two components, that is random component and mean value, and after that the mean value is the amount of some components. Linear model of additive in general from device one factor with design random complete can be differentiated to become two, that is remain and random model. Remain model is model where using treatment on trial come from limited population and the election of treatment is determined directly by the researcher Obtained conclusion of limited remain model is just on treatment which is experimented and cannot be generalized. While random model is model where treatment which is experimented is random example of treatment population. Obtained conclusion of random model apply in general to all treatment population.

Additive Model one way classification (design random complete) is formulated as follows:

$$y_{ij} = \mu + \alpha_j + e_{ij} \quad , \text{ with } i = 1, 2, \dots, a \quad (2.1)$$

$$\text{var}(\alpha_i) = \sigma_a^2; \text{var}(e_{ij}) = \sigma_e^2; \text{all covariance is zero}; \quad (2.2)$$

$$j = 1, 2, \dots, n \quad \text{for balance data}; \quad (2.3)$$

$$j = 1, 2, \dots, n_i, \forall i, \quad \text{for unbalance data}; \quad (2.4)$$

where,

y_{ij} = value perception of treatment of to-i at of to-j.

μ = mean values

α_i = influence of treatment of to-i.

e_{ij} = error obtains get treatment of to-i at of to-j.

with model assumption remain to that is:

$$\sum \alpha_i = 0, \text{ and } \text{var}(e_{ij}) = \sigma_e^2 \quad \forall_{ij} \text{ and also } e_{ij} \sim N(0, \sigma_e^2)$$

while for random model that is:

$$E(\alpha_i) = 0, \text{ var}(\alpha_i) = \sigma_a^2, \text{ var}(e_{ij}) = \sigma_e^2 \quad \forall_{ij}, \text{ and } e_{ij} \sim N(0, \sigma_e^2).$$

(Vincent Gaspersz, 1991)

Hypothesis examinee form shall be as follows:

$H_0: \alpha_1 = \dots = \alpha_i = 0$ (all treatment do not have an effect on to respond which very)

$H_1: \alpha_i \neq 0$ (at least there is one treatment having an effect on to respond perceived)

or,

$H_0: \mu_1 = \dots = \mu_a$ (all treatment give respond the is sameness)

$H_1: \mu_i \neq \mu_i^*$ (at least there is treatment couple giving respond the is sameness)

For one way classification for **a** treatment and **n** same repeat, hence experiment data for ANAVA can be is compiled in tabulates form data like at Table 2.1 as following:

Table 2.1. Data tabulation for one way classification composing from *a* treatment and *n* repeat

Repeat	Treatment				
	1	2	...	A	
	y_{11}	y_{21}	...	y_{a1}	
	y_{12}	y_{22}	...	y_{a2}	
	
	y_{1n_i}	y_{2n_i}	...	y_{an_i}	
Amount	$y_{1\circ}$	$y_{2\circ}$...	$y_{a\circ}$	$y_{\circ\circ}$
Mean	$\bar{y}_{1\circ}$	$\bar{y}_{2\circ}$...	$\bar{y}_{a\circ}$	$\bar{y}_{\circ\circ}$

Source : Ronald E. Walpole, 1986.

For same repetition, degree of freedom (df) of as follows :

df treatment = $a - 1$

df error = $a(n - 1)$

df Total = $an - 1$

For one way classification consisting of *a* treatment and n_i which is different repeating, hence perception data can be compiled in the form of tabulation data like at Table 2.2 as following:

Table 2.2: Data tabulation for one way classification composing from a treatment and n_i repeat

Repeat	Treatment						
	1	2	...	i	...	a	
	y_{11}	y_{21}	...	y_{i1}	...	y_{a1}	
	y_{12}	y_{22}	...	y_{i2}	...	y_{a2}	
	
	y_{1n_i}	y_{2n_i}	...	y_{in_i}	...	y_{an_i}	
Amount	y_{1o}	y_{2o}	...	y_{io}	...	y_{ao}	y_{oo}
Mean	\bar{y}_{1o}	\bar{y}_{2o}	...	\bar{y}_{io}	...	\bar{y}_{ao}	\bar{y}_{oo}

Source: Ronald E. Walpole, 1986.

where:

y_{io} = amount all perceptions in sample of treatment to- i

\bar{y}_{io} = perception mean in treatment to- i

y_{oo} = amount all perceptions.

\bar{y}_{oo} = mean all perceptions (general mean)

Pursuant to above perception data can be made by analysis of variance with degree of freedom as follows:

$$\text{df treatment} = a - 1$$

$$\text{df error} = \sum_{i=1}^a (n_i - 1)$$

$$\text{df total} = \sum_{i=1}^a n_i - 1$$

Variance of total can elaborated as follows:

$$y_{ij} - \bar{y}_{oo} = (y_{ij} - \bar{y}_{io}) + (\bar{y}_{io} - \bar{y}_{oo})$$

$$(y_{ij} - \bar{y}_{oo})^2 = (\bar{y}_{io} - \bar{y}_{oo})^2 + (y_{ij} - \bar{y}_{io})^2 + 2(\bar{y}_{io} - \bar{y}_{oo})(y_{ij} - \bar{y}_{io})$$

$$(y_{ij} - \bar{y}_{oo})^2 = (\bar{y}_{io} - \bar{y}_{oo})^2 + (y_{ij} - \bar{y}_{io})^2 + 2(\bar{y}_{io} - \bar{y}_{oo})(y_{ij} - \bar{y}_{io})$$

and then if amount for all treatment (sum square total) becoming :

$$\sum_{i=1}^a \sum_{j=1}^n (y_{ij} - \bar{y}_{oo})^2 = \sum_{i=1}^a \sum_{j=1}^n (\bar{y}_{io} - \bar{y}_{oo})^2 + \sum_{i=1}^a \sum_{j=1}^n (y_{ij} - \bar{y}_{io})^2$$

Because,

$$\sum_{i=1}^a \sum_{j=1}^n 2(\bar{y}_{io} - \bar{y}_{oo})(y_{ij} - \bar{y}_{io}) = \sum_{i=1}^a \left[\sum_{j=1}^n (y_{ij} - \bar{y}_{io}) \right] (\bar{y}_{io} - \bar{y}_{oo}) = \sum_{i=1}^a 0(\bar{y}_{io} - \bar{y}_{oo}) = 0$$

So,

$$SST = \sum_{i=1}^a \sum_{j=1}^n (\bar{y}_{io} - \bar{y}_{oo})^2 + \sum_{i=1}^a \sum_{j=1}^n (y_{ij} - \bar{y}_{io})^2$$

or,

$$SST = SST + SSE \quad (2.5)$$

For treatment with repeat every same treatment (balance data) can formulated as follows:

$$FK = \frac{y_{\infty}^2}{an} \quad (2.6)$$

$$\begin{aligned} SST &= \sum_{i=1}^a \sum_{j=1}^n (y_{ij} - \bar{y}_{\infty})^2 \\ &= \sum_{i=1}^a \sum_{j=1}^n y_{ij}^2 - 2 \sum_{i=1}^a \sum_{j=1}^n y_{ij} \bar{y}_{\infty} + \sum_{i=1}^a \sum_{j=1}^n \bar{y}_{\infty}^2 \\ &= \sum_{i=1}^a \sum_{j=1}^n y_{ij}^2 - 2 \bar{y}_{\infty} \sum_{i=1}^a \sum_{j=1}^n y_{ij} + an \bar{y}_{\infty}^2 \\ &= \sum_{i=1}^a \sum_{j=1}^n y_{ij}^2 - 2 \frac{y_{\infty}}{an} y_{\infty} + an \left(\frac{y_{\infty}}{an} \right)^2 \\ &= \sum_{i=1}^a \sum_{j=1}^n y_{ij}^2 - 2 \frac{y_{\infty}^2}{an} + \frac{y_{\infty}^2}{an} \\ &= \sum_{i=1}^a \sum_{j=1}^n y_{ij}^2 - \frac{y_{\infty}^2}{an} \\ &= \sum_{i=1}^a \sum_{j=1}^n y_{ij}^2 - FK \end{aligned} \quad (2.7)$$

$$\begin{aligned} SST &= \sum_{i=1}^a \sum_{j=1}^n (\bar{y}_{i\circ} - \bar{y}_{\infty})^2 \\ &= \sum_{i=1}^a \sum_{j=1}^n \bar{y}_{i\circ}^2 - 2 \sum_{i=1}^a \sum_{j=1}^n \bar{y}_{i\circ} \bar{y}_{\infty} + \sum_{i=1}^a \sum_{j=1}^n \bar{y}_{\infty}^2 \\ &= \sum_{i=1}^a \sum_{j=1}^n \left(\frac{y_{i\circ}}{n} \right)^2 - 2 \bar{y}_{\infty} \sum_{i=1}^a \sum_{j=1}^n \bar{y}_{i\circ} + an \bar{y}_{\infty}^2 \\ &= n \sum_{i=1}^a \left(\frac{y_{i\circ}}{n} \right)^2 - 2 \frac{y_{\infty}}{an} \left(n \sum_{i=1}^a \frac{y_{i\circ}}{n} \right) + an \left(\frac{y_{\infty}}{an} \right)^2 \\ &= \sum_{i=1}^a \frac{y_{i\circ}^2}{n} - 2 \frac{y_{\infty}}{an} \sum_{i=1}^a y_{i\circ} + \frac{y_{\infty}^2}{an} \\ &= \sum_{i=1}^a \frac{y_{i\circ}^2}{n} - 2 \frac{y_{\infty}^2}{an} + \frac{y_{\infty}^2}{an} \\ &= \sum_{i=1}^a \frac{y_{i\circ}^2}{n} - \frac{y_{\infty}^2}{an} \\ &= \sum_{i=1}^a \frac{y_{i\circ}^2}{n} - FK \end{aligned} \quad (2.8)$$

$$SSE = \sum_{i=1}^a \sum_{j=1}^n (y_{ij} - \bar{y}_{i\circ})^2$$

$$\begin{aligned}
&= \sum_{i=1}^a \sum_{j=1}^n y_{ij}^2 - 2 \sum_{i=1}^a \sum_{j=1}^n y_{ij} \bar{y}_{i\cdot} + \sum_{i=1}^a \sum_{j=1}^n \bar{y}_{i\cdot}^2 \\
&= \sum_{i=1}^a \sum_{j=1}^n y_{ij}^2 - \frac{2}{n} \sum_{i=1}^a y_{i\cdot} y_{i\cdot} + n \sum_{i=1}^a \left(\frac{y_{i\cdot}}{n} \right)^2 \\
&= \sum_{i=1}^a \sum_{j=1}^n y_{ij}^2 - \frac{2}{n} \sum_{i=1}^a y_{i\cdot}^2 + \frac{1}{n} \sum_{i=1}^a y_{i\cdot}^2 \\
&= \sum_{i=1}^a \sum_{j=1}^n y_{ij}^2 - \frac{1}{n} \sum_{i=1}^a y_{i\cdot}^2
\end{aligned} \tag{2.9}$$

so that obtained :

Mean Square Treatment (MST)

$$MST = \frac{SST}{a-1} \tag{2.10}$$

Mean Square Error (MSE) :

$$MSE = \frac{SSE}{a(n-1)} \tag{2.11}$$

Table 2.3: Analysis of Variance for one way classification with balance data

Source of Variance	Degree of freedom (df)	Sum Square	Mean Square	F-count
Error	$a-1$	SST	MST	$F = \frac{MST}{MSE}$
Treatment	$a(n-1)$	SSE	MSE	
Total	$an-1$	SST		

Source: Searle, Casella, & McCulloch 1992

From additive linear model for balance data is:

$$y_{ij} = \mu + \alpha_i + e_{ij}, \text{ for } i = 1, 2, \dots, a \text{ and } j = 1, 2, \dots, n \text{ is obtained :}$$

$$\bar{y}_{i\cdot} = \mu + \alpha_i + \bar{e}_{i\cdot}, \text{ for } \bar{e}_{i\cdot} = \sum_{j=1}^n \frac{e_{ij}}{n},$$

and

$$\bar{y}_{\cdot\cdot} = \mu + \bar{\alpha}_{\cdot} + \bar{e}_{\cdot\cdot}, \text{ for } \bar{\alpha}_{\cdot} = \sum_{i=1}^a \frac{\alpha_i}{a} \text{ and } \bar{e}_{\cdot\cdot} = \sum_{j=1}^a \frac{\bar{e}_{i\cdot}}{a}.$$

Therefore,

$$\begin{aligned}
E(SST) &= E \left[\sum_{i=1}^a \sum_{j=1}^n (\bar{y}_{i\cdot} - \bar{y}_{\cdot\cdot})^2 \right] \\
&= nE \left[\sum_{i=1}^a (\bar{y}_{i\cdot} - \bar{y}_{\cdot\cdot})^2 \right] \\
&= n \sum_{i=1}^a E [(\alpha_i - \bar{\alpha}_{\cdot}) + (\bar{e}_{i\cdot} - \bar{e}_{\cdot\cdot})]^2 \\
&= n \sum_{i=1}^a [E(\alpha_i - \bar{\alpha}_{\cdot})^2 + E(\bar{e}_{i\cdot} - \bar{e}_{\cdot\cdot})^2]
\end{aligned}$$

Variance σ_e^2 and σ_a^2 , is referred as component of variance because is an component of variance from an perception. So that pursuant to definition of variance used. $E(e_{ij}) = 0$ and $E(\alpha_i) = 0$, to obtain the component $\sigma_e^2 = \text{var}(e_{ij}) = E[e_{ij} - E(e_{ij})]^2 = E(e_{ij}^2)$

$$\sigma_a^2 = \text{var}(\alpha_i) = E(\alpha_i^2)$$

Then,

$$\begin{aligned} E(SST) &= n \sum_{i=1}^a [\text{var}(\alpha_i - \bar{\alpha}_o)^2 + \text{var}(\bar{e}_{i\cdot} - \bar{e}_{\cdot\cdot})^2] \\ &= n \sum_{i=1}^a \left(\sigma_a^2 + \frac{\sigma_a^2}{a} - \frac{2\sigma_a^2}{a} \right) + n \sum_{i=1}^a \left(\frac{\sigma_e^2}{n} - \frac{\sigma_e^2}{an} - \frac{2\sigma_e^2}{nan} \right) \\ &= n \sum_{i=1}^a \left(\frac{a\sigma_a^2 - \sigma_a^2}{a} \right) + n \sum_{i=1}^a \left(\frac{an\sigma_e^2 + n\sigma_e^2 - 2n\sigma_e^2}{nan} \right) \\ &= na \left(\frac{a\sigma_a^2 - \sigma_a^2}{a} \right) + nan \left(\frac{an\sigma_e^2 + n\sigma_e^2 - 2n\sigma_e^2}{nan} \right) \\ &= na \left(\frac{a\sigma_a^2 - \sigma_a^2}{a} \right) + nan \left(\frac{an\sigma_e^2 + n\sigma_e^2 - 2n\sigma_e^2}{nan} \right) \\ &= (a-1)(n\sigma_a^2 + \sigma_e^2) \end{aligned} \quad (2.12)$$

$$E(MST) = \frac{E(SST)}{a-1} = \frac{(a-1)(n\sigma_a^2 + \sigma_e^2)}{a-1} = n\sigma_a^2 + \sigma_e^2 \quad (2.13)$$

So to obtain : $E(SSE)$

$$\begin{aligned} E(SSE) &= E \left[\sum_{i=1}^a \sum_{j=1}^n (y_{ij} - \bar{y}_{i\cdot})^2 \right] \\ &= \sum_{i=1}^a \sum_{j=1}^n E[(y_{ij} - \bar{y}_{i\cdot})^2] \\ &= \sum_{i=1}^a \sum_{j=1}^n [E(e_{ij} - \bar{e}_{i\cdot})^2] \\ &= \sum_{i=1}^a \sum_{j=1}^n [\text{var}(e_{ij} - \bar{e}_{i\cdot})] \\ &= \sum_{i=1}^a \sum_{j=1}^n \left(\sigma_e^2 + \frac{\sigma_e^2}{n} - \frac{2\sigma_e^2}{n} \right) \\ &= an \left(\sigma_e^2 - \frac{\sigma_e^2}{n} \right) \\ &= a(n-1)\sigma_e^2 \end{aligned} \quad (2.14)$$

$$E(SSE) = a(n-1)\sigma_e^2 \quad (2.15)$$

$$E(MSE) = \frac{E(SSE)}{a(n-1)} = \frac{a(n-1)\sigma_e^2}{a(n-1)} = \sigma_e^2 \quad (2.16)$$

$$\hat{\sigma}_e^2 = \frac{SSE}{a(n-1)} = SST \quad (2.17)$$

$$\hat{\sigma}_a^2 = \left(\frac{\frac{SST}{a-1} - \hat{\sigma}_e^2}{n} \right) = \frac{MST - MSE}{n} \quad (2.18)$$

(Searle, Casella, & McCulloch 1992)

For treatment with repeat every treatment difference (balance data) can be formulated as follows:

$$FK = \frac{y_{\infty}^2}{\sum_{i=1}^a n_i} \quad (2.19)$$

$$\begin{aligned} SST &= \sum_{i=1}^a \sum_{j=1}^{n_i} (y_{ij} - \bar{y}_{\infty})^2 \\ &= \sum_{i=1}^a \sum_{j=1}^{n_i} y_{ij}^2 - 2 \sum_{i=1}^a \sum_{j=1}^{n_i} y_{ij} \bar{y}_{\infty} + \sum_{i=1}^a \sum_{j=1}^{n_i} \bar{y}_{\infty}^2 \\ &= \sum_{i=1}^a \sum_{j=1}^{n_i} y_{ij}^2 - 2 \bar{y}_{\infty} \sum_{i=1}^a \sum_{j=1}^{n_i} y_{ij} + a n \bar{y}_{\infty}^2 \\ &= \sum_{i=1}^a \sum_{j=1}^{n_i} y_{ij}^2 - 2 \frac{y_{\infty}}{\sum_{i=1}^a n_i} y_{\infty} + \sum_{i=1}^a n_i \left(\frac{y_{\infty}}{\sum_{i=1}^a n_i} \right)^2 \\ &= \sum_{i=1}^a \sum_{j=1}^{n_i} y_{ij}^2 - 2 \frac{y_{\infty}^2}{\sum_{i=1}^a n_i} + \frac{y_{\infty}^2}{\sum_{i=1}^a n_i} \\ &= \sum_{i=1}^a \sum_{j=1}^{n_i} y_{ij}^2 - \frac{y_{\infty}^2}{\sum_{i=1}^a n_i} \\ &= \sum_{i=1}^a \sum_{j=1}^{n_i} y_{ij}^2 - FK \end{aligned} \quad (2.20)$$

$$\begin{aligned} SST &= \sum_{i=1}^a \sum_{j=1}^{n_i} (\bar{y}_{i\infty} - \bar{y}_{\infty})^2 \\ &= \sum_{i=1}^a \sum_{j=1}^{n_i} \bar{y}_{i\infty}^2 - 2 \sum_{i=1}^a \sum_{j=1}^{n_i} \bar{y}_{i\infty} \bar{y}_{\infty} + \sum_{i=1}^a \sum_{j=1}^{n_i} \bar{y}_{\infty}^2 \\ &= \sum_{i=1}^a \sum_{j=1}^{n_i} \left(\frac{y_{i\infty}}{n_i} \right)^2 - 2 \sum_{i=1}^a \sum_{j=1}^{n_i} \frac{y_{i\infty}}{n_i} \frac{y_{\infty}}{\sum_{i=1}^a n_i} + \sum_{i=1}^a n_i \left(\frac{y_{\infty}}{\sum_{i=1}^a n_i} \right)^2 \\ &= \sum_{i=1}^a n_i \left(\frac{y_{i\infty}}{n_i} \right)^2 - 2 n_i \frac{y_{\infty}}{\sum_{i=1}^a n_i} \left(\sum_{i=1}^a \frac{y_{i\infty}}{n_i} \right) + \left(\frac{y_{\infty}}{\sum_{i=1}^a n_i} \right)^2 \\ &= \sum_{i=1}^a \frac{y_{i\infty}^2}{n_i} - 2 \frac{y_{\infty}}{\sum_{i=1}^a n_i} y_{\infty} + \frac{y_{\infty}^2}{\sum_{i=1}^a n_i} \end{aligned}$$

$$\begin{aligned}
&= \sum_{i=1}^a \frac{y_{i\cdot}^2}{n_i} - 2 \frac{y_{\cdot\cdot}^2}{\sum_{i=1}^a n_i} + \frac{y_{\cdot\cdot}^2}{\sum_{i=1}^a n_i} \\
&= \sum_{i=1}^a \frac{y_{i\cdot}^2}{n_i} - \frac{y_{\cdot\cdot}^2}{\sum_{i=1}^a n_i} \\
&= \sum_{i=1}^a \frac{y_{i\cdot}^2}{n_i} - FK \tag{2.21}
\end{aligned}$$

$$\begin{aligned}
\text{SSE} &= \sum_{i=1}^a \sum_{j=1}^{n_i} (y_{ij} - \bar{y}_{i\cdot})^2 \\
&= \sum_{i=1}^a \sum_{j=1}^{n_i} y_{ij}^2 - 2 \sum_{i=1}^a \sum_{j=1}^{n_i} y_{ij} \bar{y}_{i\cdot} + \sum_{i=1}^a \sum_{j=1}^{n_i} \bar{y}_{i\cdot}^2 \\
&= \sum_{i=1}^a \sum_{j=1}^{n_i} y_{ij}^2 - 2 \sum_{i=1}^a y_{i\cdot} \frac{y_{i\cdot}}{n_i} + n_i \sum_{i=1}^a \left(\frac{y_{i\cdot}}{n_i} \right)^2 \\
&= \sum_{i=1}^a \sum_{j=1}^{n_i} y_{ij}^2 - 2 \sum_{i=1}^a \frac{y_{i\cdot}^2}{n_i} + \sum_{i=1}^a \frac{y_{i\cdot}^2}{n_i} \\
&= \sum_{i=1}^a \sum_{j=1}^{n_i} y_{ij}^2 - \sum_{i=1}^a \frac{y_{i\cdot}^2}{n_i} \tag{2.22}
\end{aligned}$$

so that obtained:

Mean Square Treatment (MST)

$$MST = \frac{SST}{a-1} \tag{2.23}$$

Mean Square Error (MSE)

$$MSE = \frac{SSE}{\sum_{i=1}^a (n_i - 1)} \tag{2.24}$$

Table 2.4: Analysis of Variance for one way classification with unbalance data

Source of Variance	Degree of freedom (df)	Sum Square	Mean Square	F-count
Treatment Error	$a - 1$	SST SSE	MST MSE	$F = \frac{MST}{MSE}$
Total	$\sum_{i=1}^a n_i - 1$	SSTt		

Source : Searle, Casella, & McCulloch 1992

so that obtained.

$$E(SST) = \left(\sum_{i=1}^a n_i - \frac{\sum_{i=1}^a n_i^2}{\sum_{i=1}^a n_i} \right) \sigma_a^2 + (a-1)\sigma_e^2 \quad (2.25a)$$

$$SST = \left(\sum_{i=1}^a n_i - \frac{\sum_{i=1}^a n_i^2}{\sum_{i=1}^a n_i} \right) \hat{\sigma}_a^2 + (a-1)\hat{\sigma}_e^2 \quad (2.25b)$$

$$E(SSE) = \left(\sum_{i=1}^a n_i - a \right) \sigma_e^2 \quad (2.26a)$$

$$SSE = \left(\sum_{i=1}^a n_i - a \right) \hat{\sigma}_e^2 \quad (2.26b)$$

$$\hat{\sigma}_e^2 = \left(\frac{SSE}{\sum_{i=1}^a n_i - a} \right) = MSE \quad (2.27)$$

$$\hat{\sigma}_a^2 = \frac{SST - (a-1)\hat{\sigma}_e^2}{\left(\sum_{i=1}^a n_i - \frac{\sum_{i=1}^a n_i^2}{\sum_{i=1}^a n_i} \right)} = \frac{(a-1)(MST - MSE)}{\left(\sum_{i=1}^a n_i - \frac{\sum_{i=1}^a n_i^2}{\sum_{i=1}^a n_i} \right)} \quad (2.28)$$

IV. APPLICATION

This data is secondary data that gotten from Clean Water Processing Installation of Area Drinking Water Company PDAM in Makassar. Data is about the amount of clean water debit per days from January to December 2008, i.e. for 365 days that is figured in Figure 1.

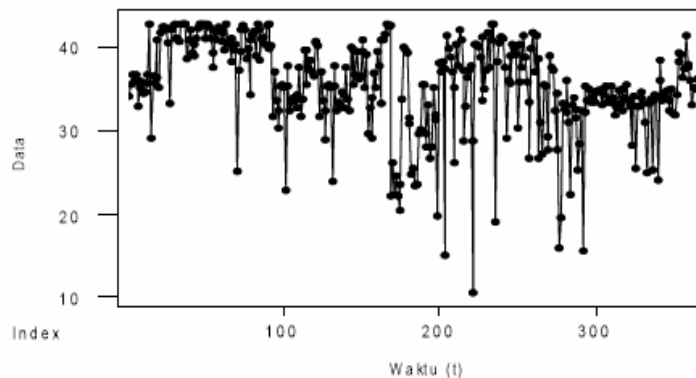


Figure 1: Plotting original data

According to autoregressive analysis, it is estimated that the model for data centered is autoregressive model AR (1), with its autoregressive model is:

$$\hat{Z}_t = (0,4734) Z_{t-1}$$

From the approximation of autoregressive model AR(1) above, the next step is calculating the original residue value by using equation: $\varepsilon_t = Z_t - \hat{Z}_t$

Where $\varepsilon_t = Z_t - \hat{\beta}Z_{t-1}$; for $t = 2, 3, \dots, 365$

For $t = 2$, the original residue value is:

$$\varepsilon_2 = Z_2 - \hat{\beta}Z_1 = 0,0848 - ((0,4734) \times (-1,4172)) = 0,7557$$

For $t = 3$, the original residue value is:

$$\varepsilon_3 = Z_3 - \hat{\beta}Z_2 = 1,2108 - ((0,4734) \times (0,0848)) = 1,1707$$

And so onto the next t .

The statement of hypothesis as follow:

H_0 : residue data of autoregressive model is from a normal distribution population.

H_1 : residue data of autoregressive model is from an

According to the original residue value, the next step is calculating statistical Bera-Jarque test for the original residue by using equation (10):

$$JB = m \left(\frac{\hat{\mu}_3^2}{6} + \frac{(\hat{\mu}_4 - 3)^2}{24} \right)$$

where

$$m = n - p = 365 - 1 = 364$$

$$\hat{\mu}_3 = \frac{1}{m} \sum_{t=p+1}^n \varepsilon_t^3 = \frac{(0,7557^3) + (1,1707^3) + \dots + (0,9946^3)}{364} = -176,201$$

$$\hat{\mu}_4 = \frac{1}{m} \sum_{t=p+1}^n \varepsilon_t^4 = \frac{(0,7557^4) + (1,1707^4) + \dots + (0,9946^4)}{364} = 4294,45$$

So that statistical Bera-Jarque test for the original residue is:

$$\begin{aligned} JB &= m \left(\frac{\hat{\mu}_3^2}{6} + \frac{(\hat{\mu}_4 - 3)^2}{24} \right) \\ &= 364 \left(\frac{(-176,201)^2}{6} + \frac{(4294,45 - 3)^2}{24} \right) = 281201041 \end{aligned}$$

Statistical value of Bera-Jarque test above is compared with critical value that be calculated by using bootstrap parametric simulation. For getting the critical value, the first step is generate the residue data $\tilde{\varepsilon}_t$ with $m = 364$ from normal distribution with mean 0 and variants $\hat{\sigma}_\varepsilon^2$, where $\hat{\sigma}_\varepsilon^2$ is acquired from equation (13).

Mean from the original residue for autoregressive model, AR(1) is:

$$\bar{\varepsilon} = \frac{\sum_{t=p+1}^n \varepsilon_t}{m} = \frac{(0,7557) + (1,1707) + \dots + (0,9946)}{364} = 0,005$$

So that, variants is:

$$\begin{aligned} \hat{\sigma}_\varepsilon^2 &= \frac{\sum_{t=p+1}^n (\varepsilon_t - \bar{\varepsilon})^2}{m - 1} \\ &= \frac{((0,7557) - (0,005))^2 + ((1,1707) - (0,005))^2 + \dots + ((0,9946) - (0,005))^2}{364 - 1} \\ &= 4,9286 \end{aligned}$$

According to the information above, residue data measure 364 is generated from normal distribution with mean 0 and variants 4,9286.

According to residue data above can be formed bootstrap data sample Z_t^* for $t = 2, 3, \dots, 365$ recursively. The first value of Z_t^* is generated randomly from the data that is centered $\{Z_t; t = 1, 2, \dots, 365\}$, by using Minitab software be acquired its first value, i.e. $Z_1^* = 5,4278$.

For $t = 2$, the value of its bootstrap data sample is:

$$Z_2^* = \hat{\beta} Z_1^* + \tilde{\varepsilon}_2 = (0,4734) \times (5,4278) + (-2,7949) = -0,2253$$

For $t = 3$, the value of its bootstrap data sample is:

$$Z_3^* = \hat{\beta} Z_2^* + \tilde{\varepsilon}_3 = (0,4734) \times (-0,2253) + 2,3107 = 2,2041$$

And so on for the other t . After getting data of bootstrap, the next step is calculating the value of estimation parametric $\hat{\beta}^*$ for data of bootstrap Z_t^* , i.e.:

$$\hat{\beta}^* = \frac{\sum_{t=2}^n Z_t^* Z_{t-1}^*}{\sum_{t=2}^n Z_{t-1}^{*2}}$$

with the value of estimation parametric model AR(1), hence its estimation of autoregressive model is:

$$\hat{Z}_t^* = (0,4295) Z_{t-1}^*$$

The value of bootstrap residue for the model above is calculated by using this formula:

$$\varepsilon_t^* = Z_t^* - Z_{t-1}^*$$

$$\varepsilon_t^* = Z_t^* - \hat{\beta}^* Z_{t-1}^* ; \text{ where } t = 2, 3, \dots, 365$$

For $t = 2$, the residue value of its bootstrap is:

$$\varepsilon_2^* = Z_2^* - \hat{\beta}^* Z_1^* = -0,2253 - (0,4295) \times (5,4278) = -2,5568$$

For $t = 3$, the residue value of its bootstrap is:

$$\varepsilon_3^* = Z_3^* - \hat{\beta}^* Z_2^* = 2,2041 - (0,4295) \times (-0,2253) = 2,3008$$

And so on for the other t . the next step is calculating the statistic value of Bera-Jarque test for residue data bootstrap by using equation:

$$JB^* = m \left(\frac{\hat{\mu}_3^{*2}}{6} + \frac{(\hat{\mu}_4^* - 3)^2}{24} \right)$$

where

$$m = n - p = 365 - 1 = 364$$

$$\hat{\mu}_3^* = \frac{1}{m} \sum_{t=p+1}^n \varepsilon_t^{*3} = \frac{(-2,5568^3) + (2,3008^3) + \dots + (1,3413^3)}{364} = 333,07$$

$$\hat{\mu}_4^* = \frac{1}{m} \sum_{t=p+1}^n \varepsilon_t^{*4} = \frac{(-2,5568^4) + (2,3008^4) + \dots + (1,3413^4)}{364} = 1354,0267$$

$$JB_1^* = m \left(\frac{\hat{\mu}_3^{*2}}{6} + \frac{(\hat{\mu}_4^* - 3)^2}{24} \right) = 364 \left(\frac{(333,07)^2}{6} + \frac{(1354,0266 - 3)^2}{24} \right) = 34413404$$

The process of generating residue data with $m = 364$ of normal distribution with mean 0 and variants $\hat{\sigma}_\varepsilon^2$, in order to get the value of statistical Bera-Jarque test for bootstrap residue repeated for $B = 1000$ times. So that, we will get the value of JB^* as many as 1000.

With level $\alpha = 0,10$, critical value that be looked for is the value JB^* in the $(1-\alpha) \times B$ number. $B = 0,90 \times 1000 = 900$. The value of the 900th JB^* is 67911810. Because the value of statistical test $JB = 281201041 > 67911810$, so the null hypothesis is rejected and the conclusion is residue data of Autoregressive model is from an up normal distribution population.

F-Test or ANAVA is used for testing mean difference of sampling cluster more than two clusters which is difference because of using some treatment level on one independent variable (x).

Conditions or assumption which is needed for F-testing follows:

1. Observation is doing in random or free, means that choosing every sample of population must free to opportunity for choosing.
2. Respond Variable which is measure must in interval or rational scale.
3. Observation data which is taken must normal distribution or at least follows normal distribution.
4. Observation datas must have variance homogen between comparing treatment.

Statistical F-Test is identifying as comparing of two random variables χ^2 which is free, and each variables is divided with degree of freedom. So, can be wrote $F = \frac{U/v_1}{V/v_2}$, U and V expressing the random variables, each variables χ^2 distribute with degree of freedom v_1 and v_2 . When S_1^2 and S_2^2 random sample variance has size n_1 and n_2 which is taken from two normal populations, each of variance σ_1^2 and σ_2^2 , and known that $\chi_1^2 = \frac{(n_1-1)s_1^2}{\sigma_1^2}$ and $\chi_2^2 = \frac{(n_2-1)s_2^2}{\sigma_2^2}$ expressing two random variables which χ^2 distribute with each degree of freedom $v_1 = n_1 - 1$ and $v_2 = n_2 - 1$. Then, because two samples are taken as random so the two random independents each other variables. With $\chi_1^2 = U$ and $\chi_2^2 = V$, be found statistical $F = \frac{S_1^2 / \sigma_1^2}{S_2^2 / \sigma_2^2} = \frac{\sigma_2^2 S_1^2}{\sigma_1^2 S_2^2}$ test that has distribution F with degree of freedom $v_1 = n_1 - 1$ and $v_2 = n_2 - 1$. So that if

the value of hunting F is more than F_{α, v_1, v_2} then the null hypothesis is refused.

Estimation is effort for getting value prediction or value interval as value estimate parameter population. The estimation can produces many kinds of estimation that must be chose what is the best to be used as its population parameter estimation. How to show negative value estimate that can be used from variance analysis method. There is nothing intrinsic in this method to avoid it. This is not only a simple case, but also in this models which have many factors, the two cases are balance and unbalance in data.

V. CONCLUSION

From analysis that has been done for balancing data or unbalancing data, can be concluded that cause component of variance has negative values on one way classification (random complete design) is :

1. Application of random complete design that does not precise
2. One or more of the unfulfilled assumption.

Data of clean water debit PDAM Makassar show that autoregressive model AR(1) i.e $\hat{Z}_t = (0,4833)Z_{t-1}$ and autoregressive model AR(1) bootstrap is $\hat{Z}_t^* = (0,43001)Z_{t-1}^*$, because plot of ACF function that is seem significant descend exponentially and plot of PACF function has significant when it is broken after the first lag. It is meant that there is no autocorrelation in residue or there is no relation between the latest (ϵ_t) and the previous residue (ϵ_{t-1}).

According to the calculation result that is acquired by using bootstrap parametric simulation can be calculated that residue data for autoregressive model AR(1) from a population that does not have normal distribution.

References:

- [1] Ahmad Ansori Matjrik dan I Made Sumertajaya. (2002). *Perancangan Percobaan Jilid I Edisi Kedua*. IPB. Bogor.
- [2] Ashari, SE. Akt. dan Purbayu Budi Santosa. (2005). *Analisis Statistik dengan Microsoft Excel & SPSS*. Andi. Yogyakarta.
- [3] Bhatia VK. (2000). *Variance Component Estimation with Application*. Library Avenue. New Delhi.
- [4] Charles E. McCulloch, George Casella, dan Shayle R. Searle. (1992). *Variance Components*. John Wiley & Sons. New York.
- [5] Efron, B. and Tibshirani, R. J. 1993. *An Introduction to the Bootstrap*. Chapman and Hall, Dept. BC, One Penn Plaza, New York
- [6] Hariyana. (2005). *Penaksiran Komponen Variansi Dengan Metode Maksimum Likelihood Pada Data Seimbang*. Skripsi. Fakultas Matematika dan Ilmu Pengetahuan Alam Universitas Hasanuddin. Makassar.
- [7] Haslinda. (2005). *Pengaruh Dosis Tubifex Kering terhadap Laju Pertumbuhan dan Sintasan Juvenil Ikan Hias Koi (Cyprinus Carpio)*. Skripsi. Fakultas Ilmu Kelautan dan Perikanan Universitas Hasanuddin. Makassar.
- [8] Instalasi Pengolahan Air Bersih PDAM Makassar. *Laporan Produksi dan Distribusi Air Bersih Tahun 2008*. Perusahaan Daerah Air Minum Makassar
- [9] Ika Susangka, Ir., MS. Kiki Haetami, Spt. MP., Yuli Andriani, SPi, MP. (2005). *Evaluasi Nilai Gizi Limbah Sayuran Produk Cara Pengolahan Berbeda dan Pengaruhnya terhadap Pertumbuhan Ikan Nila Gift*. Universitas Padjadjaran. Bandung.
- [10] Robert, G. D. Steel & James H. Torrie. (1993). *Prinsip dan Prosedur Statistika*. Gramedia Pustaka Utama. Jakarta.

Regularity of Global Attractor for a Strongly Nonlinear Parabolic Equation

Naimah Aris

Department of Mathematics, Hasanuddin University
Jl. Perintis Kemerdekaan KM. 10 Makassar 90245, Indonesia
e-mail: imaaris@yahoo.com

1. Introduction

'Global attractor' is a basic concept and tool to study asymptotic behaviours of solutions of nonlinear evolution equations and now we have standard monographs on this theory (cf. [2], [12], etc.). A global attractor is an invariant compact set absorbing all of the bounded sets as time goes to infinity and by use of this method we can reduce problems for motions in infinite dimensional spaces to some finite dimensional or 'finite dimensional like' ones.

In this paper, we consider global attractor for a typical strongly nonlinear parabolic equation:

$$u_t - \operatorname{div}(\sigma(|\nabla u|^2)\nabla u) + g(u) = f(x) \quad t > 0, \quad x \in \Omega, \quad (1.1)$$

$$u(x, 0) = u_0(x), \quad x \in \Omega; \quad u(x, t) = 0, \quad x \in \partial\Omega, \quad t > 0. \quad (1.2)$$

Where $\sigma(v^2)$ is a function like $\sigma(v^2) = |v|^m$ and $g(u)$ is a globally Lipschitz function.

This is one of the most typical nonlinear parabolic equations and investigated from various points of view like in [3], [1], [9], [5], [6] and [10]). In [4], it is shown the existence of a global attractor A in $L^2(\Omega)$.

The main purpose of this paper is to study the regularity of A . Under an additional assumption on the forcing term f we shall show that the global attractor A is in fact a bounded set in $W_0^{1,\infty}(\Omega)$. For the proof, Moser's technique as in [7], [8] is frequently used in deriving estimates. Theoretical considerations of the following section are mostly based on paper [10].

2. Results

In this section it should prove that the global attractor $A \subset L^2(\Omega)$ constructed in [4] is in fact

included in $W^{1,\infty}$ under an additional regularity assumption on f . Here, we assume $\partial\Omega$ is C^2 -class. Under the following assumptions,

Assumption A. $\sigma(\cdot)$ is differentiable on $R^+ = [0, \infty]$ and satisfies the condition:

$$k_0|v|^m \leq \sigma(v^2) \text{ and } k_0|v|^m \leq \sigma'(v^2)v^2,$$

and

$$k_1\sigma(v^2)v^2 \leq \int_0^{v^2} \sigma(\eta)d\eta.$$

For $v \in R$, $m \geq 0$ and k_0, k_1 are some positive constants.

Assumption B. $g(u)$ is a globally Lipschitz function on R with $g(0) = 0$.

Assumption C. f belongs to $L^\infty([0, \infty); W_0^{1,\infty}(\Omega))$.

Our result is:

Theorem 1. Under the assumptions A, B, and C the global attractor A of the problem (1.1)-(1.2) is a bounded set in $W_0^{1,\infty}(\Omega)$ and it holds that $\|u\|_{W_0^{1,\infty}} \leq C(M_1) < \infty$ if $u \in A$, where $M_1 = \|f\|_{W_0^{1,\infty}}$.

To proof the theorem, some estimates to approximate solutions need to derive. The solutions are in fact given as limits of smooth solutions of appropriate approximate equations and for the argument the solutions under consideration are sufficiently smooth may assume.

Estimates for $\|u(t)\|_2$ and $\|u(t)\|_\infty$.

Proposition 1 Let $u(t)$ be a solution of the problem (4.1)-(4.2). Then we have

$$\|u(t)\|_2 \leq C(M_0, \|u_0\|_2), \quad 0 \leq t < \infty, \quad (2.1)$$

and

$$\|u(t)\|_\infty \leq C(M_0, \|u_0\|_2)t^{-\lambda}, \quad 0 < t \leq 1. \quad (2.2)$$

Proposition 2 Let $u(t)$ be a solution of problem (1.1)-(1.2), obtain the equation

$$\|u(t)\|_\infty \leq C(M_0, \|u_0\|_2), \quad t \geq 1. \quad (2.3)$$

Estimate for $\|\nabla u(t)\|_{m+2}$

Proposition 3 Let $u(t)$ be a solution of problem (1.1)-(1.2). Then we have

$$\|\nabla u(t)\|_{m+2} \leq C(M_0, \|u_0\|_2)t^{-\lambda}, \quad 0 < t \leq 1, \quad (2.4)$$

for a certain $\lambda > 0$, and

$$\|\nabla u(t)\|_{m+2} \leq C(M_0, \|u_0\|_2) < \infty, \quad t \geq 1. \quad (2.5)$$

Estimate for $\|\nabla u(t)\|_p$

Proposition 4 For $p > m + 2$, the estimate is

$$\|\nabla u(t)\|_p \leq C(M_1, \|u_0\|_2)t^{-\mu}, \quad p > m + 2, \quad (2.6)$$

with a certain $\mu > 0$.

Similarly:

Proposition 5

$$\|\nabla u(t)\|_p \leq C(p, M_1) < \infty, t \geq 1, \text{ for any } p > m + 2. \quad (2.7)$$

Estimate for $\|\nabla u(t)\|_\infty$ by using results above, we obtain

Proposition 6

$$\|\nabla u(t)\|_\infty \leq C(M_1, \|u_0\|_2) t^{-\bar{\mu}}, \quad 0 < t \leq 1, \quad (2.8)$$

with $\bar{\mu} > 0$.

The final estimate is following

Proposition 7

$$\|\nabla u(t)\|_\infty \leq C(M_1, \|u(1)\|_\infty) < \infty, t \geq 1. \quad (2.9)$$

Proof of Theorem 1.

The regularity of the global attractor A constructed in [4] which also indicates that A is bounded in $W_0^{1,\infty}$ will be explained below.

From estimation for $\|u(t)\|_2$ in equation (2.1) we get $A \in L^2$ and A bounded in L^2 .

If $u_0 \in A$,

$$\|u(t)\|_2 \leq C(M_0). \quad (2.10)$$

Indeed, from equations (2.8) for $t = 0$, the solutions will blow up hence by taking $t = 1$, we get from (2.8) and (2.10) that

$$\|\nabla u(1)\|_\infty \leq C(M_1, C(M_0)).$$

Since $M_1 = \|\nabla f\|_{W^{1,\infty}}$ and $M_0 = \|\nabla f\|$, we have that M_1 more uniformly constant than M_0

$$\|\nabla u(1)\|_\infty \leq C(M_1). \quad (2.11)$$

Substitute equation (2.11) to (2.9) obtain the following result

$$\|\nabla u(t)\|_\infty \leq C(M_1, C(M_1)) < \infty, \quad t \geq 1.$$

Since A invariant and bounded in L^2 we see that for any $u_0 \in A$,

$$\|\nabla T(t)u_0\|_2 \leq C(M_1) < \infty, \quad t \geq 1.$$

For $u_0 \in A$. Since $T(t)A = A$ we conclude that A is include in the ball in $W^{1,\infty}$ with the radius $C(M_1)$.

3. Conclusion

In conclusion of this paper we would like to remark that under additional regularity assumption $f(x)$ and an estimate of solutions $u(t)$, $t > 0$, in $W_0^{1,\infty}$, the global attractor A is in fact a bounded set of $W_0^{1,\infty}$ which is also proved the regularity of the global attractor A .

Acknowledgement

I would like to thank professor Nakao Mitsuhiro for his guidance during my research.

References

- [1] A. Haraux, *Nonlinear evolution equations - Global behaviour of solutions*, Lecture Notes in Mathematics, 841, Springer, 1981.
- [2] A.V. Bavin, M. I. Vishik, *Attractors of evolution equations*, North-Holland, Amsterdam, 1992.
- [3] H. Brezis, *Operateurs maximaux monotones et semi-groupes de contractions dans les espaces de Hilbert*, North-Holland, Amsterdam, 1973.
- [4] J. W. Cholewa, T. Dlotko, *Global attractors in abstract parabolic problems*, Cambridge Univ. Press., 2000.
- [5] J. W. Cholewa, T. Dlotko, "Global attractor for sectorial evolutionary equations", *J.Differential Equations*, Vol.125, pp.27-39, 1996.
- [6] M. Nakao, " L^p estimates of solutions of some nonlinear degenerate diffusion equations", *J.Math. Soc. Japan*, Vol. 37, pp. 41-63, 1985.
- [7] M. Nakao, C. Chen, "Global existence and gradient estimate for the quasilinear parabolic equations of m -Laplacian type with a nonlinear convection term", *J. Diff. Eqns.* Vol. 162, pp. 224-250, 2000.
- [8] M. Nakao, Y. Ohara, "Gradient estimate of periodic solution for some quasilinear parabolic equations", *J. Math. Anal. Appl.*, Vol. 204, pp.868-883, 1996.
- [9] M.Tsutsumi, "Existence and nonexistence of global solutions for nonlinear parabolic equations", *Publ. RIMS*, Vol. 17, pp.211-229, 1993.
- [10] M. Nakao, N. Aris, "On global attractor for nonlinear parabolic equations of m -Laplacian type", *J. Math. Anal. App.*, Vol. 331, pp. 793-809, 2007.
- [11] R.A. Adams, *Sobolev space*, 2nd edition, Academic Press, New York, 2003.
- [12] R. Temam, *Infinite dimensional dynamical systems in mechanics and physics*, Springer, New York, 1997.

The Ramsey Numbers for odd Complete Bipartite Graphs

Hasmawati

Department of Mathematics
 Hasanuddin University (UNHAS)
 Jalan Perintis Kemerdekaan KM.10 Makassar 90245
hasma_ba@yahoo.com

Abstract

The Ramsey numbers for a graph G versus a graph H , denoted by $R(G,H)$ is the smallest positive integer n such that for any graph F of order n , either F contains G as a subgraph or \overline{F} contains H as a subgraph. This paper investigates the Ramsey number for complete bipartite graph $R(K_{1,p}, K_{n,m})$. The upper bound of Ramsey numbers on complete bipartite graph $R(K_{1,p}, K_{2,m})$ is $m+2p-2$ or $R(K_{1,p}, K_{2,m}) \leq m+2p-2$. In this paper, we show that the Ramsey numbers $R(K_{1,5}, K_{2,2})=8$, $R(K_{1,5}, K_{2,3})=10$, and $R(K_{1,5}, K_{2,4})=11$. Furthermore, we show that $R(K_{1,5}, K_{2,m})=m+8$ for odd m , $m = 4n-7$ and $n \geq 4$.

Keywords: Ramsey number, Star, Complete bipartite graph

1. Introduction

This problem concerns the topic of Ramsey numbers in graph theory, which is named for Frank Plumpton Ramsey, who was born on February 22, 1903 in Cambridge, Cambridgeshire, England. The special case of Ramsey's Theorem in graph theory when there are two colors will be particular interest to us. There are many interesting applications of Ramsey theory, these include results in number theory, algebra, geometry, topologi, set theory, logic, theory ergodic, information theory and theoretical computer science, Vera Rosta [10].

Throughout this paper, all graphs are finite and simple. Let G be a graph. We write $V(G)$ or V for the *vertex set* of G and $E(G)$ or E for the *edge set* of G . The graph \overline{G} is the *complement* of G . A graph $F=(V',E')$ is a *subgraph* of G if $V' \subseteq V(G)$ and $E' \subseteq E(G)$. For $S \subseteq V(G)$, $G[S]$ represents the *subgraph induced* by S in G .

Let v be any vertex in G and $S \subseteq V(G)$. The *neighborhood* $N_S(v)$ is the set of vertices in S which are adjacent to v . Furthermore, we define $N_S[v]=N_S(v) \cup \{v\}$. If $S=V(G)$, then we use $N(v)$ and $N[v]$ instead of $N_{V(G)}(v)$ and $N_{V(G)}[v]$, respectively. The *degree* of a vertex v in G is denoted by $d_G(v)$. The *minimum (maximum) degree* of G is denoted by $\delta(G)$; $\Delta(G)$. The *order* of G , denoted by $|G|$ is the number of its vertices.

Given two graphs G and H , the *Ramsey number* $R(G,H)$ is the smallest positive integer k such that for any graph F of order k the following holds: F contains G as a subgraph or \overline{F} contains H as a subgraph.

We denote the *complete graph* on n vertices by K_n . A graph G is a *complete bipartite graph* if its vertices can be partitioned into two non-empty independent sets V_1 and V_2 such that its

edge set is formed by all edges that have one vertex in V_1 and the other one in V_2 . If $|V_1| = n$ and $|V_2| = m$ then the complete bipartite graph is denoted by $K_{n,m}$. A wheel W_m is the graph on $m+1$ vertices that consists of a cycle C_m with one additional vertex being adjacent to all vertices of C_m .

Some results about the Ramsey numbers for complete bipartite graphs have been known. Burr [1] showed that $R(K_{2,3}, K_{2,3}) = 10$. Parsons [7] showed that $R(K_{1,7}, K_{2,3}) = 13$. Additionally, Lawrence [5] showed that $R(K_{1,15}, K_{2,2}) = 20$.

Several results have been obtained for $K_{1,p}$. For instance, Surahmat et al. [9] proved that for $n \geq 3$,

$$R(K_{1,n-1}, W_4) = \begin{cases} 2n + 1 & \text{if } n \text{ is even,} \\ 2n - 1 & \text{if } n \text{ is odd.} \end{cases}$$

They also showed $R(K_{1,n-1}, W_5) = 3n - 2$ for $n \geq 3$. In 2004 Chen et al. [2] generalized the results, namely $R(K_{1,n-1}, W_5) = 3n - 2$ for odd $m \geq 5$ and $n \geq m-1$. In [4], Korolova showed that $R(K_{1,n-1}, W_m) = 3n - 2$ for $n = m, m+1$, or $m+2$ where $m \geq 7$ and is odd. In 2004 Rosyida [6] gave an upper bound on the Ramsey numbers of $K_{1,p}$ versus $K_{2,m}$ as presented in Theorem A.

Theorem A. For $p \geq 3$ and $m \geq 2$, $R(K_{1,p}, K_{2,m}) \leq m+2p-2$.

Rosyida also proved the following two theorems.

Theorem B. For $m, n \geq 2$, $R(K_{1,3}, K_{n,m}) = m + n + 2$.

Theorem C. For $m \geq 2$,

$$R(K_{1,4}, K_{2,m}) = \begin{cases} m + 5 & \text{if } m \text{ is even,} \\ m + 6 & \text{if } m \text{ is odd.} \end{cases}$$

Recently, Hasmawati in [3] the Ramsey numbers for small complete bipartite graph were obtained, e.g., $R(K_{1,5}, K_{2,2}) = 8$, and $R(K_{1,5}, K_{2,4}) = 11$.

In this paper we determine the Ramsey numbers $R(K_{1,5}, K_{2,m})$ for certain values of odd m as a main result.

To obtain the main results, we need the following lemmas.

Lemma 1. Let G be a graph of order $2p + m - 5$, $p \geq 5$ and $m \geq 3$. If $\Delta(G) \leq p-2$ and G contains K_3 or $K_{2,3}$, then \overline{G} contains $K_{2,m}$.

Lemma 2. Let G be a connected $(p-2)$ -regular graph of order $2p + m - 5$, for $p \geq 4$ and $m \geq 3$. If G contains no K_3 and $K_{2,3}$, then \overline{G} contains no $K_{2,m}$.

2. Main Results

Theorem 1. $R(K_{1,5}, K_{2,3}) = 10$.

Proof. Given Consider a graph F with $|F| = 9$ with the vertex set $V_F = \{v_i; 0 \leq i \leq 8$ and the edge set $E_F = \{v_i v_{i+1}, v_i v_{i+3}\}$ with all induced in V_F and E_F are taken in modulo 9. Clearly, F is 4-regular and so contains no $K_{1,5}$. It can be verified that for every u, v in \bar{F} , $|N_{\bar{F}}(u) \cap N_{\bar{F}}(v)| \leq 2$. Hence, \bar{F} contains no $K_{2,3}$. Thus, $R(K_{1,5}, K_{2,3}) \geq 10$.

On the other hand, let F_1 be a graph of order 10. Suppose F_1 contains no $K_{1,5}$. So $d_{F_1}(v) \leq 4$ for every vertex v in F_1 . Next, we show that \bar{F}_1 contain $K_{2,3}$. Let there exist u in F_1 with $d_{F_1}(u) \leq 3$. Let w be any vertex in $N(u)$. Since $d_{F_1}(v) \leq 4$ for each v in F_1 , $|N[u] \cup N[w]| \leq 7$. If $B = F_1 / \{N[u] \cup N[w]\}$, then $|B| \geq \{10-7\}=3$. Thus, $\bar{F}_1[\{u, w\} \cup B]$ contains a $K_{2,3}$.

Now, we assume that $d_{F_1}(v) \leq 4$ for each v in F_1 . Let u, w in F_1 with (u, w) not in $E(F_1)$. Write $Z = N(u) \cap N(w)$ and $Q = F_1 / \{N[u] \cup N[w]\}$. Observe that $|Q|=|Z|$. If $N(u)$ or $N(w)$ is not independent, then F_1 contains a K_3 . By Lemma 1, \bar{F}_1 contains a $K_{2,3}$. Suppose $N(u)$ and $N(w)$ are independent sets. Then $\bar{F}_1[\{u, w\} \cup Q]$ contains a $K_{2,3}$ if $|Z| \geq 3$ and $\bar{F}_1[\{w\} \cup N(u)]$ contains a $K_{2,3}$ if $|Z| \leq 2$ (see Fig.1).

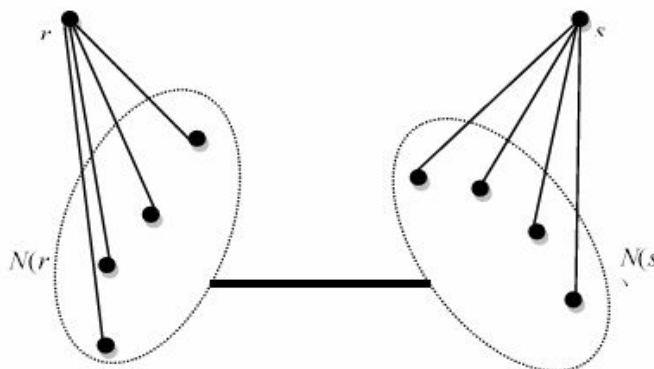


Figure 1. The illustration of proof $|Z|=0$.

Thus, we have $R(K_{1,5}, K_{2,3}) \leq 10$. The proof is now complete. ■

Theorem 2. $R(K_{1,5}, K_{2,5}) = 13$.

Proof. Given a graph F with $|F| = 12$ in Fig. 2.

We can see that the graph F is 4-regular such that contains no $K_{1,5}$. Furthermore, every two vertices in F , say u, v , $|Z(u, v)| \leq 2$ for $(u, v) \in E(F)$ and $Z(u, v) = 0$ for $(u, v) \notin E(F)$. Hence, F contains no K_3 and $K_{2,3}$. By Lemma 2, \bar{F} contains no $K_{2,5}$. So, F is good graph for $K_{1,5}$ and $K_{2,5}$. Thus, $R(K_{1,5}, K_{2,5}) \geq 1$. On the other hand, by Theorem A, we have $R(K_{1,5}, K_{2,5}) \leq 13$. ■

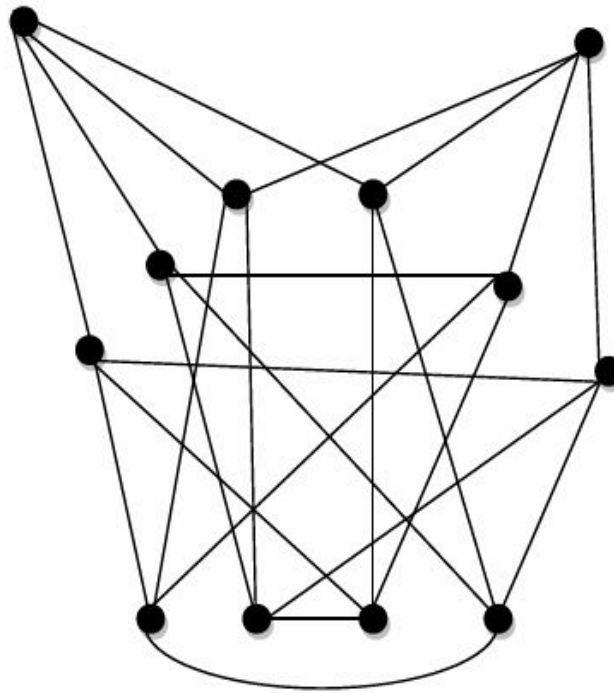


Figure 2. Good graph of $K_{1,5}$ and $K_{2,5}$.

Theorem 3. For $n \geq 4$ and $m = 4n - 7$, then $R(K_{1,5}, K_{2,m}) = m + 8$.

Proof.

By Theorem A, $R(K_{1,5}, K_{2,m}) \leq m + 8$ $m \geq 2$. Therefore, it suffices to prove that $R(K_{1,5}, K_{2,m}) \geq m + 8$ $m = 4n - 7$ $n \geq 4$. Now, we construct a graph F on $4n$ vertices as follows. Divide the vertices of F into two disjoint sets:

$$A = \{u_i : 0 \leq i \leq 2n - 1\} \text{ and } B = \{v_i : 0 \leq i \leq 2n - 1\}, n \geq 4.$$

Define

$$E_F = \{u_i v_i, u_i v_{i+2}, u_i v_{i+5}, u_i v_{i+9} : 0 \leq i \leq 2n - 1\}$$

with all induced in V_F and E_F are taken in modulo $2n$.

Clearly, F is a 4-regular and so contains no $K_{1,5}$. We can observe that for every $u, v \in V_F$, $N_{F-}(u) \cap N_{F-}(v) = \emptyset$ if $(u, v) \in E(F)$ and $|N(u) \cap N(v)| \leq 2$ if (u, v) not in $E(F)$. Hence, F contains no K_3 and $K_{2,3}$. By Lemma 2, \bar{F} contains no $K_{2,m}$. Hence, $R(K_{1,5}, K_{2,m}) \geq 4n + 1 = m + 8$ for $m = 4n - 7$, $n \geq 4$.

Thus, we have $R(K_{1,5}, K_{2,m}) = m + 8$ for $m = 4n - 7$ and $n \geq 4$. The proof is now complete. ■

3. References

1. S. A. Burr, Diagonal Ramsey numbers for small graphs, *J. Graph Theory*, **7**(1983), 67-69.
2. Y. J. Chen, Y. Q. Zhang and K. M. Zhang, The Ramsey numbers of stars versus wheels, *European J. Combin.*, **25**(2004), 1067-1075.
3. Hasmawati, The Ramsey numbers for small complete bipartite graph, JMSK, to appear.
4. A. Korolova, Ramsey numbers of stars versus wheels of similar sizes, *Discrete Math.*, **292** (2005) 107-117.
5. S. L. Lawrence, Cycle-star Ramsey numbers, *Notices Amer. math. Soc.*, **20** (1973), abstract A-420.
6. I. Rosyida, Bilangan Ramsey untuk kombinasi graf bintang dan graf bipartit lengkap, *Tesis Magister Departemen Matematika ITB*, Indonesia (2004).
7. T. D. Parson, Ramsey graphs and block designs, *Trans. Amer. Math. Soc.*, **209** (1975) 33-44.
8. T. D. Parson, Ramsey graphs and block designs I, *J. Combin. Theory, Ser. A*, **20** (1976) 12-19.
9. Surahmat and E. T. Baskoro, The Ramsey number of a path or a star versus W_4 or W_5 , *Proceedings of the 12-th Australasian Workshop on Combinatorial Algorithms*, Bandung, Indonesia, July 14-17 (2001) 165-170.
10. Vera Rosta, Ramsey Theory Applications, Hungarian Academy of Sciences, 2004.

Survival Analysis of High Dimension Microarray DNA Gene Data

Arniati J. Kalatasik¹ and Armin Lawi²

¹ Department of Information System, STMIK Kharisma Makassar
Jl. Baji Ateka No. 20, Makassar, INDONESIA

² Department of Mathematics, Hasanuddin University
Jl. Perintis Kemerdekaan Km. 10, Makassar, INDONESIA
armin@unhas.ac.id

1. Introduction

The study of microarray DNA gene data that includes the survival information of patient can be analyzed using Cox Proportional Hazard (CPH) with output as the probability of the observed object (patient) survival. However, the expression data of *Microarray* DNA gene is a high dimension data and it is difficult to analyse directly using CPH (with the assumption that the number of variables should be less or equal to the number of samples). To remedy this problem, we need to reduced the dimension without losing the information in the original data. Partial Least Square Regression (PLSR) is an elegant method that can reduce the dimension of data by extracting the usefulness information in the data. Therefore, we can have a smaller dimension of data without losing usefulness and potential elements of the data.

In this paper, we implement PLSR method in reducing the dimension data of microarray DNA gene of breast cancer patient [6]. The reduced data are used to analyze the survivalability of the breast cancer patient using CPH model.

2. Fundamental Concepts

2.1. Partial Least Square Regression

Partial Least Square Regression (PLSR) is a new method that generates and combines features in Multiple Linear Regression (MLR) and Principle Component Analysis (PCA). This method constructs predictive model of large number of factors (predictor variables) and correlated. The method extracts the latent component T which is included in high dimension predictor variables. This T component can explained the variation of the data in the model with smaller dimension number. PLSR model can generally be defined as follows.

$$\begin{aligned} Y &= TQ' + F \\ X &= TP' + E \end{aligned} \quad (1)$$

where, Y is response variable matrix with n observations as rows and q -variables as columns, T is *latent* component matrix with n observations rows dan c -variables as columns, Q' and P' are the coefficient matrices/ loading matrices with c -variables as rows dan q -variabel as columns, and F and E are the error matrices.

Latent components T is constructed from the linear combination of the original variables [2].

$$T = XW \quad (2)$$

W is a weight matrix that maximizing the covariances between response variables Y and latent component T [4]. Latent component is used as predictor changing the original variable X . After T is obtained, we have least squared solution for Equation (1) as follows.

$$Q' = (T'T)^{-1}T'Y \quad (3)$$

Then, coefficient regression matrix β for Equation (2) can be obtained as follows.

$$\beta = WQ' = W(T'T)^{-1}T'Y \quad (4)$$

where, β is parameter estimator of the regression equation. Thus, \hat{Y} can be written as follows.

$$\hat{Y} = TQ' = T(T'T)^{-1}T'Y \quad (5)$$

2.2. Cox Proportional Hazard Model

The model of Cox Proportional Hazard (CHP) is given as follows [3].

$$h(t) = h_0(t) \exp(\beta x) \quad (6)$$

where, $h_0(t)$ is the baseline hazard function (unknown), β is the regression coefficient (unknown), and x is the predictor variables.

The β parameter estimator in CHP model is obtained by the estimator of Maximum Likelihood (ML). As a logistic regression, ML estimates β parameter by maximizing the likelihood function which is denoted L. Likelihood function in the CHP model is known as Partial Likelihood (PL). This is because L only evaluating the probability of the fail subject (patient) without considering censored patient. Typically, PL can be expressed as a multiplication product of some likelihood for all k fail times (deads). Therefore, at the j -th fail time, L_j is the likelihood of the fail at the time k considered the object (patient) can survive at time k .

$$L = L_1 \times L_2 \times \dots \times L_k = \prod_{j=1}^k L_j \quad (7)$$

2.3. Survivor Function Estimation

Based on [1] in the prediction phase, proportional hazard that is fitted to k components of PLS is

T_1, \dots, T_k as covariates. Let $S_0(t) = \exp\left[-\int_0^t h_0(u) du\right]$ is the baseline unspecified survivor function.

The its survivor function can be given as follows.

$$S(t, T_k) = S_0(t)^{\exp(\beta T_k)} \quad (8)$$

3. Result and Discussion

Based on data in [6], we have 4,651 gene expressions (as predictor variables) of 78 breast cancer patients (samples). The predictor variables are reduced using PLS method. In PLS itself, we use Cross Validation (CV) so as to know the number of the best variables to use. By implementing PLS and CV, we have reduced the variables to 45 and the residual histogram plot are shown in Figure 1.

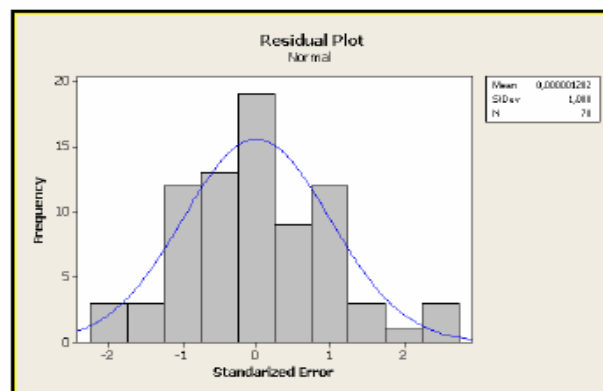


Figure 1. Residual histogram plot of the reduced 45 variables

From Figure 1, it is easy to see that the residual data follows normal distribution. The multicollinearity test is also shown that the reduced 45 variables are independent or there is no strong correlation amongst variables. The determination coefficient R^2 , which describes variation of Y variable that can be explained by the 45 variables, is 1.00 and the R^2 (adj) is also 1.00. Therefore, the PLS model with 45 variables can explain the variety of data (Y) is 100%, and it really gives a good reduction for the regression model.

The reduced variables then are used into Cox Proportional Hazard function in order to evaluate survival probability of the patients. However, we should firstly evaluate all variables to determine which variable is give strong influence with significany level 5% (Sig < 0.05). The result shows variables (gene expression) that have strong influences to the patient survivalbility are the variable 1, 2, 3 and 5. Survivalbility of the variables are shown in Table 1.

Table 1. Survivalbility of Breast Cancer Patients

Gene Expression	Time (Month)	Baseline Cum Hazard	At Mean Covariates		
			Survival	SE	Cum Hazard
1	3	0,059	0,988	0,011	0,012
	10	0,118	0,977	0,016	0,023
	56	2,596	0,598	0,056	0,513
2	3	0,012	0,988	0,012	0,012
	10	0,025	0,976	0,017	0,024
	56	0,533	0,597	0,056	0,516
3	3	0,009	0,991	0,009	0,009
	10	0,018	0,982	0,013	0,019
	56	0,446	0,632	0,059	0,46
4	3	0,011	0,99	0,01	0,01
	10	0,021	0,979	0,015	0,021
	56	0,505	0,608	0,057	0,497
6	3	0,012	0,988	0,012	0,012
	10	0,024	0,976	0,017	0,025
	56	0,51	0,598	0,056	0,515
5	3	0,011	0,99	0,01	0,01
	10	0,021	0,979	0,015	0,021
	56	0,505	0,608	0,057	0,497

From Table 1, it can be seen for the influence of gene expression 1 that on 3 months the patient survival probability is 0.988 with standard error 0.012. In the same month period, the risk of breast cancer patient to fail (dead) is 0.012. In the next 7 months the survival probability of the patient is decreasing to 0.976 by the increasing risk to fail becomes 0.24. In the month 59, the survivability to live is 0.568 and the risk to fail is going balanced with 0.565.

The high survival probability is given by the influence of variable 3 (i.e., the gene expression 3). It can be seen that patient survivability in 2 months and 59 months are, respectively, 0.991 dan 0.603. It can also be said that the highest decreasing of survivability is given in 3 months and 59 months by the influence of gene expression 1 (i.e., can reach 42%), and the lowest risk is given by variable 3 around 38.8%. Therefore, we can said that the gene expression 3 has strong influence to the patient survivability. The graphs of survival and hazard functions of the variable 3 are given in Figure 3 and Figure 4, respectively.

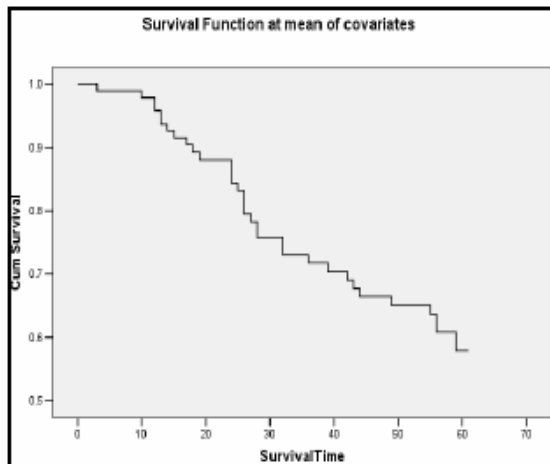


Figure 2. Patient survivability by variable 3

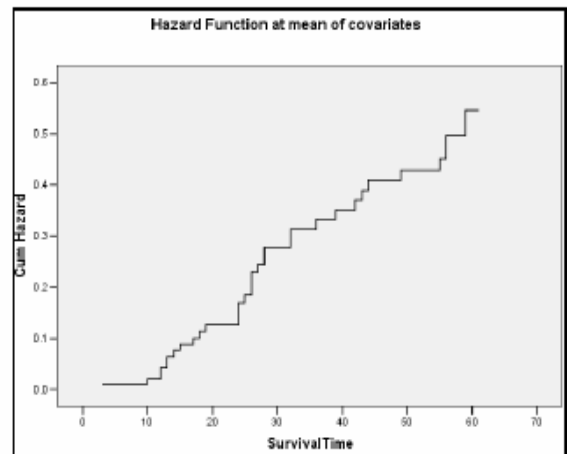


Figure 3. Hazard Function of Gene Expression 3

4. Conclusion

Expression data of Microarray DNA gene is a high dimension data that can be reduced using PLSR method without losing all the information of the original data. The patient survivability can thus be analyzed using Cox Proportional Hazard (CPH). Based on our result for the case of breast cancer, the number of gene expression data are 4,751 and they can be reduced to 78 variables. According to its PRESS value, the best number of variables that can be used are 45. From these 45 variables, the significant influence to the patient survivability is given by variable 1, 2, 3, 4 and 6. The highest influence to the patient survivability is given by the combination of gene expressions in variable 3.

References

- [1] Bastien, Philippe. *PLS-Cox Model: Application to gene expression*. <http://cedric.cnam.fr/PUBLIS/RC1001.pdf>, 2004.
- [2] Boulesteix, A.-L. and Strimmer, K. *Partial Least Square: A Versatile Tool for The Analysis of High-Dimensional Genomic Data*. Department of Medical Statistic and Epidemiology, Germany, 2006.
- [3] Febiruri, Nur I. *Penggunaan Model Resiko Proporsional Cox Dengan Pendekatan Bayesian Semiparametrik Menggunakan Gamma Proses Prior*. Undergraduate Project Paper Dept. Mathematics Hasanuddin University. Makassar, 2008.
- [4] Naes, T., Isaksson, T., Fearn, T., and Davies, T. *A User Friendly to Multivariate Calibration and Classification*. NIR Publications, Chichester, West Sussex, UK., 2004
- [5] Tobias, D. Randall, *An Introduction to Partial Least Squares Regression*. SAS Institute Inc., <http://www.ats.ucla.edu/stat/sas/library/pls.pdf>, 1995.
- [6] <http://www.plosbiology.org/article/info:doi/10.1371/journal.pbio.0020108> #pb io0020108-Alizadeh1

Classifying Cervical Cancer Stadium Level using Fuzzy Decision Support System

Greby Febriastuti and Armin Lawi

Department of Mathematics, Faculty of Mathematics and Natural Sciences, Hasanuddin University
Jl. Perintis Kemerdekaan Km. 10, Makassar 90245, INDONESIA
armin@unhas.ac.id

1. Introduction

Cancer is the most malignant disease and cause death nowadays in the world. One of the most dangerous of all cancers which attacked 34% women in Indonesia is cervical cancer. Currently, the cervical cancer is ranked as the top three among the various types of cancer that causes death to women in the world [1]. In Indonesia, more than 15,000 cancer cases are detected by the cervical cancer every year. The main problem in treating the cervical cancer by paramedical is, of course, firstly to determine the evaluation of stadium level of the cervical cancer. After the stadium level is determined, good treatments to the patient can surely be decided.

In this paper, we purpose a powerful decision support system (DSS) using fuzzy system which helps in evaluating and determining the level of the stadium on cervical cancer. We use parameters of symptoms and signs of cervical cancer, i.e., decreasing of the human-immune, drastic weight loss, lower abdominal pain, enlarged abdomen, the presence of vaginal bleeding, anaemia symptoms, the patient experienced vaginal discharge, high dose consumption of birth control that can cause irregular bleeding and enlargement of cervical tissues.

2. Fuzzy Decision Support System

The fuzzy decision support system in classifying the stadium level of cervical cancer is conducted as the following steps.

2.1. Fuzzyfication

This process serves to convert an analog quantity into fuzzy input and determining the degree of membership of each crisp input. In this step we evaluate the degree of membership of each input parameter, i.e., the decreasing human-immune, drastic weight loss, lower abdominal pain, enlarged abdomen, the presence of vaginal bleeding, the symptoms of anaemia, the patient experienced vaginal discharge, high dose consumption of birth control that can cause irregular bleeding and enlargement of cervical tissues. We use trapezium membership functions to all parameters in this step. For instance, we use the following trapezoidal membership function for the weight loss parameter.

$$\mu_{rendah} = \begin{cases} 1, & x < 5 \\ \frac{8-x}{3}, & 5 \leq x \leq 8 \\ 0, & x \geq 8 \end{cases} \quad (1)$$

$$\mu_{sedang} = \begin{cases} 0, & x < 5 \\ \frac{x-5}{3}, & 5 \leq x < 8 \\ 1, & 8 \leq x < 14 \\ \frac{20-x}{6}, & 14 \leq x < 20 \\ 0, & x \geq 20 \end{cases} \quad (2)$$

$$\mu_{tinggi} = \begin{cases} 0; & x < 14 \\ \frac{x - 14}{6}; & 14 \leq x < 20 \\ 1; & x \geq 20 \end{cases} \quad (3)$$

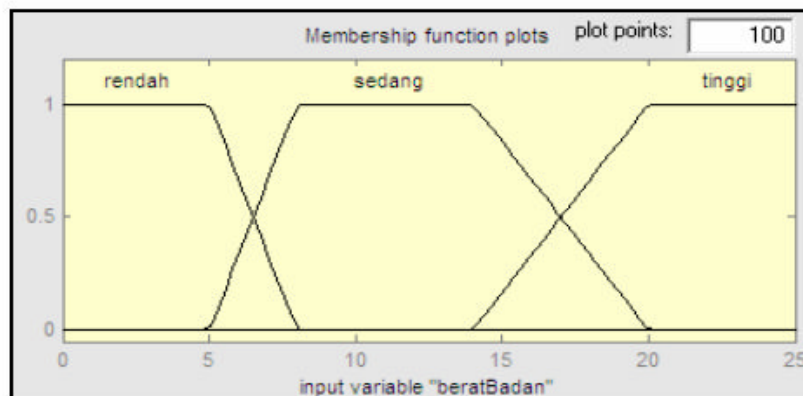


Figure 1. Membership Function for Weight-Loss

2.2. Inferencing

Inferencing is a process of making and evaluation rules to generate the output of each rule. The rules which are used for the decision support system of cervical cancer are as follows.

- R₁:** IF immune height AND weight loss slightly AND lower abdominal pain AND history of stomach AND low bleeding slightly enlarged AND low anemia AND history of vaginal discharge is rarely AND low use of family planning AND small cervical cancer tissue THEN cervical cancer Stage I.
- R₂:** IF immune is weight loss AND weight loss is medium AND lower abdominal pain AND history of stomach AND bleeding slightly enlarged AND anemia are whitish AND history of vaginal discharge is rarely AND the use of family planning is low AND medium cervical cancer tissue THEN cervical cancer Stage II.
- R₃:** IF immune is weight loss AND weight loss is medium AND abdominal pain AND stomach is enlarged AND bleeding are whitish AND anemia are whitish AND history of vaginal discharge AND the use of family planning is whitish AND medium cervical cancer tissue THEN cervical cancer Stage III.
- R₄:** IF immune is low AND weight loss is high AND lower abdominal pain AND history of stomach AND bleeding highly AND anemia are highly AND history of vaginal discharge (often) AND the use of family planning is high AND medium cervical cancer tissue THEN cervical cancer Stage IV.

2.3. Composition

This process serves to combine the output of all rules in determining the level of the stadium on cervical cancer. In this step, we use the Mamdani method.

2.4. Defuzzyfication

This process is a computation to the crisp output. There are several methods can be used in this step. In this paper we use the *centroid* method. Crisp solution obtained by taking the centre point of a fuzzy area using the following functions.

If the parameter is in discrete case we use

$$z = \frac{\sum_{i=0}^n z_i \times \mu_c(z_i)}{\sum_{i=0}^n \mu_c(z_i)} \quad (4)$$

And, we use the following centroid for continue case.

$$z = \frac{\int_{\mathcal{R}_c} z \mu_c(z) dz}{\int_{\mathcal{R}_c} \mu_c(z) dz} \quad (5)$$

3. Classifying the Stadium Level

The overall steps in classifying the stadium level of the four steps which are mentioned in the previous sections can be described as follows.

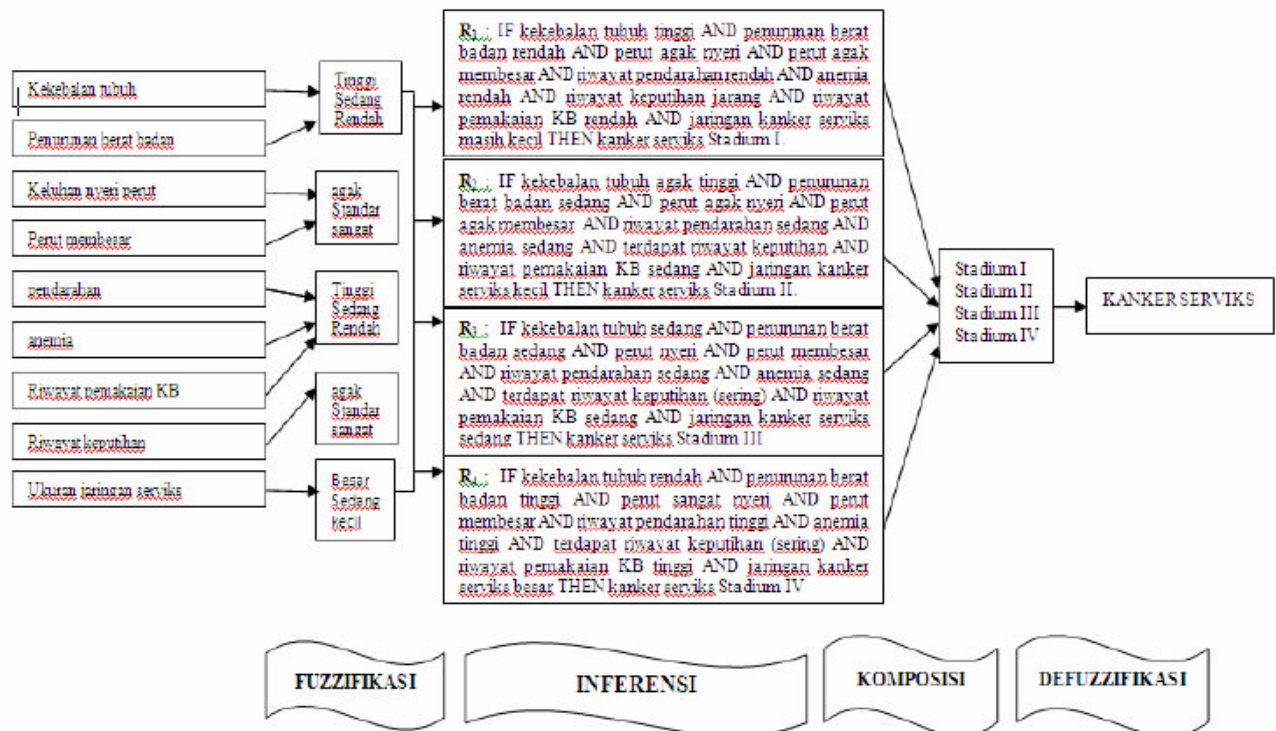


Figure 2. Overall steps in classifying the stadium level

The result of the evaluation process in the fuzzy decision system, of course, is determining the level of the stadium level of cervical cancer. This framework has been applied for the all data of observed patients on cervical cancer at Wahidin Sudirohusodo General Hospital. The result of the determination stadium levels obtained using fuzzy decision system was the same as determining the level of stage cervical cancer conducted by the medical. For instance, the system determining the level of cases of cervical cancer stage using fuzzy logic is conducted as follows.

A woman with symptoms of cervical cancer with the characteristics of: anemia, vaginal discharge, vaginal bleeding during the past 11 months, lower abdominal pain, cervical cancer tissue 0.4 cc.

A. Fuzzyfication

$$\begin{aligned}\mu_{\text{anemiaSEDANG}} &= 0,75 \\ \mu_{\text{keputihan}} &= 0,75 \\ \mu_{\text{pendarahanSEDANG}} &= \frac{16 - 11}{6} = 0,833 \\ \mu_{\text{pendarahanTINGGI}} &= \frac{11 - 10}{6} = 0,167 \\ \mu_{\text{PerutNyeri}} &= 0,75 \\ \mu_{\text{SEDANG}} &= 1\end{aligned}$$

B. Inferencing

Based on existing data, the obtained predicate rules are as follows.:

$$\begin{aligned}\alpha_{\text{predikat1}} &= \min [0,75 ; 0,75 ; 0,833 ; 0,75 ; 1] = 0,75 \\ \alpha_{\text{predikat2}} &= \min [0,75 ; 0,75 ; 0,167 ; 0,75 ; 1] = 0,167\end{aligned}$$

C. Composition

Membership functions of the resulted of this composition is

$$\mu_z = \begin{cases} 0,067x - 2,33 ; 35 \leq x \leq 46,25 \\ 0,0274x - 1,101 ; 46,25 \leq x \leq 67,505 \\ 0,0078x - 0,363 ; 46,25 \leq x \leq 67,505 \\ 0,013x - 0,902 ; 67,505 \leq x \leq 80 \end{cases} \quad (6)$$

D. Defuzzyfication

The he resulting fuzzy value is 61.32. In the variable domain of cervical cancer, this value is including at Stadium III of cervical cancer.

4. Conclusion

Decision support system using fuzzy logic can be implemented to assist in determining the level of the stadium on cervical cancer. This system has been applied for observed patients on cervical cancer at Wahidin Sudirohusodo General Hospital, and the result of the determination stadium levels obtained using fuzzy decision system was the same as determining the level of stage cervical cancer conducted by the medical.

References

- [1] Anonim, 2006. *Kanker Leher Rahim*. <http://www.medicastore.com>
- [2] Buckland, Mat. 2005. *Fuzzy Expert System*. <http://digilib.petra.ac.id/>
- [3] Dwiono, Wakhyu. 2008. *Fuzzy Logic System*. <http://trensains.com/fuzzy.htm>

Quality of Service Measurement In Virtual Server

Ida Nurhaida¹, N. N. R.A. Mokobombang², E. Palantei²

¹Computer Science Faculty, Mercu Buana University
Jalan Raya Meruya Selatan, Kembangan, Jakarta Barat 11650

²Electrical Engineering Department, Hasanuddin University, Makassar, Indonesia 90245

E-mail: (idarivan@yahoo.com) ; novvra@yahoo.com; elvas_palantei@unhas.ac.id

Abstract

Server Virtualization Technology is sharing a physical machine by several server operating systems. Each role can be run on an isolated virtual environment so that it becomes relatively more secure and easier to manage. The main advantage offered by the use of virtual technology is promising a reliable infrastructure and allow maximum use of a server. This is because generally in the scale of enterprise, a dedicated server runs only one role. The typical server utilization range is about 10% - 20%. This situation is not ideal when compared with the total cost of ownership for the server machine.

The implementation of virtual technology that utilizes virtual server resources maximally is expected not to reduce its scalability. Therefore in this research, the scalability performance virtual servers will be measured in terms of quality of service (QoS) including *delay*, *jitter*, *throughput*, *round trip time*, and *packet loss*. The scenario used is to merge three servers with different role as database server, email server, and active directory server into a single physical machine. Next, the server is connected to a network that has four workstations. QoS measurement has done using *wireshark*. At the end of this research the expected results obtained through the measurement can provide some information about the virtual server's scalability.

Keywords: *Virtualization Technology, Virtual Server, Virtual Machine, Scalability, QoS*

I. Introduction

Virtualization is becoming a key feature of Grids where it essentially provides the feature of abstracting some specific characteristics of the Grid infrastructure [2]. The concept of a Virtual Machine (VM) is not recent and was proposed very early in the history of computers. Virtualization is a major part of today's data centers. The operating efficiencies offered by virtualization allow organizations to dramatically reduce operational effort and power consumption. Virtualization technology can be a key factor in helping the organization optimizes IT [4]. The optimization should be able to realize power savings and substantially improve resource utilization. Virtualization is more useful in application testing, staging, and moving workloads into production. While IT may still be viewed as a cost center, virtualization can make IT department become much more efficient. Virtualization is also crucial when it comes to simplified backup and disaster recovery because downtime caused by catastrophic events will be reduced from days to hours or even minutes. Virtualization ensures that applications remain available, independent of hardware servicing. In more advanced organizations, business units can acquire their own infrastructure through self-service provisioning of virtual machines. In fact, dynamic provisioning can enable business units to automatically bring new resources online (or take services offline) as workload demands require. Migration of workloads can also happen automatically and without interrupting users, and problems can be detected and mitigated with minimal manual effort.

One way to benefit from Virtual Machine (VM) is to run multiple VM on the same physical machine [3]. There is no set limit to the number of virtual machines that can be configured, but no more than 256 virtual machines can be booted simultaneously on a single VM Host. Each virtual machine is isolated from the others. The VM Host administrator allocates virtual resources to the guest. The guest accesses the number of CPUs that the VM Host administrator allocates to it. CPU use is governed by an entitlement system which can adjust to maximize CPU use and improve performance.

A symmetric multiprocessing system can run on the virtual machine if the VM Host system has sufficient physical CPUs for it. Because multiple virtual machines share the same physical resources, I/O devices can be allocated to multiple guests, maximizing use of the I/O devices and reducing the maintenance costs of the data center. By consolidating systems onto one platform, data center requires less hardware and management resources.

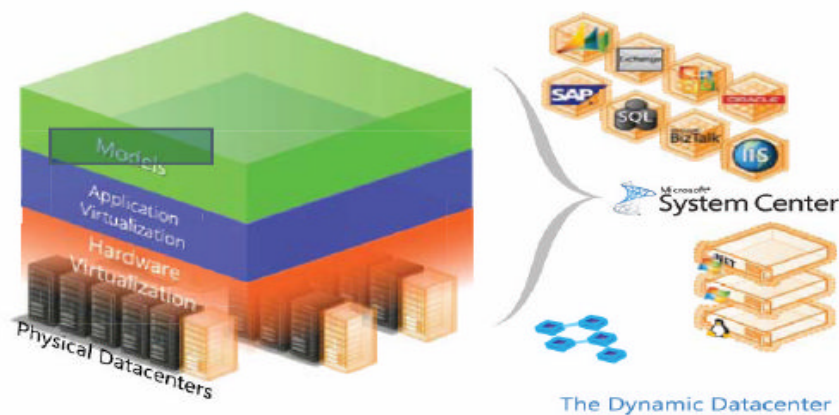


Figure 1: Dynamic Data Centre [4]

Another use for virtual machines is to duplicate operating environments easily, maintaining isolation on each virtual machine while managing them from a single, central console [7]. Virtual Machine allows administrator to create and clone virtual machines with a simple command interface. Administrator can modify existing guests and arrange networks that provide communication through the VM Host's network interface or the guest local network. Because all the guests share the same physical resources, administrator can be assured of identical configurations, including the hardware devices backing each guest's virtual devices. Testing upgraded software and system modifications is a simple matter of entering a few commands to create, monitor, and remove virtual machines.

Taking into account that different applications have different resource requirements, an application could not need all of the resources provided in the physical node [1]. As a consequence, the application could underutilize some of the physical resources (such as CPU or network interfaces). Unlike the traditional approach, with virtualization, we can boot different isolated operating systems sharing the multiplexed physical resources of an equipment. The isolation is achieved through the concept of the VM, which is an *efficient, isolated duplicate* of the real machine.

The rest of this paper is organized as follows. In section 2 describe methodologies and metrics system that used to evaluate the Quality of Service (QoS) of virtual machine. In section 3 report the experiments to validate QoS measurement. Finally, the conclusion is in section 4.

II. Methodology and Metric System

Typically, in this paper QoS measurement for single machine compared to basic operating system. This is the main focus for virtual system. In particular, several measurement tests with different scenario applied in both two systems, traditional and virtual. Firstly, consolidate three physical servers into one physical server. The server consists of virtual machines implemented from each server in traditional server. In server performance's testing, scenario test applied according to each server role as follows:

- Database Server
- Email Server
- Active Directory Server

Scenarios of these experimental are access server's application from workstations together at the same time for certain duration in both traditional and virtual. The parameters measured by average from experimental perform for five times each. Comparison between traditional server and virtual server perform in the same software and hardware related to each server's role as a database server,

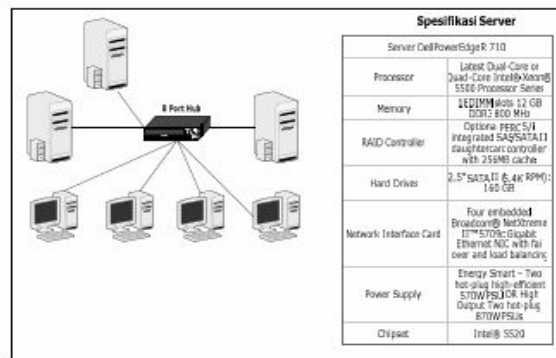


Figure 2: Network Topology with Traditional Server

active directory (AD) server, and mail server. The first phase of implementation began with the installation of three servers and four workstations to be connected in a LAN. Step-by-step traditional network configuration is as follows:

1. Installing Windows Server 2008 operating system on the server.
2. Installing the system in accordance with the role each server, MS-SQL 2008 and MS-Exchange 2003.
3. Installing the operating system Windows XP Professional Service Pack 2 on a workstation.
4. Installing hardware drivers needed.

IP addresses is provisioning on the computer servers and workstations in accordance with their respective NIC interfaces. In this configuration, each server is assigned an IP address 192.168.71.141 to AD Server, Exchange Server to 192.168.71.143, and 192.168.71.143 to SQL Server. While each workstation assigned an IP address from 192.168.71.231 to 192.168.71.234.

Network topology in virtual server implementation is consists of one virtual server and four workstations that are connected to the hub by RJ 45 cable. Virtual server performs the role in accordance with the functions of each server in the traditional network.

After the measurement of traditional networks, the next stage is done by installing a virtual server that contains one host partition and three guest partition with a different role. Network configuration steps are as follows:

1. Installing VMWare ESX 3.5 operating system on the server.
2. Installing a virtual machine and guest operating systems. For the guest operating system used Windows Server 2008.
3. Installing hardware drivers needed.
4. Provision of IP addresses on a virtual server for both host and guests.
5. IP workstation that is used together with traditional IP network.

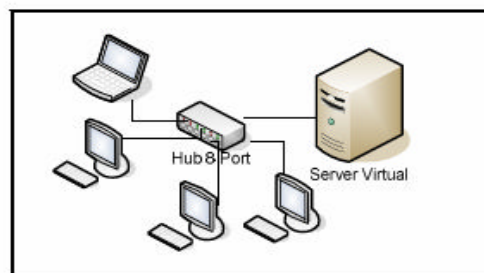


Figure 3: Network Topology with Virtual Server

The test was performed in two stages in traditional LAN and LAN with server virtual. Testing applied in both servers have done in the initial conditions and conditions burdened by the application. The QoS parameters measurement used as the nature for analyzing network performance, including delay, jitter, packet loss, throughput, and round trip time. Data were collected using Wireshark software.

Capturing streaming audio and video data by running Netmeeting program is done in two stages:

1. Streaming audio and video made between user1 and user2.
2. Streaming audio and video made between user1 and user2, user3 and user4 while transferring files.

Table 1: Results Measurement of QoS Parameters on Streaming Audio and Video Conference

Without Burdened				With Burdened		
Server	Delay (ms)	Jitter (ms)	Throughput (Kbps)	Delay (ms)	Jitter (ms)	Throughput (Kbps)
Streaming Audio						
Tradisional	30.52	7.87	16.97	30.88	7.90	16.81
Virtual	30.49	7.76	17.03	30.86	7.80	16.88
Video Conference						
Tradisional	94.92	0.58	188.21	94.97	0.59	107.90
Virtual	96.99	0.59	189.02	98.93	0.95	187.99

III. Testing Results

Table 1 show data average obtained in this research. The QoS parameters namely packet loss, round trip time, and round trip loss cannot be measured. This is due to a local network both traditional and virtual in good condition so that no packets have failed or corrupted. Graphic image streaming audio QoS parameters measurement can be seen in Figure 4 and Figure 5. While the image of the measurement for video conferencing can be seen in Figure 6 and Figure 7.

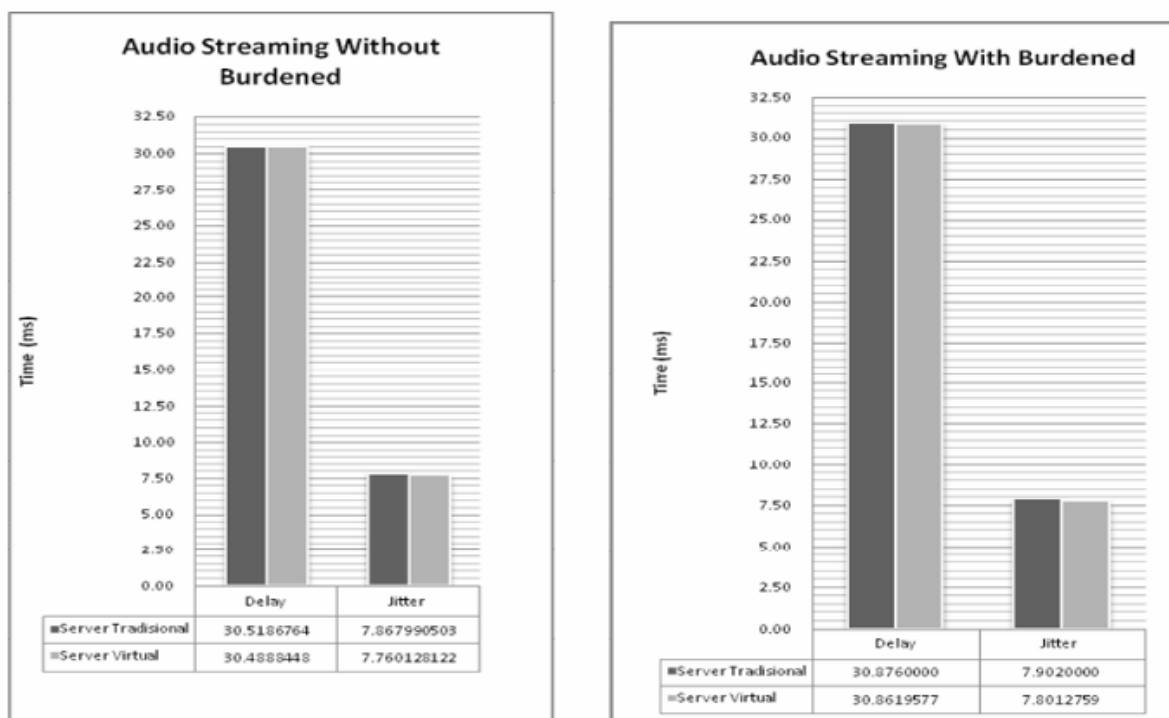


Figure 4: Streaming Audio on traditional servers and virtual servers

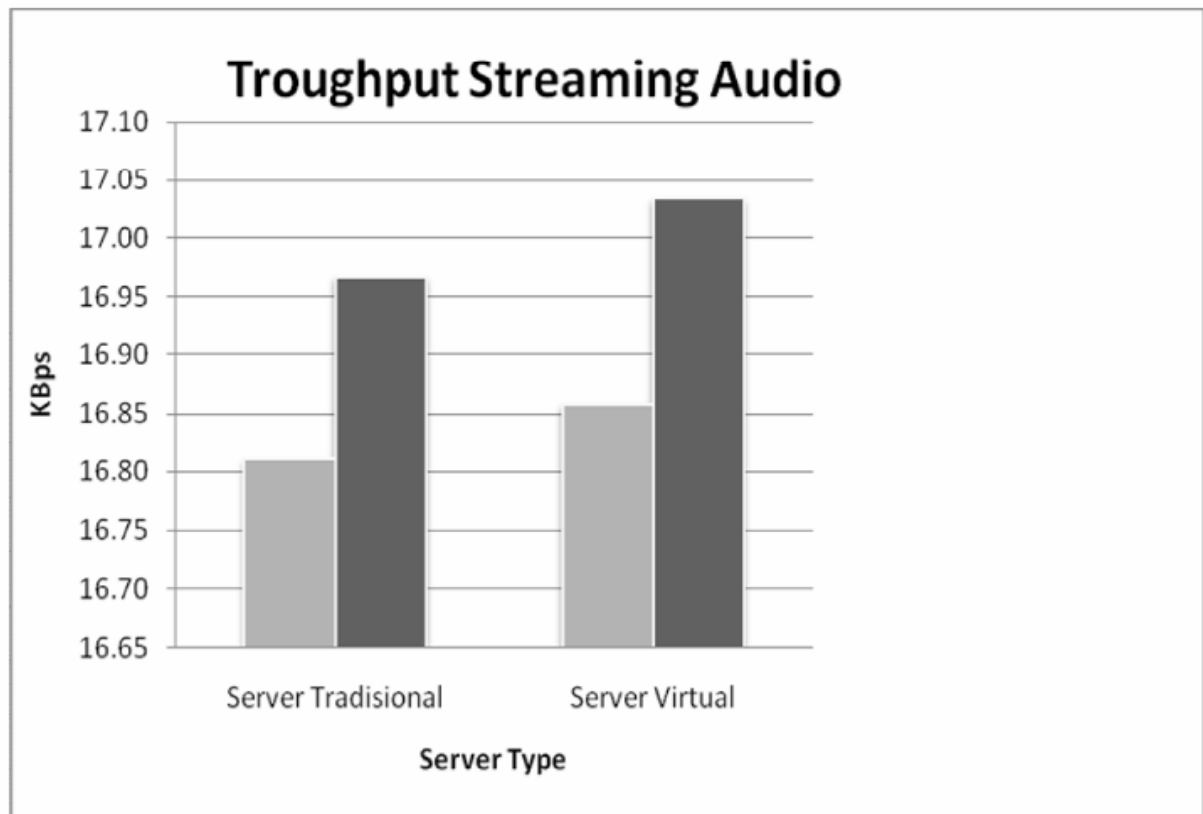


Figure 5: Streaming Audio on traditional servers and virtual servers

Based on measurement results obtained by the values of delay and jitter between streaming audio and video conferencing, it can be seen that the result both types of servers are not much different. However, throughput on the virtual server obtained a better value than traditional servers.

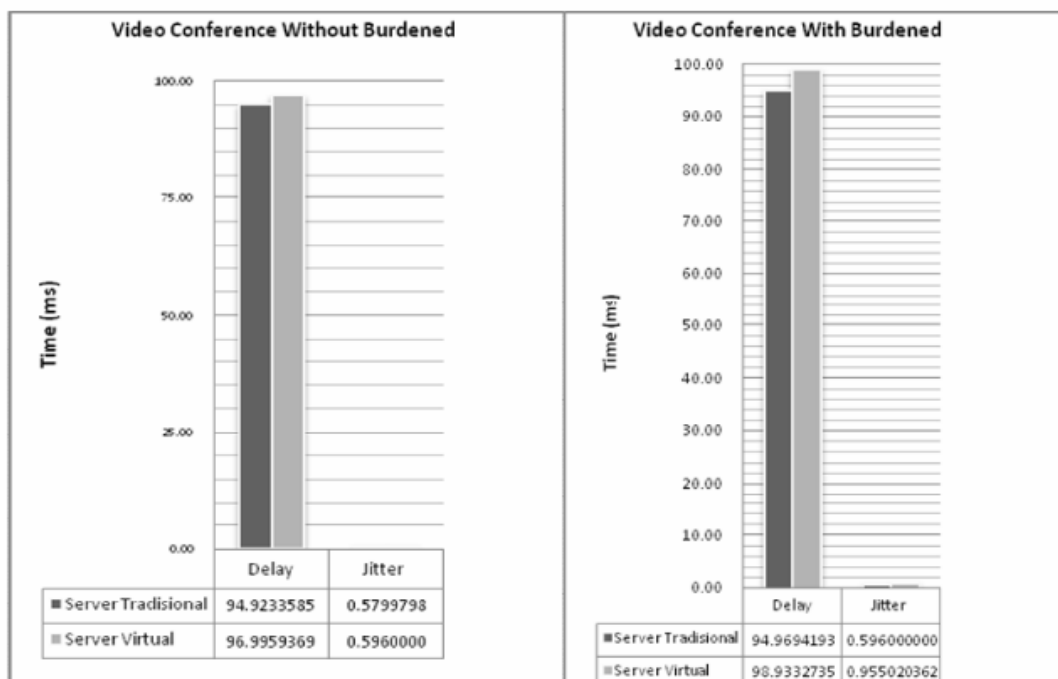


Figure 6: Video Conference on traditional servers and virtual servers

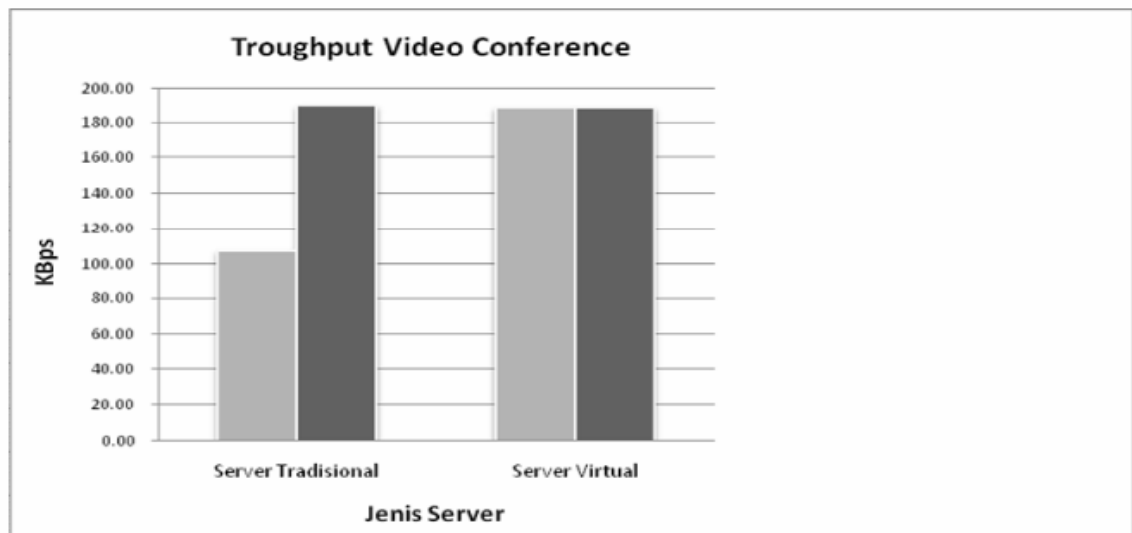


Figure 7: Throughput Video Conference

QoS parameter measurements have been obtained the following results:

1. Streaming Audio

According to Table 1 streaming audio delay and jitter values obtained for the virtual server is better than traditional servers with difference 0.03 and 0.11 ms for the experiment without any burden. Measurements of streaming audio with burden have obtained values 0.014 ms and 0.1 ms. In the throughput measurement, result for the virtual server is better than traditional servers, while differences without burden obtained 0.067 Kbps and differences testing with burden obtained 0048 Kbps. The difference was not significant due to the streaming audio bit rate is relatively very small.

2. Video Conference

The value of delay and jitter in traditional server server is better than virtual with a difference 2.073 ms and 0.016 ms for the testing applied without any burden. As for testing with burden obtained by the differences of 3.96 ms and 0.36 ms. Throughput measurement result for the virtual server is better than traditional servers. For without any burden, the difference obtained 0.81 Kbps, otherwise 80.69 Kbps to testing with burden. When the conference was ongoing, sound came faster than the video. This is because the audio jitter is smaller than the jitter in streaming video. This occurs naturally due to its delay variation is lower so it will reach the destination earlier than a bigger jitter.

Based on the results of QoS parameters measurement on streaming audio and video conferencing, it can be seen that the throughput on the virtual server is better than traditional servers. To explain this, there are several considerations about the physical aspects in relation to the optimization of networks:

1. The connection between client and server in local network which is connected by the same switch. If the client and server use a different switch then it must consider how many network hops required by the package to achieve the two systems.
2. NIC type used by both machines to interact with each other. NIC to the server class generally offers better performance.
3. The size of packets transmitted via the network.

Network throughput is highly dependent on network configuration and application specifications. On the physical environment, CPU usage plays a significant role to achieve the expected network throughput. In order to produce a higher throughput requires more CPU resources. The impact of the availability of CPU resources for virtual network throughput applications also plays an important role. Running a virtual server requires a certain amount of CPU resources depends on server configuration. CPU usage on a virtual server is higher than with traditional servers. This is due to the features provided by the virtual technology that allows for dynamic allocation of resources

more flexibly in accordance with the applications needs. Planning the network throughput applications that run on virtual server is same with the planning of throughput network applications that run on physical systems. Similarly with the physical platform, the entire system's performance depends on the network physical elements, network stack implementation, running application and network traffic. Higher CPU usage required by the transaction network in running a virtual application.

Virtual infrastructure allows the implementation of a transparent network configuration. When a workload is run in a virtual machine, network mechanisms used by the workload is similar when running on physical machines using the physical NIC. Maximum throughput obtained by the virtual machine can be compared with throughput on the physical server.

Another issue affecting the network throughput involves network usage patterns. Although the traffic generated by the same application, but the results can differ depend on user and access time. For example, for CRM applications can generate steady streams of small packets when used by a sales representative. But traffic can be bursty and contains a large package when it is used to create activity reports. A few things into consideration traffic patterns are:

1. The frequency of transactions that led to large-sized package.
2. Data packets size.
3. Sensitivity of the data loss. For example, streaming multimedia applications using UDP can still be understood by the user despite data loss.
4. Traffic Directiveness, data to be transmitted downstream (from server to client) more than data upstream.

4 Conclusions

1. Performances of LAN with traditional servers and LAN with virtual servers do not show significant differences. However, the resulting throughput on the LAN with a virtual server is better than the LAN with a traditional server. On audio streaming throughput for the experiment without burden have difference obtained 0067 Kbps and 0048 Kbps for testing with burden. It is case can be explained that the virtual server can use CPU resources more efficient and dynamically in accordance with the needs of the running application. A CPU resource is an important factor for throughput.
2. Based on the results of measurements show that maximum utilization of infrastructure resource does not affect the quality of services that can be perceived by the user. User does not feel any differences in server systems used on the local network.

References

- [1] Fernando Rodriguez-Haro, Felix Freitag, Leandro Navarro, Enhancing Virtual Environments with QoS-aware Resource Management, *Ann. Telecommun.* (2009) 64:289–303 DOI 10.1007/s12243-009-0106-1, Received: 1 May 2008 / Accepted: 10 February 2009 / Published online: 21 April 2009 © Institut TELECOM and Springer-Verlag France 2009
- [2] Scalability Comparison of Four Host Virtualization Tools, Benjamin Quérier, Vincent Neri, Franck Cappello, *J Grid Computing* (2007) 5:83–98 DOI 10.1007/s10723-006-9052-6, Received: 15 February 2006 / Accepted: 11 July 2006 / Published online: 19 September 2006 © Springer Science + Business Media B.V. 2006
- [3] Hewlett-Packard Development Company, L.P., HP Integrity Virtual Machines A.03.00 Installation, Configuration, and Administration, 3rd Edition, 15-16, 2007
- [4] Microsoft Corporation, *Virtualization from Data Center to the Desktop*, © 2007 Microsoft Corporation www.microsoft.com/virtualization, last accessed September 27, 2009